THE ROLE OF THE NEUROPEPTIDE PRECURSOR VGF IN THE GLIOBLASTOMA MULTIFORME MICROENVIRONMENT AND ITS EFFECTS ON MICROGLIA CELLULAR FUNCTIONS

INAUGURAL-DISSERTATION
TO OBTAIN THE ACADEMIC DEGREE
DOCTOR RERUM NATURALIUM (DR. RER. NAT.)
SUBMITTED TO THE DEPARTMENT OF BIOLOGY,
CHEMISTRY AND PHARMACY
OF FREIE UNIVERSITÄT BERLIN

BY

FELIPE DE ALMEIDA SASSI

FROM PORTO ALEGRE, BRAZIL

2016

This work was carried out at the *Max-Delbrück Zentrum für Molekulare Medizin in the Helmholtz Association* from April 2013 to July 2016 under the supervision of Prof. Dr. Helmut Kettenmann.

1st Reviewer: Prof. Dr. F.G. Rathjen
Max-Delbrück-Zentrum für Molekulare Medizin
Developmental Neurobiology
Robert Rössle Str. 10
13125 Berlin

2nd Reviewer: Prof. Dr. H. Kettenmann
Max-Delbrück-Zentrum für Molekulare Medizin
Cellular Neurosciences
Robert Rössle Str. 10
13125 Berlin

Date of defense:
13.10.2016

I. Acknowledgements

I would like to first thank Professor Helmut Kettenmann for trusting me a PhD position at his distinguished lab and giving me the opportunity to work on this exciting project in such a productive environment. I appreciate all his support, guidance and supervision which made me a much better scientist than when I started. I also would like to thank the MDC for the financing and fantastic support.

I would like to thank Dr. Susanne Wolf for her trust and faith both on the project and in me and for the constant supervision. I thank Dr. Dolores Hambardzumyan for welcoming me as her temporary student in Cleveland, for helping so much my project and always being available. I thank Marcus Semtner for sharing his great knowledge. I thank Professor Stephen Salton for his collaboration and for providing the VGF antibodies and knockout mice which made this project so interesting.

I thank my students Martin Mersch and Josien Visser for helping me during this journey and trusting me as a supervisor, thank you for the great work! I thank my collaborators Philipp Jordan and Stefan Wendt for all the good discussions. I thank all my dear lab colleagues who make this lab so unique and easy to work with. Thank you all for the amazing time!

I would also like to thank the best technical assistants a lab can have: Regina Piske, Nadine Scharek, Michaela Segeer-Zografakis, Hanna Schmidt and Sophie Neuber.

I would like to sincerely thank our dear Birgit Jarchow for the constant help and care.

I finally want to thank my mother for letting me take her heart along with me to Berlin and for being my number one fan. I could not find enough words to thank all the love from my father, my family and friends: you inspire and make me feel as happy as someone could be.

Last, I would like to dedicate my thesis to my love Stefan Davids, who has been in this journey with me all along giving an unbelievable amount of support and making any challenge easy to face and every achievement a great victory.

Thank you all from the bottom of my heart!

II. Table of contents

III. List of figures

IV. List of tables

V. List of Abbreviations

AMP	Adenosin monophosphate
ANOVA	Analysis of variance
ATP	Adenosin triphosphate
BDNF	Brain-derived neurotrophic factor
C3AR1	Complement C3a receptor-1
CGC	Cerebellar granule cells
CM	Conditioned medium
CNS	Central nervous system
CRE	Cyclic AMP-response element
dLGN	Dorsal lateral geniculate nucleus
ECM	Extracellular matrix
ELISA	Enzyme-linked immunosorbent assay
GBM	Glioblastoma multiforme
gC1qR	Globular head of the complement component C1q receptor
GDNF	Glial cell-derived neurotrophic factor
GEM	Genetically-engineered mice
GFAP	Glial fibrillar acidic protein
GPCR	G protein-coupled receptor
IFN-γ	Interferon gamma
IL	Interleukins
LGG	Low grade gliomas
LPS	Lipopolysaccharides
MAPK	Mitogen-activated protein kinases
MHC	Major histocompatibility complex
MRI	Magnetic resonance imaging
NGF	Nerve growth factor
NPC	Neural progenitor cells
OPC	Oligodendrocyte precursors cells

PC	Prohormone convertases
PNS	Peripheral nervous system
RT-qPCR	Quantitative reverse transcription polymerase chain reaction
TAA	Tumor-associated astrocytes
TAM	Tumor-associated macrophages
VEGF	Vascular endothelial growth factor
WHO	World health organization
WT	Wild-type

For all the units the International System of Units prefixes were used.

1. Introduction

I. The neuropeptide precursor VGF: a recent history

VGF (non-acronymic) mRNA was first identified in 1985 by Andrea Levi at the National Institute of Health in the laboratory of Bruce Macdonald Paterson as a result of his investigation on neural sympathetic and sensory differentiation induced by nerve growth factor (NGF) using rat pheochromocytoma PC12 cells as a model. The study published in Science (Levi et al., 1985) describes a mRNA with a rapid increase after NGF stimulation, with peak at five hours. The mRNA hybridized with the cDNA clone *Vgf8a* from a 5000 clones library, but the authors at the time did not find any sequence homology at the National Sequence Data Bank and only after four years of research the group published in *The EMBO Journal* (Possenti et al, 1989) the first comprehensive study on the newly discovered neuropeptide precursor, shedding light on the identity and function of the gene, later named as VGF (originally the name was *Plate V nerve Growth Factor inducible gene*). The paper describes the complete sequence (**Figure 1, left**) of the mRNA and amino acids that were deduced by overlapping cDNA clones from PC12 and rat brain libraries. Making use on immunoblotting and immunostaining (**Figure 1, right**) the authors could also localize VGF in the cytoplasm of PC12 cells and more precisely in secretory vesicles and perinuclear regions and indeed the VGF amino acid rat sequence is anticipated by a secretory leader sequence of 22 amino acids that promotes translocation to the endoplasmic reticulum. The identified protein presented different peptide sizes (90 and 75 kDa) consistent with proteolytic processing and more importantly, they could assess that VGF was being secreted through the regulated secretory pathway upon stimulation with the different agents tested and by depolarization.

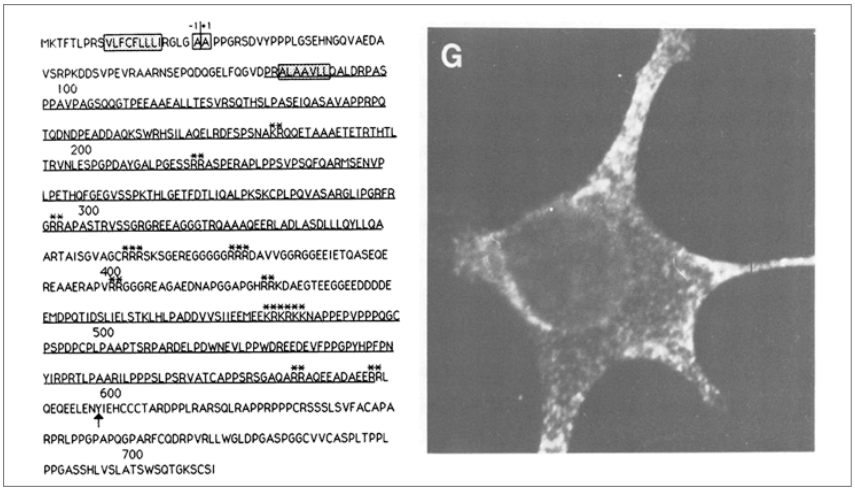

Figure 1: VGF protein sequence and localization.

(**Left**) Sequencing of the *Vgf8a* clone acquired with overlapping cDNA clones. (**right**) First immunostaining of VGF in PC12 cells after NGF stimulation. Adapted from Possenti et al. (*The EMBO Journal,* 1989).

In the same year van den Pol and colleagues (van den Pol et al. 1989) published that VGF protein expression throughout the central nervous system (CNS) had a spatial temporal pattern, with an abundant staining in neurosecretory cells of the hypothalamus . The area with the most abundant staining for VGF was the dorsal lateral geniculate (dLGN), which receives a major sensory input from the retina.

In 1991 Stephen Salton (Salton et al., 1991) using the same approach as Andrea Levi - cDNA cloning from mRNA upregulated in PC12 cells after NGF stimulation - published the *Vgf* genomic sequence and for the first time the gene structure for VGF was studied. In his research he confirmed the previous findings stating that "*In the cascade of events which ultimately results in the neural differentiation of PC12 cells in the presence of NGF, the VGF gene encodes the most rapidly and selectively regulated, nervous system-specific mRNA"* and also described induction of VGF mRNA by bFGF, aFGF, insulin and depolarization. In the sequence of the promoter besides canonical TATAA box and a CCAAT elements they localized a cyclic AMP-response element (CRE) that could explain the regulation of VGF gene expression by neurotrophins and depolarization, this finding was later confirmed by introduction of mutations in the CRE sequence that abolished *Vgf* transcription induced by NGF (Hawley et al., 1992). As predicted by the author the discovery of VGF gene sequence enabled a better assessment of VGF mRNA distribution and regulation.

Besides VGF expression in the CNS, VGF protein products were also described in several neuronal groups of the peripheral nervous system (PNS) and endocrine organs, including primary sensory and enteric neurons, and in endocrine cells of the adrenal medulla, adenohypophysis and gut (Ferri et al., 1992). The authors also considered precursor roles for VGF and biogically active derived peptides, highlighting the C-terminal region of the protein as most prominent in terms of biological function. **Figure 2** illustrates VGF distribution in the different organs.

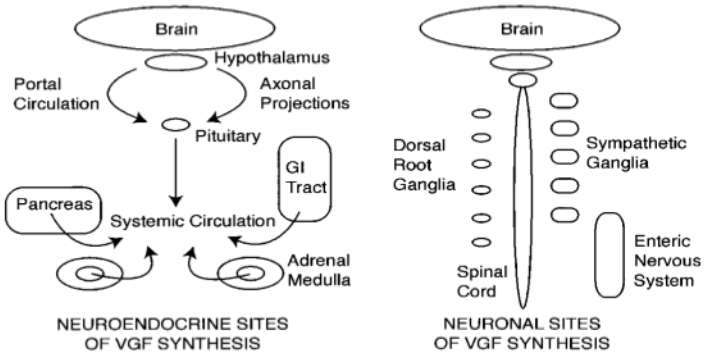

Figure 2: Vgf distribution

VGF protein and mRNA have been detected in a number of neuroendocrine tissues. Schematic representation of the sites of VGF synthesis in the adult with arrows representing possible routes of release of VGF peptides into the circulation. This image and capture were extracted from Salton et al. (*Frontiers in Neuroendocrinology*, 2000).

Following the above cited many other publications came out in the 1990s from different groups trying to uncover the molecular regulation of rapid VGF induction. **Table 1** summarized the main findings. Several studies worked on VGF protein and mRNA expression as well, mapping VGF across the entire rat brain, spinal cord, olfactory bulb and retina (van den Pol et al., 1994; Snyder and Salton, 1998). *Vgf* human sequence was first published at the Society for Neuroscience conference in 1992 (Canu et al., 1992) and the human promoter was fully characterized five years later by the same authors (Canu et al., 1997).They found in certain regions of the promoter 75-85% of homology with the already published rat sequences and different consensus sequences of transcription factors, including the cyclic AMP response element and Activation Protein 1 element and an upstream sequence that could act as a *Vgf* silencer and prevent its transcription in non-neuroendocrine cells. The human VGF gene is

located on 7q22.1 and is comprised of two exons, but only exon 2 comprises the complete coding-sequence. The 2.5 Kbp transcript encodes a protein of 615 aminoacids (two less than in rodents) that have several regions of high sequence conservation across mammals, specially the C-terminal domains (Bartolomucci et al., 2011).

Table 1: First findings in VGF research

Authors	Year	Findings
Levi et al.	1985	VGF mRNA, inducible by NGF
Possenti et al.	1989	mRNA/Amino acid sequence; VGF is a polypeptide; VGF localization in secretory vesicles from the regulated secretory pathway
Van den Pol et al.	1989	VGF immunostaining throughout the rat CNS and development
Salton et al.	1991	*Vgf* rat genomic sequence;
Trani et al.	1995	Description of pro-VGF processing
Canu et al.	1997	*Vgf* human promoter characterized

1.I.1. **Precursor processing and derived peptides**

Despite the previous hints that VGF undergoes proteolytic processing, only ten years after its discovery the protein was characterized as a polypeptide (pro-VGF) and its peptides were finally identified (depicted in **Figure 3**). The first VGF peptide isolated was the C-terminal Peptide V or AQEE-30 (VGF-derived peptides are named after the four N-terminal amino acids and sequence length according to Levi et al., 2004) (Liu et al., 1994). One year later a description of the different processed peptides in the rat CNS and their differential distribution in several brain areas was published (Trani et al., 1995). Making use of an antibody against the N-terminal regions of VGF most of the areas presented 90 kDa and 80 kDa precursor polypeptides but using an antibody against the C-terminal specifically smaller amounts of peptides with 20

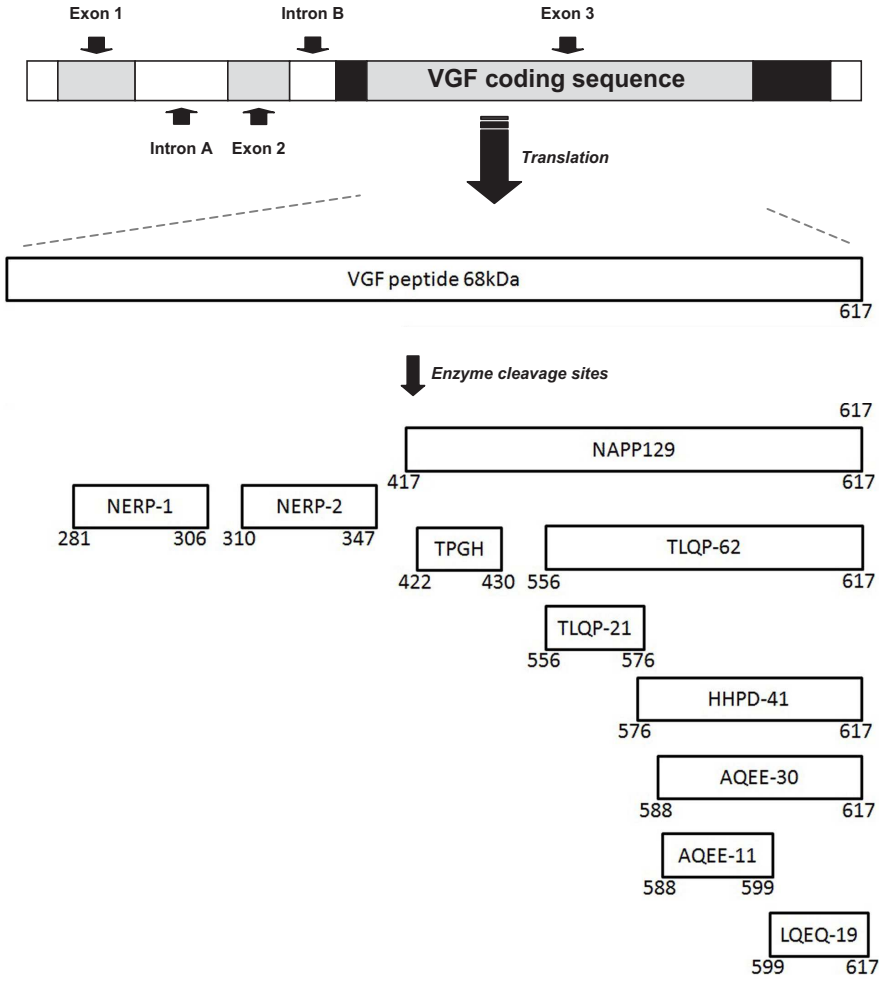

Figure 3: VGF processing and derived peptides

Vgf gene and peptides: *vgf* is a single copy gene and corresponding protein sequence is encoded by the exon 3, while the untranslated region contains two small introns. The *vgf* gene encodes a polypeptide of 615 (humans) and 617 (rat/mouse) amino acids which is cleaved into a number of smaller biologically active peptides. Caption and top picture with *vgf* gene copied and modified from Jethwa & Ebling (*Neuroendocrinology,* 2008) and bottom picture with the derived peptides from Lewis et al. (*Frontier in Endocrinology*, 2015).

(VGF20, or NAPP-129), 10 (VGF10 or TLQP-62) and 18 kDa were also observed. The processing was inhibited by the fungal metabolite BFA which interrupts the vesicular vectorial transport of protein toward the cell surface, causing the accumulation of the immature secretory vesicles at the endoplasmic reticulum, which indicates that the vesicles containing the peptides are part of the regulated secretory pathway. Later, in 2002, the authors isolated and characterized a few of the described peptides (Trani et al., 2002). Trani and collaborators found that the proteolytic post-translational processing at

specific cleavage sites yields several VGF peptides by the prohormone convertases (PC), PC1/3 and PC2, with both PC targeting the cleavage site at NAPP-129, but only PC1/3 cleaves the amino acid sequence *Arg-Pro-Arg* at the position 555 that will generate TLQP peptides. Salton et al., 2000 describes at least ten conserved regions on the VGF protein murine and human sequence that are potential cleavage sites and so far actually ten different peptides with known biological activity were already described although some with unknown activity and many more could be discovered in the future (Ferri et al., 2011; Lewis et al., 2015). The fine regulation of VGF was further elucidated with the finding that VGF sorting is dependent on the prohormoneconvertase catalytic activity on a regulatory sequence (^{564}*Arg-Arg-Arg*^{566}) at the C-terminal region of the protein (Garcia et al., 2005), which together with the N-terminal signal was necessary and sufficient to target the polypeptide to the regulated secretory pathway in both PC12 and the rat insulin secreting beta cell derived line INS-1 (**Figure 4)**. All the characteristics, including tight regulation and processing, storing into secretory vesicles and regulated release, involved in VGF regulation determined its protein classification as part of the granin family of peptides (Bartolomucci et al., 2011). This family of peptide precursors distinguishes from the others by higher precursor sizes and lower pI values. Members of the granin family include the chromogranins (A and B), secretogranins (II and III), and related proteins (7B2, NESP55, proSAAS and VGF).

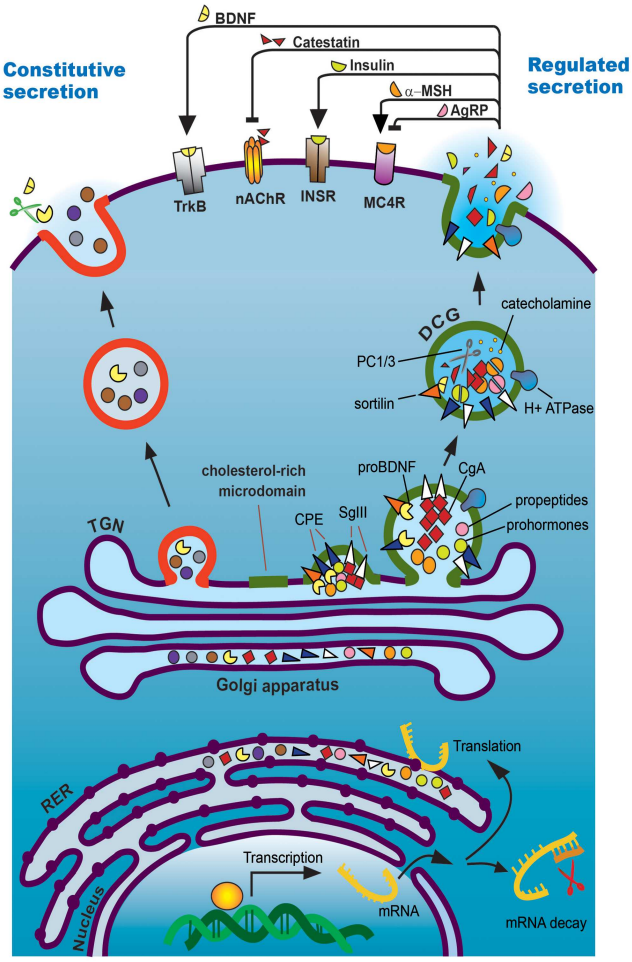

Figure 4: The regulated secretory pathway

Neurons and neuroendocrine cells make use of the regulated secretory pathway in order to achieve a tight control in different steps of the production, processing and delivery of hormones and regulatory neuropeptides, which are first synthesized at endoplasmic reticulum and sorted to large dense core vesicles in the Golgi apparatus. Granules are transported toward the plasma membrane and mature into competent organelles for secretagogue-induced exocytosis. Granules are then docked, and primed, before finally releasing their processed contents after fusing with the plasma membrane. The whole process is spatially and temporally coordinated. Imaged adapted from Lin & Salton (*Frontiers in Endocrinology,* 2013) and caption from Vazquez-Martinez & Gasman (*Frontiers in Endocrinology,* 2014).

1.I.2. **VGF neuronal functions**

Until VGF peptides were isolated and studied individually, the main function of VGF was thought to be associated with neural development. In this regard, some

evidence pointed to VGF having a role in synaptogenesis, but also later studies showed an involvement in neuronal differentiation through neurite growth and possibly neuroprotection. Lombardo and colleagues were the first to propose that VGF could be involved in synaptogenesis: they showed that VGF distribution correlated with the process of synaptogenesis both temporally, at different stages of development (El6, El8, P0, P4, P10, P15, P23) and spatially at the geniculocortical pathway from the thalamic area called dorsal lateral geniculate nucleus (dLGN) to the adult post natal visual cortex. More specifically, their findings show VGF being synthesized by thalamic cells, and then transported to the axonal terminals in the developing cortical layers from E18, when in the rat, afferents connections arrive at the cortical subplate (Lombardo et al., 1995). The VGF expression stayed high until the first postnatal weeks, when the new synapses are already established with the definitive target neurons at the layer IV. Interestingly, the blockade of afferent retinal activity induces a dramatic but reversible reduction of VGF mRNA in the dLGN neurons.

Supporting this hypothesis another study came out one year later (Benson and Salton, 1996) demonstrating high VGF expression in a small population (6%) of GABAergic neurons of hippocampus cultures from P18 rats. The VGF immunolocalization became polarized to axons at the onset of dendrite maturation, supporting a role in synaptogenesis in favor to axon polarization. Later Sato and collaborators (Sato et al., 2012) confirmed that VGF is transported from the sensory thalamic nuclei throughout thalamocortical axon terminals. Furthermore, they showed with in vitro and ex vivo experiments from cortical cultures that VGF increases dendritic growth, specifically of spiny stellate neurons and also survival of multipolar neurons without interfering with cell fate of these cells. In line with these results VGF overexpression was also shown to promote neurite extension and viability under ischemia in PC12 in a recent study (Sakamoto et al., 2015).

Regarding hippocampal synaptic plasticity a study (Alder et al., 2003) demonstrated that VGF might play a role in synaptic plasticity associated with learning, since it was induced after treatment of hippocampal cells with brain-derived neurotrophic factor (BDNF), which promotes synaptic strengthening associated with learning. The authors observed an induction of VGF mRNA after hippocampus-

dependent tasks and also identified a dose-dependent enhancement of synaptic charge using the synthetic C-terminal peptide TLQP-62, showing that the C-terminal cleavage products of VGF are biologically active. Thakker-Varia and colleagues found in 2007 that VGF was downregulated in animal models of depression and that it had anti-depressant activity upon its infusion in the hippocampus of mice subjected to forced swim test, which is used to assess antidepressant-like behaviors. Chronic treatment with VGF enhanced proliferation of hippocampal progenitor cells both in vitro and in vivo with long-term survival and differentiation of the progenitors, meaning that the antidepressant activity of VGF was likely to be involved with increased neurogenesis. This research group also went further on the investigation and found that TLQP-62 specifically increases the pool of Type 2a neural progenitor cells (NPC) by enhancing their proliferation and reducing the number of differentiated daughter cells (Thakker-Varia et al., 2014). This effect seems to be mediated by mutual interaction with BDNF receptor TrkB and also by synaptic activity through signaling cascades downstream of the glutamate receptors (PKD and Ca2+-calmodulin-dependent protein kinase II).

More recently, 2015, in an elegant study, Lin and colleagues from Salton's research group showed many aspects of TLQP-62 and BDNF interaction to regulate memory consolidation but not acquisition resulting in synaptic plasticity through TrkB receptor activation in a positive feedback loop. TLQP-62 peptide modulated synaptic plasticity through BDNF-TrkB-dependent alterations of the actin cytoskeleton, as a result of Rac1 increased mRNA levels and cofilin protein phosphorylation which were induced after contextual fear memory training in the dorsal hippocampus of wild-type mice, but not in germline VGF heterozygous knock-out mice. Phosphorylation of cofilin, which regulates actin dynamics, and activation of Rac1, an upstream factor of cofilin-regulated actin polymerization are involved in synaptic plasticity related to memory. TLQP-62 also caused acute cofilin phosphorylation in hippocampal slices via BDNF-dependent signaling. They showed that the effects are most likely are due to VGF expression in excitatory neurons during memory formation and also stated that VGF processing and the corresponding receptor distribution can modulate memory consolidation in a versatile fashion, as administration of TLQP-21 showed opposite effects of TLQP-62 by impairing fear memory under the same training protocol.

In addition to its role on energy balance, which will be further explained, TLQP-21 was already shown to have neuroprotective functions on cerebellar granule cells (CGC) (Severini et al., 2008). In this study the authors reduced the potassium and serum concentration from the cultures in order to induce cellular death. Upon simultaneous treatment with different doses of TLQP-21 a subpopulation of cells presented activation of mitogen-activated protein kinases (MAPK) Erk1/2 accompanied by increase intracellular calcium and also phosphorylation of Akt which resulted in reduced DNA fragmentation and increased survival of the cells (more than 20% compared to control), probably related to anti-apoptotic mechanisms mediated by the stress-activated protein kinase JNK pathway. Such pathways, especially MAPK Erk1/2 are already known to regulate neuronal cell death, providing a hint for the mechanism of action of TLQP-21. The authors took care to use a MEK1/2 inhibitor, which completely reduced the protective effect of TLQP-21 on the potassium deprivation-induced cellular death.

A research group studying endoplasmic reticulum stress role on amyotrophic lateral sclerosis (Shimazawa et al., 2010) proposed another role for VGF in neuronal function. They found VGF to be upregulated by the small molecule SUN N8075 while screening for substances protecting cells from ER stress. The mRNA upregulation occurred through ERK1/2, AKT, and CREB1 pathway. Making use of knockdown and overexpression of VGF in the human neuroblastoma SH-SY5Y cell line they found that SUN N8075 inhibited endoplasmic reticulum stress-induced neuronal cell death by tunicamycin via VGF expression, pointing out that VGF plays a critical role in motor neuron survival. SUN N8075 treatment also ameliorated spinal cord gliosis on an animal model of amyotrophic lateral sclerosis, which showed decreased VGF immunoreactivity. Although the authors did not study any peptide-specific effect, the results highlight a neuroprotective function of the VGF precursor protein.

1.I.3. **VGF knockout characterization**

Despite the very exciting findings of VGF regulation on neuroplasticity, with the first publication of the VGF-deficient mouse (Hahm et al., 1999) a novel role for VGF was discovered and took the spotlight, deviating the focus of research from neural development to neuroendocrinology. Although at birth the knockout pups did not show any obvious alterations, starting at post-natal day 3 (P3), after weaning VGF mutant mice maintained body weights 50–70% of those of wild-type (**Figure 5)**. The mice typically also have a drastic reduction in peripheral fat and leptin levels and a greater elevation in basal metabolic rate, which is associated with hyperactivity. mRNAs levels of hypothalamic peptides such as Neuropeptide Y and Agouti-related peptide, which work on the central control of energy balance, were similar to a gene expression profile seen in normal mice fasted for 48 hours. Fasted mutant mice had a food intake similar to wild-type. Such neurons control food intake and energy output through communication with peripheral fat stores through hormones like leptin (Levi et al., 2004). VGF-deficient mice have also significant reproductive abnormalities, probably from a dysregulation of the hypothalamic–pituitary–gonadal axis, as VGF is expressed in the pituitary. Taken together the phenotype of the VGF knockout mouse shows that VGF is essential for energy homeostasis and metabolism. Hahm et al., 2002, further explored the VGF-deficient mouse, crossing it with knockouts for leptin (ob/ob) and Agouti-related peptide (Ay /a), which cause an obese phenotype. Interestingly, VGF knockout blocked the development of obesity in Ay /a mice, but not in ob/ob mice (only attenuated weight gain) indicating that VGF is required for the development of diet-induced obesity and obesity caused by decreased activity in the melanocortin satiety pathway.

As example of the complexity related to VGF function is the fact that VGF-deletion phenotype is the final result of a sum of consequences from the absence of the several derived peptides, which have different, and possibly even opposite biological activities. When researchers isolated the peptide TLQP-21 (Bartolomucci et al., 2006) and injected it chronically into rat brains, they found a striking contrast with the VGF-

deficient anabolic phenotype with increased resting energy expenditure, rectal temperature, and serum E without affecting body weight or food intake. Therefore delicate temporal and spatial regulation of VGF processing probably account for its fine-regulated functions, depending on different physiological signals and states.

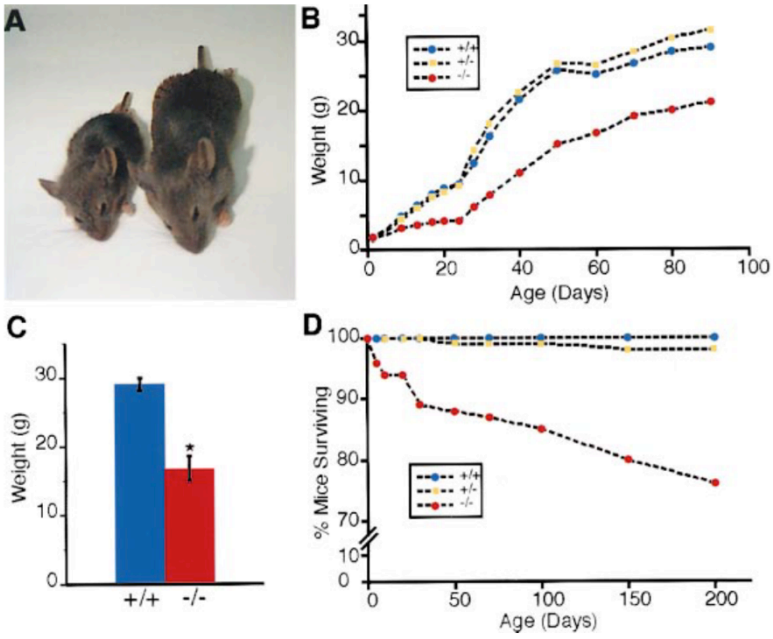

Figure 5: VGF-deficient mice phenotype

(**A**) VGF-deficient mice are smaller and leaner and (**B,C**) gain less weight compared to wild-type littermates. (**D**) mice also have decreased survival, mostly around weaning age. Extracted from Hahm et al. (*Neuron,* 1999).

1.I.4. **VGF-derived peptides regulation in physiology**

To date, VGF-derived peptides have been studied in the most variable physiological contexts such as blood pressure, reproduction, circadian cycle, gut contraction and reproduction (**Table 2)**. So far the most studied peptide (Font: http://www.ncbi.nlm.nih.gov/pubmed), with most known biological functions is the TLQP-21:

Table 2: Biological functions of the most studied VGF-derived peptides

Peptide	Biological Role	Study (as example)
TLQP-21	Cell survival	Severini et al., 2008
	Energy Balance	Bartolomucci et al., 2006
	Lipolysis	Possenti et al., 2012
	Reproduction	Pinila et al., 2010; Aguilar et al., 2013
	Digestive function	Severini et al., 2009
	Blood pressure	Fargali et al., 2014
	Pain	Rizzi et al., 2008; Chen et al., 2013; Fairbanks et al., 2014
TLQP-62	Hippocampal function	Lin et al., 2015
	Neurogenesis	Thakker-Varia et al., 2014
	Insulin secretion	Petrocchi et al., 2015
	Pain	Moss et al., 2008
NERP-1	Body fluid homeostasis	Toshinai et al. 2009
	Penile erection	Melis et al., 2012
NERP-2	Body fluid homeostasis	Toshinai et al. 2010
	Feeding	Melis et al., 2012
	Insulin secretion	Moin et al., 2012; Kim et al., 2015
AQEE-30	Penile erection	Succu et al., 2004; 2005
	Thermal hyperalgesia	Riedl et al., 2009
LQEQ-19	Penile erection	Succu et al., 2004; 2005
	Thermal hyperalgesia	Riedl et al., 2009

Besides the already cited functions, the peptide has been studied with regard to its gastrointestinal and metabolic functions (Bartolomucci et al., 2008), regulation of rat gastric motor functions involved with stomach emptying (Severini et al., 2009), protecting the gastric mucosa exposed to ethanol (Sibilia et al., 2010), inhibiting gastric acid secretion through endogenous somatostatin and prostaglandins (Sibilia et al., 2012) and stimulating exocrine pancreatic secretion of amylase (Petrella et al., 2012). In the endocrine context, in addition to the previous findings, TLQP-21 was found to increase lipolysis, decreasing adipocyte size via noradrenaline/β-adrenergic receptors pathways (Possenti et al., 2012). The peptide was able to enhance pancreatic islet β-cell survival and function by preventing the β-cells from apoptosis and increasing their proliferation, as a result there was enhanced glucose-stimulated insulin secretion, also shown in human cells, and improving glucose tolerance in vivo (Stephens et al., 2012). More evidence of its involvement with glucose homeostasis and cellular protection came with

a studied that shows TLQP-21 protecting vascular endothelial cells from high glucose injury via upregulation of glucose-6-phosphate dehydrogenase, which is known as the main source of nicotinamide adenine dinucleotide phosphate, a reducing agent, able of restoring the redox status of the endothelial cells thus inhibiting the high-glucose-induced apoptosis (Zhang et al., 2013). In a different topic TLQP-21 was shown to have a role in mammotrophic cell differentiation, also by causing a trophic effect on a GH3 cell line and increasing prolactin and VGF-itself expression (Petrocchi Passeri et al., 2013). Regarding reproduction, TLQP-21 was shown to modulate pituitary hormone secretion such as luteinizing hormone and follicle-stimulating hormone (Pinila et al., 2010; Aguilar et al., 2013); also, levels of TLQP-21 were shown to change with estrous cycle (Noli et al., 2014). An independent study has shown TLQP-21 to regulate the formation of secretory vesicles in adrenal cells and catecholamine levels therefore decreasing blood pressure (Fargali et al., 2014). Besides that, other C-terminal peptides were also shown to have biological activity in rats: two studies from the same group (Succu et al., 2004; 2005) showed that injection of AQEE-30 and LQEQ-19 in the paraventricular nucleus of the hypothalamus caused penile erection mediated by nitric. Another study using the same peptides showed that they caused thermal hyperalgesia depended on the activation of the mitogen-activated protein kinase p38 in microglia cells (Riedl et al., 2009); this study will be further explored in the context of microglia. Finally, TLQP-21 seems to be involved in pain modulation, changing the response to inflammatory pain caused by formalin in mice (Rizzi et al., 2008). Fairbanks and others, 2014, further explored the involvement of this peptide in persistent pain: they observed that the spinal effects of TLQP-21 in thermal hyperalgesia were similar to AQEE-30 and LQEQ-19 and dependent on P38 activation, suggesting a role of microglia in intermediating the effects. Moreover, the pain response was inhibited by a cyclooxygenase inhibitor, indicating that the effects of TLQP-21 are mediated by p38-dependent release of prostaglandins from microglia. The longer peptide TLQP-62, was also shown to induce long lasting mechanical and cold allodynia by intrathecal application to rats, which suggests a role for this peptide as well in neuropathic pain (Moss et al., 2008).

Following TLQP-21, there is an increased interest in studying NERP peptides. Neuroendocrine regulatory peptides or NERP were first identified from human medullary thyroid carcinoma secretion by peptidomic analysis of peptides with C-terminal amidation, which is a common posttranslation modification in peptides hormones (Yamaguchi et al., 2007). The human NERP-1 is made of 26 amino acids, and that of rat NERP-1 of 25, both human and rat NERP-2 have 38 amino acids NERP-3 (VGF 180-209) was identified later in extracts of rat brain and gut as a 30 amino acids peptide and was shown to control fluid balance as an autocrine activator of arginine vasopressin release (Fujihara et al., 2012). Antibodies against NERP inhibited vasopressin reduction in response to water loading suggesting a function in body fluid homeostasis by controlling vasopressin release from the hypothalamus (Toshinai & Nakazato, 2009). Anti-NERP-2 decreased food intake and intracerebroventricular administration of NERP-2 increased body temperature, oxygen consumption, and locomotor activity in rats. Importantly, the biological effects were dependent on the orexin pathway (Toshinai, 2010). Besides that, Melis et al., 2012, showed that NERP-2 facilitates feeding by acting in the lateral hypothalamus, adding evidence for this action to be through orexin and also that NERP-1 facilitates penile erection by acting in the arcuate nucleus with an independent mechanism of action. NERP-2 was shown to regulate glucose-stimulated insulin secretion (Moin et al., 2012) and regulate insulin secretion through the regulation of insulin secretory granules (Kim et al., 2015).

1.I.5. **TLQP-21 receptors**

In 2013, two studies reported for the first time the identification of VGF-derived peptides functional receptors in the same volume of the Journal of Biological Chemistry. The first study (Hannedouche et al., 2013) used the Chinese hamster ovarian cell line CHO-K1 and rat ovarian tumor cell line O-342/DDP to screen for a receptor for TLQP-21. Using Fluo-4 calcium assay as readout of the cell response they observed a dose-dependent response after ATP priming to the peptide in the two cell lines. The

inhibition of the signal by pertussis toxin suggested that the receptor could be a Gi/Go-coupled receptor. With the use of a third cell line CCL39 that did not evoked calcium signal for TLQP-21 they could compare the transcriptome of responding versus not responding cells by genome-wide sequencing and in the analysis they checked for upregulated G protein-coupled receptors (GPCR) in the responding cells. The identification of the complement C3a receptor-1 (C3AR1) as a target for TLQP-21 in the rodent cell lines was possible with the use of subsequence screenings with siRNAs and receptor antagonists against the candidates. The only siRNAs that reduced the TLQP-21 calcium signal significantly was those against C3AR1. In addition they used a very well-studied selective antagonist SB290157 (Ames et al., 2001) that completely blocked the response when applied with TLQP-21. They proved the receptor to be functionally responding as TLQP-21 increased migration of the mouse RAW264.7 that was blocked by the antagonist. The authors found human TLQP-21 to be 5% less potent than rodent and they do not discard the possibility of human cells having another TLQP-21 receptor as they could not translate all the findings to human cells.

The complement system is a danger sensing system component of normal plasma that evolved as part of the innate immune system to 'complement' the antibacterial activity by opsonization of bacteria by antibodies. The complement system is also independent from antibodies in early phases of infection (Janeway et al., 2001). The anaphylatoxins and its receptors are involved in pro-inflammatory responses of allergy, autoimmunity, neurodegenerative diseases, cancer and infections (Klos et al., 2009). C3AR1 is a GPCR expressed on cells of myeloid origin, including microglia, but also activated astrocytes, endothelial cells and other cell types, being involved in many biological processes, including neurogenesis and hormone release, insulin resistance, macrophage infiltration and homing of hemopoietic progenitor cells to bone marrow (Klos et al., 2013). Furthermore, C3AR1-deficient mice are resistant to diet-induced obesity mediate insulin resistance and have altered metabolism phenotypes (Mamane et al., 2009) also observed in VGF-knockout mice (Cero et al., 2014). Intracellular signal transduction of C3AR1 response is carried through pertussis-toxin-sensitive Gαi - proteins and mobilizes calcium fluxes from the extracellular medium in neutrophilins (Norgauer et al., 1993). Our group (Möller et al., 1997) has also shown that in primary

microglia cultures C3a signal transduction involves PTX-sensitive G-protein, but removal of calcium from the extracellular solution did not eliminate the response, only the plateau phase and also limited the response to the initial peak, suggesting that the first response is dependent of internal stores, but subsequent activation of the receptor requires extracellular calcium.

In a more recent and detailed publication (Cero et al., 2014) the authors describe the exact mechanism of binding of the TLQP-21 peptide to the C3AR1 receptor. First they confirm the specificity to the receptor using photoaffinity labeling experiments, and when using also the antagonist SB290157 there was a reduction in the crosslinking with membranes of 3T3L1 and CHO cells. They calculated the half-maximal effective concentration (EC_{50}) for mouse and human TLQP-21 in HTLA cells transfected with the human C3AR1 receptor and found them to be 5 and 22 times lower than that of C3a, respectively. Using nuclear magnetic resonance the authors showed that in aqueous solutions the peptide helix is essentially unstructured in random coil conformations. Interestingly, incubating the peptide with cells that express C3AR1 TLQP-21 underwent a disorder-to-order transition (**Figure 6)**, shifting from random coil to a-helical conformation upon binding, which did not occurred in C3AR1 knock-out cells or to much lower extend when in the presence of the antagonist. In this system the authors did not predict a second binding site of TLQP-21 in 3T3L1 and CHO cells and that TLQP-21 has not structure or function similarity with other complement ligands such as C1q.

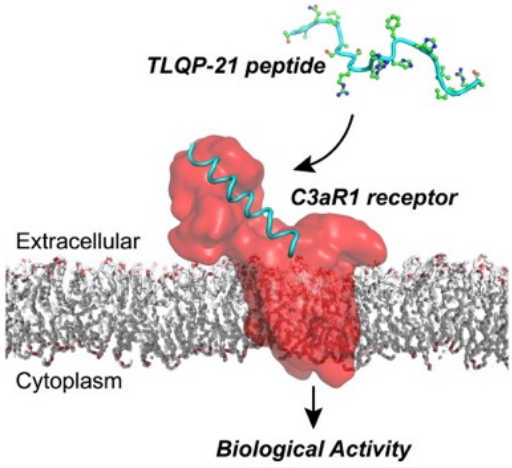

Figure 6: TLQP-21 mechanism of binding to C3AR1.

TLQP-21 undergoes a disorder-to-order transition, shifting from from random coil to a-helical conformation upon binding to the receptor. Graphic abstract from Cero et al. (*Structure,* 2014).

The second article, in the subject of analgesics research for neuropathic pain, came out only a few months after Hannedouche's publication as VGF was among the genes regulated in the associated nerve inflammation (Chen et al., 2013). Using the same readout, calcium imaging, the authors found response from TLQP-21, but not TLQP-62 or LQEQ-19 in primary marrow-derived primary macrophages and microglia cells, without ATP priming (as the first study needed for ovarian cells) in concentrations as low as 10 nM. The transient increase in intracellular calcium signal was independent from extracellular calcium; therefore it is released from intracellular calcium stores such as endoplasmic reticulum or mitochondria. Interestingly, further applications of TLQP-21 only, showed no response, indicating desensitization of the receptor. Using chemical cross-linking conjugation to a modified peptide (biotin attached via the amide bond at the N terminus and an extra cysteine residue at the C terminus) combined with mass spectrometry for analysis of the eluted potential receptor-TLQP-21-complex the authors identified the globular head of the complement component C1q receptor, gC1qR. Both macrophages and microglia were shown to express the receptor and upon silencing with siRNAs against gC1qR or blocking with two different monoclonal antibodies the calcium response to TLQP-21 was substantively reduced. Finally, treatment of rats with partial sciatic nerve ligation using a gC1qR-neutralizing antibody resulted in a delayed onset of nerve injury-associated mechanical hypersensitivity, corroborating for a functional complex of TLQP-21 and gC1qR. The results suggest that in some cells there could be a collaboration or interaction between gC1qR and C3AR1 in TLQP-21 response. gC1qR is the first subcomponent of the classical pathway for complement activation and it has been shown to bind to many different ligands necessary for immune surveillance. The receptor is ubiquitously expressed and also is present in different compartments of the cell. It also plays a role in different pathologies other than infection, such as carcinogenesis (Peerschke et al., 2006).

1.I.6. **VGF in disease**

VGF dysregulation has been so far associated with many pathologies. For its functions in metabolism, lipolysis and insulin regulation, VGF loss has been reported in obese patients and diabetes type II (D'Amato et al., 2015), but more interestingly VGF dysregulation has been reported in neurological and psychiatric diseases. For example, there are solid evidences for increased levels of VGF fragments in schizophrenia and also the N-terminal VGF23–62 fragment was increased in the cerebrospinal fluid of major depression patients (Huang et al., 2006). In contrast, another study reported that C-terminal peptides possess antidepressant activities (Jiang & Salton, 2013), highlighting the different regulation of individual VGF peptides. In addition, several studies reported a VGF reduction in amyotrophic lateral sclerosis, proposing it as a possible biomarker and also in frontotemporal dementia and Alzheimer's disease (Bartolomucci et al., 2011). The identification of VGF as a biomarker for several neurological diseases put it in the spotlight of basic and clinical research, for it is most likely to play a role in the course of such pathologies. Understanding VGF regulation and activity in such contexts is of great relevance and will therefore help unrevealing VGF different functions also in physiology.

1.I.7. **VGF and neoplasia**

VGF has been identified in different screenings as a prominent biomarker for several neoplasias (Bartolomucci et al., 2011), most of them are unsurprisingly secretory endocrine and neuroendocrine tumors. The first study to detect VGF in tumor cells was published already in 1992 (Rossi et al., 1992) reporting pro-VGF expression in murine and human neuroblastoma lines. Later different VGF-derived peptides were also reported in mouse neuroblastoma secretome by another study (Rozek et al., 2013). Importantly, VGF expression was upregulated in neoplasias derived from tissues that

normally express very low levels of the protein, such as stomach and lungs, suggesting that VGF precursor and products are important for and associated with proliferative endocrine and tumor cells. It is also possible that VGF expression is associated with energy balance abnormalities presented by some of the tumor patients with paraneoplastic syndrome (Rindi et al, 2007). Some of these tumors include breast cancer (Annaratone et al., 2014), lung cancer (Matsumoto et al., 2010), insulinoma, gastrointestinal cancers, parathyroid adenoma, medullary thyroid, parathyroid adenoma, pheochromocytoma and pituitary cancer (Rindi et al, 2007).

For its fine regulation and multiple functions, VGF is likely to play a different role in each cancer, especially when accounting for tumor heterogeneity. In non-neuroendocrine tumors, VGF was already shown to display a very different regulation as two publications of the same group recently demonstrated with the epigenetic study of VGF promoter in ovarian cancer (Brait et al., 2013) and urothelial cell carcinoma (Hayashi et al., 2014). The first study shows promoter hypermethylation, and therefore silencing of VGF in 43% of the cases analyzed (158 of 366), in contrast to the absence of hypermethylation in control, this was correlated with overall survival and prognostic factor for ovarian cancer and when VGF was overexpressed in corresponding cancer cell lines the cell growth was inhibited. The second study shows similar regulation being completely methylated in different urothelial cell carcinoma cell lines, VGF was re-expressed with an inhibitor of DNA methylation and forced ectopic expression in bladder cancer cell lines inhibited cell growth as seen in the colony formation assay.

VGF's many functions are therefore now emerging as promising targets for cancer therapy and its regulation as biomarkers for several diseases including different types of cancers. Many other tumors types, like those in the CNS are still not studied for VGF expression or its regulation and the available literature at the present time is not yet robust enough to uncover VGF possible roles in these severe pathologies. With the emergency of novel screenings and more information on VGF-derived peptide receptors and the corresponding signaling and targets it is expected that the causal link between VGF and disease becomes more evident.

II. Gliomas and glioblastomas

Gliomas are the most common primary tumors of the CNS and comprise a group of several histologically and molecularly diverse tumors originally derived from glial progenitors that undergo malignant transformation. Classification of gliomas is variable and with the advent of new molecular technologies it is possible to combine classical histological classification with new molecular subtypes to define a glioma type and subtype. According to Perry and Wesseling, 2016, the glial tumors can be histologically stratified in specific types illustrated in **Figure 7**. Many factors help the neuropathologist make the initial histological classification of the tumors starting with the clinical information, radiologic findings from magnetic resonance imaging (MRI) including macroscopic evaluation. Such details must be combined with molecular and genetic analysis, which can correlate better with glioma biology than the histologic diagnosis, to be inserted within the world health organization (WHO) for final classification of the gliomas. Most of the gliomas in adults are classified as diffuse,

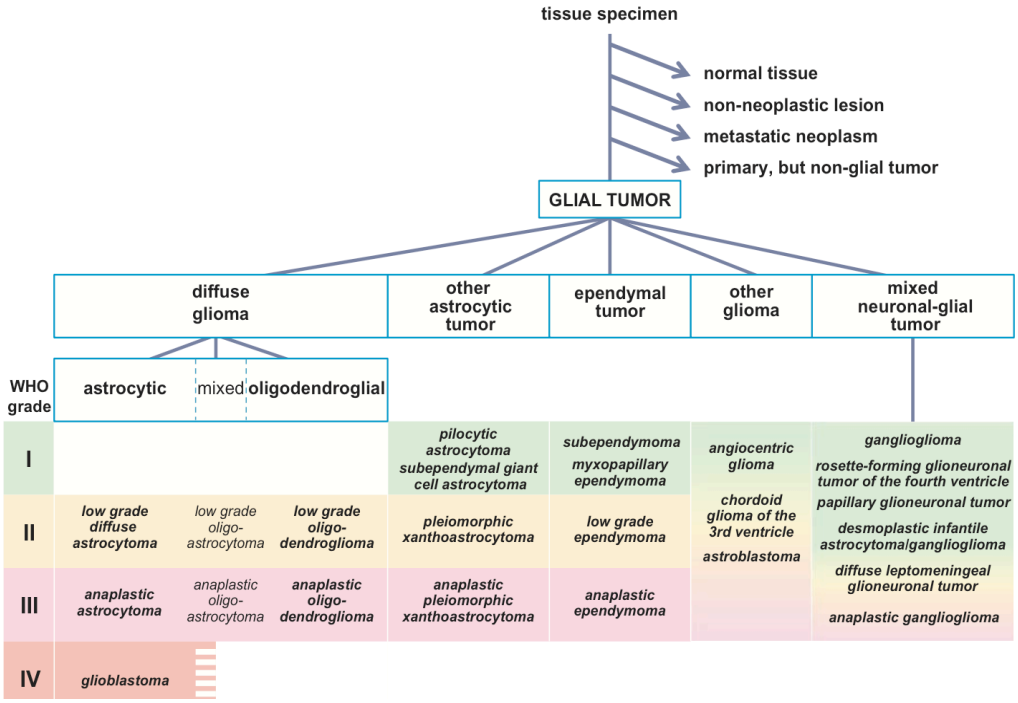

Figure 7: Decision tree for histologic diagnosis of glial and neuronal-glial central nervous system neoplasms

Figure extracted from Perry & Wesseling (*Handbook of Clinical Neurology*, 2016)

which present infiltration within the CNS parenchyma and aggregation of around neurons and blood vessels (Perry & Wesseling, 2016). Such tumors can be further classified according the resemblance of the tumor cells to nonneoplastic glial cells, namely astrocytic, oligodendroglial, or mixed oligodendroglial-astrocytic. They can then be graded as WHO grade II (low-grade), III (anaplastic), or IV (glioblastoma), following the natural progression of the tumors, which depends on the morphologic features, such as mitotic activity, microvascular content, and necrosis.

Among gliomas, the glioblastoma multiforme (GBM) is the most common and aggressive type, and patients frequently relapse or become refractory to conventional therapies (**Figure 8**). Glioblastomas are derived from the malignant transformation of neural and glial precursors, such as the oligodendrocyte precursors cells (OPC) or neural stem cells residing in the cortex and subventricular zone, where post-natal neurogenesis is thought to occur (Hambardzumyan et al., 2011; Liu et al., 2011; Siebzehnrubl et al., 2011). Accordingly, quiescent OPC were recently shown to be permissive of dynamic multistep malignant transformation in the adult upon deletion of p53 and NF1 generating GBM with proneural-like signature in mice (Galvão et al., 2014).

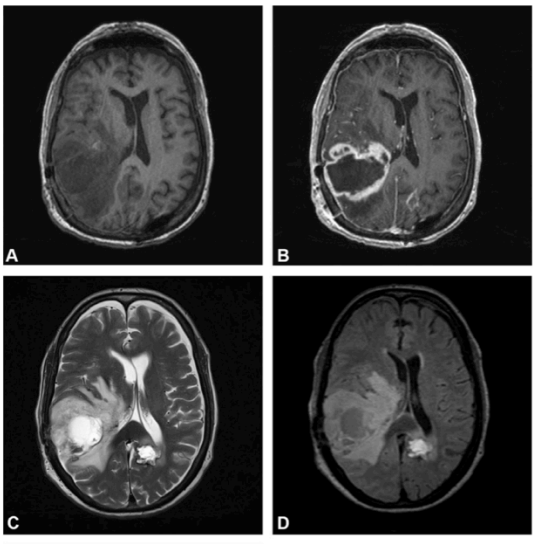

Figure 8: Neuroimaging of glioblastoma.

Magnetic resonance imaging (MRI), T1-weighted (**A**), gadolinium-enhanced (**B**), T2-weighted (**C**), fluid-attenuated inversion recovery (FLAIR, **D**). Reproduced from Wirsching et al., (*Handbook of Clinical Neurology*, 2016).

In numbers GBM represent 45.6% of the primary malignant brain tumors with an annual incidence of 3.1 per 100 000 (in the USA) of which only 5% of all patients will survive after 5 years of the diagnosis (Ostrom et al., 2014). Causes and risks factor for GBM are not well defined, besides ionizing irradiation of the brain, which can be a risk factor. GBM are more frequent in older, male and white patients, but there is no association with smoking, mobile phone use or other carcinogenic agents reported (Wirsching et al., 2016).

1.II.1. **Molecular classification**

According to the International Society of Neuropathology brain tumor diagnosis is based on four layers of classifications:

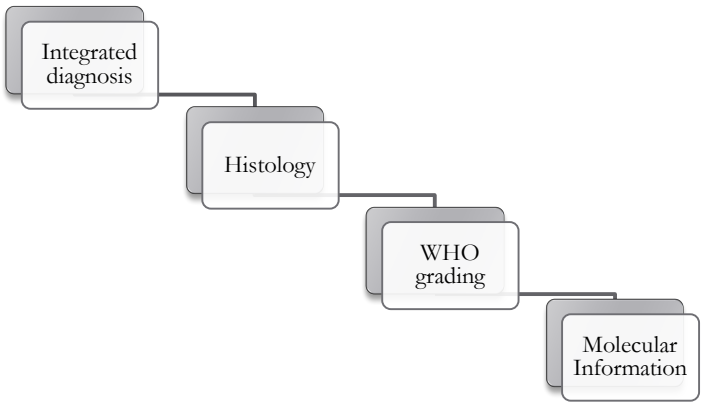

Figure 9: Different layers of information for brain tumor classification

Such system is important for the tumor species not only to be defined for accurate clinicopathologic predictions and therapeutic planning (Louis et al., 2014), but also helps the understanding of the pathogenesis of gliomas. Since recently, genetic alterations comprise an important factor in glioblastomas characterization. The molecular markers identified by isocitrate dehydrogenase 1 or 2 (IDH1 or IDH2) gene

mutations or wild-type comprise the main divisor for glioblastoma molecular subtypes with distinct biology and clinical behavior (Masui et al., 2016). IDH are part of the TCA cycle in glucose metabolism and when mutated can cause abnormalities on the epigenetic regulation and gene expression through the over-production of the product 2-hydroxyglutarate, which will finally result in tumorigenesis (Liu & Ling, 2015).

IDH wild-type glioblastomas are the major group with more than 90% of all glioblastomas in patients with median age of 62 years (against 44 years in IDH-mutants) and a median overall survival after standard surgery, radiotherapy and chemotherapy of only 15 months (against 31 months in IDH-mutants) and extensive necrotic areas (Louis et al., 2016). Such IDH wild-type usually do not present progression from lower-grades lesions, but patients develop the tumor de novo. The molecular hallmarks distinguishing glioblastoma IDH mutant from wild-type are listed in **Table 3.**

Table 3: Molecular aberrations in Glioblastomas.

Adapted from Masui et al., 2016.

Alteration	Glioblastoma, IDH mutant	Glioblastoma, IDH wild-type
Epigenetic	G-CIMP	MGMT promoter methylation
Genetic	IDH1 or IDH2, TP53, ATRX mutations; CDKN2A/p14ARF deletion	TERT, PTEN, TP53, PIK3CA, PIK3R1, NF1, H3F3A mutations; EGFR, PDGRA, MET, CDK4, CDK6, MDM2,MDM4 amplifications; EGFRvIII deletion
Chromosomal	trisomy 7 or 7q gain, LOH 17p, 10q deletion	trisomy 7 or 7q gain, monosomy 10, double minute chromosomes

1.II.2. **Molecular subtypes of glioblastoma**

Glioblastomas can also be classified according to their gene expression profiles based on large-scale molecular analyses such as those provided by The Cancer Genome Atlas Network. Based on gene expression, DNA copy number and somatic mutations profiles GBM can be further stratified into Proneural, Neural, Classical, and Mesenchymal biological subtypes (Verhaak et al., 2010) which responded differently to therapy and have specific prognosis. Such subtypes also resemble the gene signature of different neural lineages. Find b elow a list of characteristics for each of the subtypes:

Proneural - alterations in PDGFRA expression, TP53 mutations, and point mutations at IDH1. High expression levels of genes associated with oligodendrocytic developmental genes (PDGFRA, OLIG2, and NKX2-2). Better prognosis and increased survival, but no survival benefit from aggressive therapy.

Mesenchymal - deletions and low expression of NF1 and PTEN. Express astrocytic and higher expression of mesenchymal markers (CD44 and MERTK). High expression of genes in the tumor necrosis factor super family pathway and NF-kB pathway, such as TRADD, RELB, and TNFRSF. Inflammatory infiltration and necrosis. Poor response to radiotherapy and shorter survival (Bhat et al., 2013).

Classical - Chromosome 7 amplification paired with chromosome 10. High-level EGFR amplification. High expression of astrocytic markers. Neural precursor and stem cell marker NES, as well as Notch (NOTCH3, JAG1, and LFNG) and Sonic hedgehog (SMO, GAS1, and GLI2) signaling pathways are highly expressed.

Neural - expression of neuron markers, such as NEFL, GABRA1, SYT1, and SLC12A5.

The clustering of glioblastomas by gene expression may be useful for classifying tumor specimens but the limits of these classes are not well defined and stable (Masui et al., 2016) as there may be intratumoral heterogeneity of expression at the single-cell level (Patel et al., 2014).

1.II.3. **Tumor models**

Initially, gliomas were obtained from mutating mice with DNA alkylating agents treatment, but such models offer undefined genetic background, generating big variations for every tumor. Nowadays, several tools are available for studying a specific type of glioblastoma. Cell cultures are a good initial option for drug development, but any further assessment regarding, tumor-host and tumor microenvironment must be done in vivo. Xenograft models (orthotopical injection of tumor cells in immunodeficient mice) are frequently used for in vivo cancer studies for allowing easy visualization, but they lack stepwise genetic changes involved in tumorigenesis and rarely recapitulate etiology, pathobiology, and biochemistry of human tumors (Fomchenko & Holland, 2006). The use of genetically-engineered mice (GEM) for the generation of spontaneous tumors circumvent many of these limitations, despite their complications regarding poor reproducibility, low tumor penetrance and prolonged tumor formation latency. Ideally mouse models should possess the following characteristics: cellular heterogeneity similar to the human glioma, orthotropic, must show invasive and angiogenic-like growth with no encapsulation, be highly reproducible with predictable growth, and must mimick the therapeutic response of the human glioma (Stylli et al., 2015). Gain or loss-of-functions models can be achieved by creating conditional knockout mice containing floxed alleles excised upon Cre/Flp-mediated recombination (Stylli et al., 2015).

Somatic cells can be genetically modified by viral vectors, usually single-stranded RNA murine or avian viruses (Fomchenko & Holland, 2006). The RCAS/tv-a system can be used to initiate tumors in mice with known glioma oncogenic drivers

with the use of the avian replication-deficient ALV-splice acceptor retroviral vector carrying an oncogene, such as PDGF and Kras, and mice genetically engineered to express tv-a receptor that binds RCAS into targeted engineered brain cells. The retroviruses can be delivered to cultured cells and secondarily transferred into mice or used for direct in vivo infections. These transgenic tv-a mice can then be crossed onto specific genetic backgrounds to model the effects of genetic aberrations such as tumor suppressor loss on glioma formation and response to therapy (Fomchenko & Holland, 2006; Hambardzumyan et al., 2009). The current most used models for GBM research are listed in **Table 4.**

Table 4: Mouse models for GBM

Adapted from Stylli et al., 2015.

Model	Strategy
C6	Xenograft
GL261	Xenograft
U251MG	Xenograft
U87MG	Xenograft
V12Ha-ras	Transgenic/GFAP promoter
GFAP-Cre	Flox NF1, + p53 knockout
GFAP-T121 tg	PTEN knockout
NESTIN-CreER	Flox NF1, Flox PTEN, Flox p53
PTEN-/- and K-ras	RCAS/tv-a; cre-lox system – deletion of PTEN/nestin
p53-/-and Nf1-/-	GFAP-driven cre-lox system - deletion of Nf1
PDGFB and Ink4a-Arf-/-	RCAS/tv-a; cre-lox system – deletion of PTEN
PDGFB and p53-/-	Transgenic mice/GFAP

1.II.4. **Glioblastoma treatment**

In most of the cases, when possible after detection of the tumor by MRI and characterization of the biopsy the first step is the removal of the main tumor bulk by surgical resection. After that, the treatment with concomitant chemotherapy with temozolomide and radiotherapy is common, although the addition of temozolomide only prolongs overall survival from 12.1 months to 14.6 months (Stupp et al., 2005). Moreover, temozolomide is only recommended for patients (especially elderly ones), with methylation of the promoter of the O6-methylguanine-DNA methyltransferase, which functions as a DNA repair enzyme that can counteract the efficacy of chemotherapy with temozolomide (Masui et al., 2016). On the contrary, therapy with Lomustine and/or the antiangiogenic bevacizumab (antibody against vascular endothelial growth factor, VEGF) is recommended, although current evidence only shows benefit in overall survival associated to the proneural subtypes GBM (Wirsching et al., 2016). Failure of treatment and relapse are common in GBM therapy. Many factors contribute to that. First, GBMs are usually detected upon the incidence of neurological symptoms, rendering it a disease that is unfortunately diagnosed already at an advanced stage, which makes it more difficult to treat. Second, GBM are highly invasive and the spreading to the brain parenchyma may prevent appropriated surgical resection. Third: genetic and cellular heterogeneity of GBM my cause molecular adaptation due to selection of resistant cell population, like glioma-initiating cells (Patel et al., 2014; Wirsching et al., 2016). In this context, advance in therapy depends on identifying agents that affect molecular targets that are relevant to specific subgroups of patients (Thomas et al., 2014).

1.II.5. **The glioma microenvironment**

As one of the first steps of tumorigenesis, tumor cells establish themselves in niches proper for their proliferation (Sassi et al., 2012) where they can construct a microenvironment of their own recruiting and interacting with a set of cell types known to contribute in several ways to the biology of brain tumors (and other tumor types) through a very complex regulatory signaling mechanism (Hanahan & Weinberg, 2011). The tumor network consists of different parenchyma and immune cell types besides the cancer cells and cancer stem cells themselves. The extracellular matrix proteins and soluble signaling factors and cytokines also take part in the constant crosstalk between cancer and the niche and the balance of these feedbacks determines tumor fate.

The main non-tumor cell population found in the glioblastoma bulk are the tumor-associated macrophages (TAM), which are composed of a mix of microglia, the brain resident macrophages, and infiltrating monocytes and macrophages derived from blood monocytes (Charles et al., 2011), that can easily cross the disrupted blood-brain barrier from glioma-associated vasculature (Watkins et al., 2014). Under physiological conditions, microglia are the dominant and most abundant macrophages residing inside the CNS. They are very active cells, that constantly survey the surrounding for maintenance of homeostasis In case of abnormalities and damage they can change their state into a more vigilant phenotype, which upon damage can become reactive (Hanisch and Kettenmann, 2007). In pathological conditions monocytes from bone marrow migrate into the CNS and contribute to a proportion of mononuclear phagocytes together with the resident microglia cells.

It seems that the infiltration of TAM increases with tumor grade, reaching up to 30 % of the malignant tumors mass, meaning that they have a role in tumor progression and malignancy (Badie et al., 2000; Hussain et al., 2006). Other tumor-associated cell populations include oligodendrocyte precursors, involved with neo-vascularization of gliomas (Huang et al., 2014); neural precursor cells, which are attracted to the tumor from different neurogenic brain areas and promote several anti-tumorigenic effects (Glass et al., 2005; Stock et al., 2012; Goffart et al., 2014).

Moreover, endothelial cells adhere with glioma stem cells in the perivascular niche and increase their secretion of growth-promoting factors that increase glioma cells stemness (upregulation of self-renewal markers, such as related transcription markers) via Nitric oxide, TGF-beta and Notch pathways (Sharma & Shiras, 2015). Tumor-infiltrating lymphocytes are also part of the tumor microenvironment, comprising a mixed population of both CD8 cytotoxic T lymphocytes, which are crucial components of the tumor-specific adaptive immunity that attacks tumor cells and (Charles et al., 2011) CD4 T cells, including CD4 regulatory T cells, which suppress anti-tumor immunity and promote tumor. Therefore the balance of both population sizes and activities might dictate tumor progression. In this line of investigation a study found that in GBM there are higher CD4 lymphocyte infiltration levels (compared with lower grade gliomas) in combination with low CD8 levels, which together are associated with unfavorable prognosis in human patients (Han et al., 2014).

Tumor-associated astrocytes (TAA) are also very important for the GBM microenvironment. Although astroglia cells were traditionally thought to be mainly associated with brain structure and support, astrocytes play an important role in the maintenance of CNS homeostasis: by glutamate uptake at synapses, modulation and control of synaptic activity, blood brain barrier composition and different roles in neuropathologies, such as glial scar formation (Kimelberg & Nedergaard, 2010; Oberheim et al., 2012). Astrocytes upregulate the glial fibrillar acidic protein (GFAP) and display cellular hypertrophy in the presence of injury: the so called reactive astrogliosis (Lorger, 2012). Reactive astrocytes have a remarkable heterogeneity both in function and molecular phenotype (for example not all astrocytes express GFAP) (Lorger, 2012). In the glioma microenvironment astrocytes may contribute to tumor invasion and migration as one study showed that astrocytes produce pro-matrix metalloproteinase 2 (pro-MMP2), which is cleaved by plasmin into active MMP2, when glioma cells produce plasminogen, later converted to plasmin. This was associated with glioma invasion (Le et al., 2003). Other studies also showed that astrocytes may contribute to tumor progression through secretion of substances that promote cancer cell proliferation (like growth factors, interleukins and transforming growth factor beta), suppression of adaptive immune responses through the repression of microglial

activation and induction of T-cell apoptosis (Lorger, 2012). TAA were already associated with increasing grade in PDGF-induced gliomas (Becher et al., 2008). In addition, also in proneural GBM TAAs present a unique gene signature that is associated with overall patient survival (Katz et al., 2012).

1.II.6. **Tumor-associated macrophages**

Tumor associated macrophages (TAM) are recruited to the tumor by their attraction to multiple soluble factors released by glioma cells. Some of these factors include ATP, chemokines, complement receptor ligands, like C5a and neurotransmitters, such as glutamate (Hambardzumyan et al., 2015). These factors are crucial for the glioma microenvironment because they dictate the amount of TAM infiltrating the tumor, which can ultimately affect the tumor growth and survival of the host: when monocyte chemoattractant protein-1 was transfected into rat gliomas, there was a massive increase of microglia cells in the tumor, promoting tumor growth in vivo only (meaning that the effect is depend on the microenvironment, specifically microglia) and reducing the rat survival (Platten et al., 2003).

Once recruited, microglia and infiltrating monocytes become activated, acquiring an amoeboid and phagocytic morphology, and converging to a phenotype unique for the glioma microenvironment, which is very similar for the two cell populations, making them difficult to distinguish (Hambardzumyan et al., 2015). The idea of microglia activation towards a phagocytic phenotype is a very old one, and there is a report for their large presence inside glioma, where they promote phagocytosis of the products of cerebral destruction (making room for the tumor to grow), from as early as 1925 (Penfield, 1925; **Figure 10**).

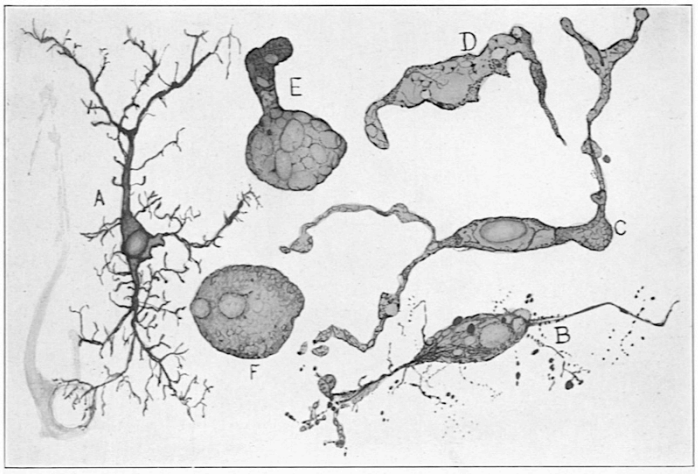

Figure 10: Microglia activation in gliomas

Resident microglia change their shape from ramified (A) to amoeboid (B-F) when associated to brain tumors. Original from Penfield (*The American journal of pathology*, 1925)

TAM have a phenotype that is very different from classical macrophage polarization derived from in vitro characterizations. Typically, when studying macrophage activation, different states, or polarized subpopulations are identified that have specific response to a stimulus, in terms of receptor expression, cytokine and chemokine production. This plasticity in response allow the macrophages and microglia to have multiple roles in physiology and pathology, as presenting antigens, modulating inflammation and performing phagocytosis (Kennedy et al., 2013; **Figure 11**). Classic M1 state results from toll-like receptor 4 activation (with lipopolysaccharides, LPS) or interferon gamma, IFN-γ receptors leading to activation of transcription factors NF-κB and STAT1 and increased expression of CD86 and major histocompatibility complex (MHC)-II followed by release of pro-inflammatory cytokines, such as interleukines IL-1α, IL-1β, TNF-α, IL-6, IL-12, IL-23 and the chemokines CCL2 and CCL20. Also part of the antibacterial defense mechanism, there is an inducible nitric oxide synthase-mediated nitric oxide production, which generates reactive oxygen and nitrogen species (Kennedy et al., 2013; Orihuela et al., 2014).

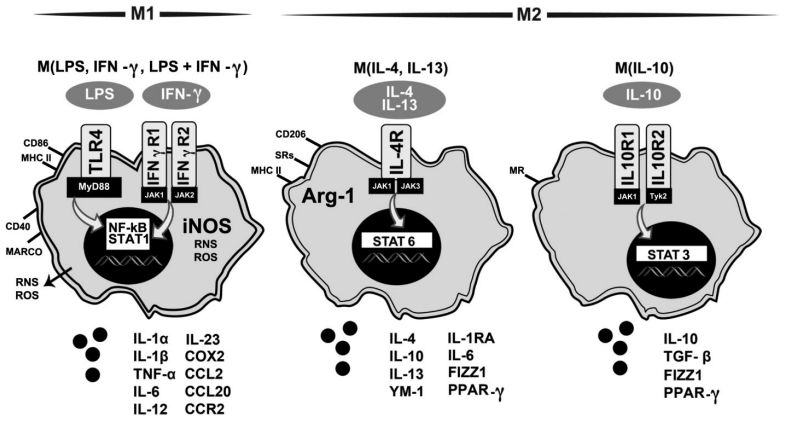

Figure 11: Macrophage polarization states

M1 and M2 phenotypes are an outcome from the stimulation of macrophages with different factors, which lead to the production of inflammatory cytokines and chemokines, through NF-kB and STAT1 (M1) or anti-inflammatory through STAT6 or STAT3 activation (M2).Both states have unique receptor expression signature. Image from Orihuela et al. (*British Journal of Pharmacology*, 2014).

An opposite activation-state, so called M2, was shown to be achieved by stimulation with several factors, like IL-4, IL-10 and IL-13. Binding to the interleukin receptors 4 or 10 causes activation of STAT6 and increase in Arg-1, CD206 and mannose receptors expression, shifting the cells towards an anti-inflammatory phenotype with a release of anti-inflammatory factors: IL-4, IL-6, IL-10, IL-13, IL-1RA, TGF-β, FIZZ1, and PPARγ (Orihuela et al., 2014). This suggests an activation state proper for tissue repair, promoting remodeling of the extracellular matrix (ECM) and angiogenesis. Other alternative states include M2a, associated with allergy; M2b, involved in immunoregulation and M2c, which affects immunoregulation, matrix deposition and tissue remodeling (Hambardzumyan et al., 2015).

Interestingly, studies with TAM in vivo, showed that these cells can express markers from both polar states (producing anti and pro-inflammatory molecules) and also they produce other molecules involved with tissue remodeling and angiogenesis such as VEGF, MMP-2,9 and 14 (Hambardzumyan et al., 2015). In fact, when analyzed by RNA microarray sorted TAM show a mixture of M1 and M2a, b, c-specific genes, furthermore 59% of the genes differently expressed from control do not belong to classic and alternative M1 and M2 phenotypes (Szulzewsky et al., 2015). Accordingly,

there are studies showing that genes from both phenotypes can affect tumor growth and host survival in similar ways, meaning that is more relevant studying individual targets associated in TAM rather than in M1/2-polarization phenotypes (Hambardzumyan et al., 2015).

In this regard, TAM and tumor cells interact with each other through a very complex crosstalk that is still not fully understood. Nonetheless, there is solid evidence that tumor cells can recruit and reprogram microglia, so that they collaborate to tumor growth and invasion.. Several factors released from TAM have been reported to promote glioma proliferation and migration: upon colony stimulating factor 1 stimulation derived from tumor cells microglia release epidermal growth factor (EGF), which stimulates glioblastoma cell invasion and migration (Coniglio et al., 2012). In addition, transforming growth factor-β derived from microglia increases glioma cell migration, and production of MMP-2. Via TLR2 activation with tumor derived versican, TAM also produce MMP14 which activates pro-MMP2 in the extracellular space. MMP14 expression positively correlates with the glioma malignancy grade (Markovic et al., 2009; Vinnakota et al., 2013; Hu et al., 2014).

2. Aim of the thesis

VGF is a neuropeptide precursor that regulates several aspects of brain function and many other endocrine processes involved in metabolism. Accordingly, the dysregulation of the different VGF-derived peptides has been associated with many metabolic and neurological disorders. In this regard VGF has been also proposed as a biomarker for secretory cancers, but the literature in this topic is still scarce. Glioblastomas are very malignant brain tumors that have different molecular subtypes, which present different clinical behavior. Factors involved in the communication of the tumor cells with their associated microenvironment can become targets for tumor therapy as they are essential for dictating the course of the pathology. So far, VGF expression in glioblastomas has not been reported and little is known about VGF function in cancer. Therefore the aim of this work is to elucidate the mechanisms involved in VGF expression in glioblastoma multiforme and characterize its effects on microglia cells, which are the main non-tumor cell population in the tumor niche.

Specific aims include:

1. Do GBM subtypes present differential VGF expression?
2. Does VGF expression affect GBM-related survival?
3. Which cells express VGF in the tumor microenvironment?
4. How is VGF expression regulated?
5. Do VGF derived peptides affect tumor growth?
6. How do microglia cells respond to VGF-derived peptides?
7. Does VGF stimulation affect microglia innate biological functions?

3. Materials and Methods

I. Materials

For the development of this work and obtaining of the results the following materials were used (other materials are stated at the following Methods section):

Table 5: Cell culture reagents

Product	Supplier
Accutase	Life Technologies GmbH, Darmstadt, Germany
B27 minus vitamin A	Life Technologies GmbH, Darmstadt, Germany
Clodronate, Disodium Salt	Merck KGaA, Darmstadt, Germany.
Dulbecco's phosphate-buffered saline (DPBS)	Life Technologies GmbH, Darmstadt, Germany
Dulbecco's Modified Eagle Medium (DMEM)	Life Technologies GmbH, Darmstadt, Germany
DMEM/F-12, GlutaMAX™ supplement	Life Technologies GmbH, Darmstadt, Germany
Dimethyl sulfoxide	Sigma-Aldrich, Munich, Germany
Fetal calf serum (FCS)	Life Technologies GmbH, Darmstadt, Germany
Geltrex™ LDEV-Free Reduced Growth Factor Basement Membrane Matrix	Life Technologies GmbH, Darmstadt, Germany
Glucose	Braun Melsungen, Germany
Heat-inactivated horse serum	Life Technologies GmbH, Darmstadt, Germany

Hank's balanced salt solution (HBSS)	Life Technologies GmbH, Darmstadt, Germany
Insulin	Life Technologies GmbH, Darmstadt, Germany
L-Glutamine	Life Technologies GmbH, Darmstadt, Germany
Penicillin/Streptomycin	Life Technologies GmbH, Darmstadt, Germany
RPMI 1640	Life Technologies GmbH, Darmstadt, Germany
Recombinant human epidermal growth factor	Cell Systems, Washington, USA
Recombinant human fibroblast growth factor	Cell Systems, Washington, USA
Trypsin-EDTA	Life Technologies GmbH, Darmstadt, Germany
Vitamin C	Sigma-Aldrich, Munich, Germany

Table 6: Drugs and chemicals

Product	Supplier
4′,6-Diamidin-2-phenylindol (DAPI)	Sigma-Aldrich, Munich, Germany
Adenosine-5'-Triphosphate (ATP)	Sigma Aldrich, St. Louis, USA
Agarose	Lonza, Cologne, Germany
Agarose - Low-melting point	Promega Corporation, Madison, USA
Alamar blue	Invitrogen, Darmstadt, Germany
Aqua Poly mount	Polysciences Europe GmbH, Eppelheim, Germany
Bovine serum albumine (BSA)	Carl Roth GmbH, Karlsruhe, Germany
β-mercaptoethanol	Merck, Darmstadt, Germany
Citric acid	Vector Laboratories, Burlingame, USA
Ethidium bromide	Carl Roth GmbH, Karlsruhe, Germany

Fluo 4 AM	Life technologies, USA
Fluoresbrite® BB Carboxylate Microspheres 4.50µm	Polysciences Europe GmbH; Hirschberg an der Bergstrasse, Germany
FuGENE 6 Transfection Reagent	Promega GmbH, Mannheim, Germany
Histo-Clear	Thermo Fisher Scientific, Inc., Waltham, USA
Ketamin 10%	WDT, Garbsen, Germany
Lipofectamine-RNAiMAX Transfection Reagent	Invitrogen, Darmstadt, Germany
Lipopolysaccharide (LPS)	Alexis Biochemicals (Lausen, Switzerland)
Low melting point agarose	Promega, Wisconsin, USA
Normal donkey serum (NDS)	Sigma-Aldrich, Munich, Germany
Opti-MEM I Reduced Serum Media	
Pierce ECL Western Blotting Substrate	Thermo Fisher Scientific, Rockford, USA
Ponceau S solution	Sigma-Aldrich, Munich, Germany
Paraformaldehyde	Merck, Darmstadt, Germany
Protease inhibitor cocktail	Roche, Berlin, Germany
Propidium iodide	Invitrogen, Darmstadt, Germany
RIPA buffer	Sigma-Aldrich, Munich, Germany
Puromycin	Sigma-Aldrich, Munich, Germany
Rompun	Bayer HealthCare AG, Lerverküsen, Germany
Scrambled non-targeted siRNA	Dharmacon, Chicago, USA
siRNA VGF (on target plus SMARTpool)	Dharmacon, Chicago, USA
Sodium dodecylsulfate polyacrylamide (SDS)	Sigma-Aldrich, Munich, Germany
Sucrose	Merck, Damstadt, Germany
SuperScript II reverse transcriptase	Invitrogen, Darmstadt, Germany
SYBR green Select Mastermix	Life technologies, USA
Tissue Tek Compound (OCT)	Weckert Labortechnik, Kitzingen, Germany
Tris-base	Carl Roth GmbH, Karlsruhe, Germany

Tris-HCl	Carl Roth GmbH, Karlsruhe, Germany
Triton X-100	Carl Roth GmbH, Karlsruhe, Germany
Trypan blue	Sigma-Aldrich, Munich, Germany
Tween 20	Merck, Hohenbrunn, Germany

Table 7: Commercial kits

Product Name	Supplier
Cell proliferation Enzyme linked immunosorbent assay (ELISA) - BrdU	Roche, Berlin, Germany
BCA Protein Assay Kit	Thermo Fisher Scientific, Rockford, United States of America
ELISA ProcartaPlex Mouse Basic Kit HS	Bender MedSystems GmbH, Vienna, Austria
ELISA Mouse IL-1β/IL-1F2 Duo Set	Bio-Techne GmbH Wiesbaden-Nordenstadt Germany
ELISA Mouse IL-6	Bio-Techne GmbH Wiesbaden-Nordenstadt Germany
ELISA Mouse TNF-α	Bio-Techne GmbH Wiesbaden-Nordenstadt Germany
RNeasy Kit	Qiagen, Düsseldorf, Germany

Table 8: Antibodies

Antibody	Supplier
Cy3 anti-rabbit IgG	Jackson ImmunoResearch/Dianova, Hamburg, Germany
Cy5 anti-goat IgG	Jackson ImmunoResearch/Dianova, Hamburg, Germany
DyeLight 488 anti-mouse IgG	Jackson ImmunoResearch/Dianova, Hamburg, Germany
Goat anti-VGF (R-15)	Santa Cruz, Heidelberg, Germany
Rabbit anti-VGF (C-terminal)	Provided by Prof. Dr. Salton (Salton et al., 1995)
Goat anti-Iba1	Abcam, Cambridge, United Kingdom
Monoclonal Mouse anti-GFAP	EMD Millipore Headquarters, Massachusetts, United States of America
Rabbit anti-Olig2	EMD Millipore Headquarters, Massachusetts, United States of America

Table 9: Quantitative PCR mouse primers (5' >3')

β-actin	Forward	CCCTGAAGTACCCCATTGAA
	Reverse	GTGGACAGTGAGGCCAAGAT
VGF	Forward	TCAGTTCGGGGAAGGAGTGT
	Reverse	GGAAGGGGCCACCTAGACTT
GFAP	Forward	TCGCACTCAATACGAGGCAG
	Reverse	GTCGTTAGCTTCGTGCTTGG
Iba1	Forward	GGATTTGCAGGGAGGAAAAG
	Reverse	TGGGATCATCGAGGAATTG
C3AR1	Forward	GATTTGTTGGTGGCTCGCAG

	Reverse	ATGGCTCAGTCAAGCACACT
CX3CR1	Forward	CAGCATCGACCGGTACCTT
	Reverse	GCTGCACTGTCCGGTTGTT

Table 10: Peptides

Peptide	**Supplier**
TLQP-21 mouse	Bachem Distribution Services GmbH, Weil am Rhein , Germany
TLQP-62 mouse	Bachem Distribution Services GmbH, Weil am Rhein , Germany
Scrambled TLQP-21 mouse	Bachem Distribution Services GmbH, Weil am Rhein , Germany

Table 11: Buffers and media

DMEM complete	DMEM, 10 % FCS, 2 mM L- glutamin100 U/ml, penicillin, 100 µg/ml streptomycin
DMEM F12 complete	DMEM-F12 GlutaMAX, 1% penicillin G/streptomycin sulfate, 2x B-27 without vitamin A (1:50), HEPES (0.2 mM), supplemented with fibroblast growth factor 2 (FGF2, 20ng/ml) and epidermal growth factor (EGF, 20 ng/ml)
Cultivation Media	DMEM, contained, 25% heat-inactivated horse serum, 50mM sodium bicarbonate, 2% glutamine, 25% Hank's balanced salt solution, 1 mg/ml insulin, 2.46mg/ml glucose, 0.8mg/ml vitamin C, 100 U/ml penicillin, 100 mg/ml streptomycin and 5 mM Tris.
HEPES buffer	HEPES 4.95 mM, NaCl 150 mM, KCl 5.36 mM, MgCl2 1 mM, CaCl2 2 mM, Glucose 10 mM
0.9 % saline	0.9% NaCl, Aqua dest. sterile filtered.

1M TBS	1L destilled water, 1.21g Tris and 8.76g NaCl. pH adjusted to 7.4
Blocking buffer (immunohistochemistry)	0,1% Triton X-100, 5% donkey serum in 1 M Tris-buffered saline (TBS)

Table 12: Softwares

Program	**Company**
Adobe Creative Suite 6	Adobe Inc, San Jose, USA
GraphPad Prism	GraphPad Software Inc., La Jolla, USA
IGOR Pro 6.3	WaveMetrics, Inc., Lake Oswego, USA
ImageJ	National Institute of Health, USA
Microsoft Office	Microsoft, Redmond, USA
TIDA	HEKA, Lambrecht/Pfalz, Germany
R	R Core Team, Vienna, Austria

II. Methods

3.II.1. **The Cancer Genome Atlas analysis for survival outcome**

Memorial Sloan Kettering Cancer computational biology cancer genomics cBioPortal (http://www.cbioportal.org/public-portal/) was used to access patient clinical and survival information and tumor gene expression data. (Study: Glioblastoma multiforme, TCGA Provisional, mRNA Expression z-scores (microarray), accessed in February, 2016) (Szulzewsky et al., 2015). A z-score for a sample indicates the number of standard deviations away from the mean of expression in the reference. For mRNA expression data, typically the relative expression of an individual gene (VGF in this case) is computed and tumor to the gene's expression distribution in a reference population. That reference population is all tumors that are diploid for the gene. Subtype information was retrieved from (Verhaak et al., 2013; Brennan et al., 2013). For analysis of TCGA patient survival data the average and standard deviation of the gene expression values of all patients was calculated. Patients with a gene expression lower than the negative standard deviation were clustered into the low expression group, whereas patients with a gene expression higher than the positive standard deviation were clustered into the high expression group. Statistical significances between high and low expression groups were calculated using the Log Rank (Mantel-Cox) test. Survival plots were generated and Kaplan-Meier curves were produced using GraphPad Prism 5 software.

3.II.2. **Mice**

Animals were handled according to the rules and recommendations of the local authorities (Germany: LaGeSo, animal protocol numbers: G O 268-10, G O 343-10, G 0438-12, Cleveland, OH, USA: Institutional Animal Care and Use Committee of

the Cleveland Clinic #2013-1029) All animal experiments were conducted according to the guidelines for animal care and were approved in advance by the authorities. Animals were housed in the Cleveland Clinic Biological Resource Unit and at the animal facilities of the Max-Delbrück-Center for Molecular Medicine in the Helmholtz Association. C57BL/6 (BL6) mice were purchased from Charles River Laboratories and used for establishment of primary neonatal glial cells culture and organotypic brain slice cultures. For the production of RCAS-PDGFb/RCAS-PDGFb-RFP GBM primary tumors *Ntv-a*/*Ink4a-Arf*$^{-/-}$ and *Ntv-a*/*Ink4a-Arf*$^{-/-}$/*Pten*$^{flox/flox}$ mice were used, respectively. The genetic backgrounds of tv-a mice are FVB/N, C57BL/6, BALB/C. *CX3CR1*$^{GPF/wt}$/*CCR2*$^{RPF/wt}$ and *GFAP*$^{GFP/wt}$ mice where used for glial cell isolations from tumor-bearing and naïve mice and were all housed at the Cleveland Clinic Biological Resource Unit. The transgenic mouse strain FVB-Tg(GFAP-cre)25Mes/J (hGFAP-cre) was acquired from The Jackson Laboratory (Bar Harbor, USA) and crossed with B6-Tg(VGF^{flpflox}) kindly donated by Prof. Dr. Stephen Salton (Department of Neuroscience, Icahn School of Medicine at Mount Sinai, New York, USA; Lin et al., 2015).

3.II.3. **PDGFb-induced glioblastoma proneural model**

To study VGF regulation in GBM a murine glioma model based on somatic-cell gene transfer was used. Tumor formation is initiated by the overexpression of human PDGFb in Nestin-expressing cells in vivo. The used transgenic mice express the avian RCAS virus receptor tv-a on nestin-positive cells and also harbor germ line Ink4a-Arf loss (such locus is implicated in cell cycle regulation and is altered in 60% of GBM). *Ntv-a*/*Ink4a-Arf*$^{-/-}$ mice develop proneural high-grade gliomas 6 to 8 weeks following intracranial injection of RCAS-PDGFb-producing DF-1 chicken fibroblast cells at 4.5 to 10 weeks of age (Hambardzumyan et al. 2009).

DF-1 cells were purchased from ATCC (Manassas, VA, USA). Cells were grown at 39°C according to ATCC instructions. Transfections with RCAS-PDGFb were performed using FuGENE 6 transfection kit according to manufacturer's protocol.

This tumor model histologically resembles primary human GBM and displays several hallmarks of human GBM, such as a more invasive growth pattern, necrotic and pseudopalisading.

3.II.4. **Intracranial injections**

Injections were performed using a stereotactic frame (Stoelting, Wood Dale, IL, USA). Mice were anesthetized with intraperitoneal injections of ketamine (0.1 mg/g, Pharmazeutischen Handelsgesellschaft, Garbsen, Germany) and xylazine (0.02 mg/g, Bayer, Leverkusen, Germany), fixated in a stereotactic micromanipulator (Kopf, Tujunga, CA, USA), and a small incision was made in the skin using a scalpel. One microliter cell suspension (5×10^4 transfected DF-1 cells) was delivered very slowly using a 30-gauge needle attached to a Hamilton syringe (Hamilton, Reno, NV, USA). Coordinates for injections of DF-1 cells into *Ntv-a*/*Ink4a-Arf-/-* mice were bregma 1.5 mm anterior both laterals 1 mm in a depth of 2.0 mm from the dural surface, targeting the subventricular zone where many nestin-positive cells are localized. Post-surgery, the incision was closed with surgical suture and mice were carefully monitored. The bodyweight was periodically measured and upon tumor development, if 20% of the initial weight was lost the mice were sacrificed and tumor-bearing brains collected.

For the generation of secondary tumors $CX3CR1^{GPF/wt}/CCR2^{RPF/wt}$ and $GFAP^{GFP/wt}$ mice were operated as above and one microliter cell suspension containing $5x10^4$ RCAS-PDGFb primary tumor cells (isolation will be later described in section **3.II.7**) were delivered. Mice were monitored daily for the first two weeks and twice a day starting from day 15 post-injection for symptoms of tumor development (lethargy, hydrocephalus, head tilting).

3.II.5. **Isolation of tumor-associated glia**

For isolation of glioma-associated microglia and macrophages/monocytes from RCAS-PDGFb tumors, primary tumors were intracranially re-transplanted into *CX3CR1*$^{GPF/wt}$*/CCR2*$^{RPF/wt}$ mice to distinguish between microglia and peripheral monocytes that invaded the brain. Naïve age-matched *CX3CR1*$^{GPF/wt}$*/CCR2*$^{RPF/wt}$ mice were used as controls. 5 to 7 weeks after intracranial injection of RCAS tumor cells into *CX3CR1*$^{GPF/wt}$*/CCR2*$^{RPF/wt}$ mice these mice develop tumors that are histologically identical to the original tumors in *Ntv-a*/*Ink4a-Arf*$^{-/-}$ mice. The same procedure was done using *GFAP*$^{GFP/wt}$ for isolation of tumor-associated or naïve astrocytes.

RCAS-PDGFb-implanted mice were sacrificed 4-5 weeks post-injection. Tumor-bearing and control mice were euthanized by intraperinoneal (i.p.) injection of 200 µl pentobarbital-sodium (Narcoren, Pharmazeutischen Handelsgesellschaft) and perfused using a 0.9% NaCl solution. The brain and spleen (for naïve monocytes) were extracted and stored in ice-cold HBSS (Gibco-Invitrogen). For naïve mouse brains, the olfactory bulbs and the cerebellum were cut away using a scalpel and discarded. The rest of the tissue was used for dissociation. Tissues from 2-4 animals were pooled together for increasing the yield. In tumor- bearing mouse brains, only the visible tumor area around the injection site was isolated and was dissociated with the Neural Tissue Dissociation Kit (Miltenyi Biotec, Bergisch-Gladbach, Germany) according to the manufacturer's instructions. To remove the myelin an established protocol was used (Olah & Raj et al., 2012). In brief, the brain cell suspension was mixed with a total of 25 ml of a 22% Percoll (Th.Geyer, Renningen, Germany) solution and a layer of 5 ml cold PBS (Gibco-Invitrogen) was added on top. Centrifugation at 950 g with slow acceleration and without breaks created a gradient that separated the cell pellet on the bottom of the tube from the myelin which was carefully aspirated. Spleens were processed through a 70 µm cell strainer with a syringe plunger and the mesh rinsed with 10 ml of PBS per spleen. The cells were centrifuged and the pellet subjected to erythrocyte lysis by adding 5 ml of 1x RBC lysis buffer (Cat# 420301, Biolegend, San Diego, CA, USA). The lysis was carried out by shaking the tube mildly for 5 min at RT and subsequently stopped with 20 ml of PBS. The pellet was washed once with PBS

and resuspended in PBS, containing 0.5% FCS and 2mM EDTA (FACS buffer) for subsequent FACS isolation. 500 µl FACS buffer per $5x10^6$ cells was used for sorting at a BD FACSAria (BD Bioscience).

FACS was based on RFP and GFP positivity. *CX3CR1*$^{GPF/wt}$/*CCR2*$^{RPF/wt}$ mice display RFP$^+$/GFP^{low} macrophages/monocytes and RFP$^-$/GFP$^+$ microglia. RFP$^+$/GFP^{low} peripheral macrophages/monocytes resemble the classical CD11b$^+$/CD45^{high}/ population and the RFP$^-$/GFP$^+$ microglia resemble the classical CD11b$^+$/CD45^{low} population. For tumor-associated or naïve astrocytes the sorting was done from tumors injected in *GFAP*$^{GFP/wt}$ or non-injected mice. The astrocytes were sorted according to cell size and high expression of the GFP marker.

Generation of flow-sorted samples from re-implanted RCAS-PDGFb for qRT-PCR analysis was done in the lab of Prof. Dolores Hambardzumyan at Cleveland Clinic (Cleveland, Ohio, USA) by Dr. Ilaria Tamagno (microglia and macrophages) and me (astrocytes) during a 6 month lab rotation in Cleveland.

3.II.6. **Generation of VGF$^{-/-}$ GBM tumors**

VGF knockout mice B6-Tg(VGF^{flpflox}):FVB-Tg(GFAP-cre)25Mes/J (or simply hGFAP-cre/VGF^{flpflox})were generated at the Cleveland Clinic by crossing two transgenic mouse lines. hGFAP-cre expresses Cre recombinase under the control of the human glial fibrillary acidic protein promoter (GFAP). The mice were crossed with VGF^{flpflox} mice containing a *loxP*-flanked VGF sequence (neo cassette flp'd out and removed). Cre-mediated recombination results in tissue-specific deletion of the target during the embryonic development as onset of Cre expression begins in the forebrain by embryonic day 13.5 of development, suggesting that the hGFAP promoter is active in a multi-potential neural stem cell, causing the subsequent neural and glial progenies to lack the target gene (Zhuo et al., 2001). **Figure 12** shows that at 1 month after birth the whole adult brain is affect by hGFAP-Cre-mediated recombination, confirming this is a good strategy for knocking out targets from CNS-derived cells (excluding microglia, as they are originated from the yolk sac at the embryonic day 8.5 - Ginhoux et al., 2010).

For generation of tumors lacking VGF expression the hGFAP-cre/VGF^{flpflox} were crossed with the *Ntv-a*/*Ink4a/Arf*$^{-/-}$ mice which when infected with the RCAS virus will have their neural and glial progenitors undergo malignant transformation (as previously explained in section II: Gliomas and glioblastomas). The tumor initiating cells lacking VGF genes will give rise to primary VGF knockout tumors .

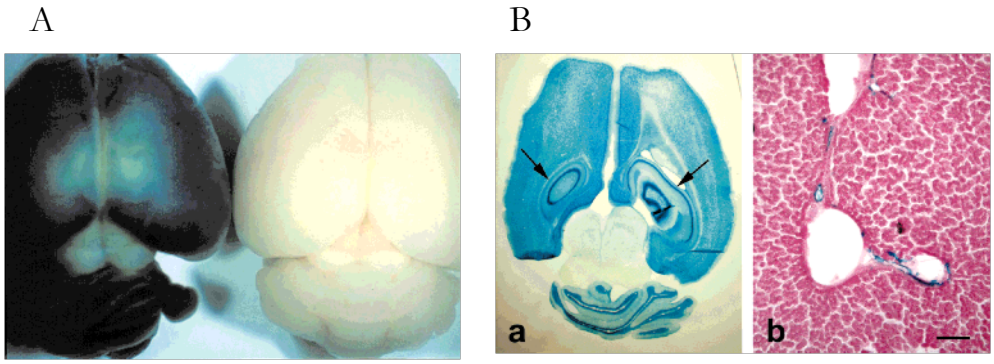

Figure 12: hGFAP-cre transgenics activation of lacZ reporter gene in brain

(**A**) X-gal stain of whole brains from hGFAP-cre/lacZ double transgenic (left) versus lacZ reporter alone (right), both 1 month old. (**B**) Histochemical detection of *lacZ* activity by X-gal staining in hGFAP-cre/R26-*lacZ* double transgenic mice. **a:** Horizontal section of brain from a 5-week-old mouse showing extensive labeling throughout the cerebral cortex and cerebellum, and lighter staining of the midbrain. Dense labeling of the hippocampi (arrows) was observed. **b:** Section of liver (counterstained with eosin) from an 11-week-old mouse showing scattered labeling of cells (likely ductal) in periportal regions. Pictures and legends adapted from Zhuo et al. (*Genesis,* 2001).

3.II.7. **Cultivation of primary RCAS-PDGFb-derived tumor cells**

RCAS-PDGFb tumors were excised from mouse brains using a scalpel, minced, and incubated with Accutase for 15 minutes at 37°C (**Figure 13)**. Tissue pieces were further mechanically dissociated using a 1 ml pipette and washed in HBSS. Cells were passed through a 70 µm cell strainer and seeded into a T25 cell culture flask. Cells were grown in DMEM F12 complete and passaged with Accutase (10 minutes followed by mechanic dissociation on ice). To promote adhesion of the cells in the absence of serum, whenever necessary (in example for BrdU-ELISA or immunocytofluorescence)

a thin layer of Geltrex in a concentration of 0.1 mg/ml (diluted in cultivation media) was used to coat the plate following manufactures instructions. All cells were maintained in a 37°C incubator with a 5% CO2 humidified atmosphere.

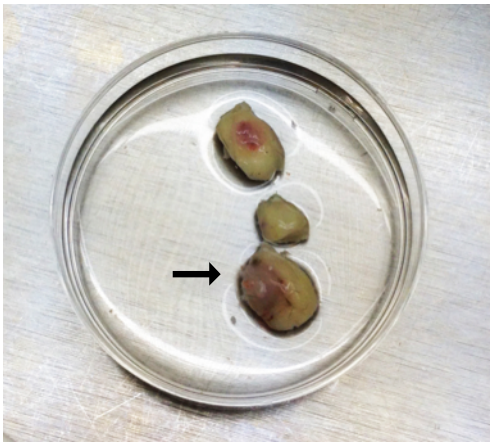

Figure 13: Isolation of RCAS-PDGFb tumor from mouse brain.

Mice bearing tumors were perfused and the brains removed from the skull. The tumor was carefully dissected from the rest of the brain and processed as previously described. Arrow shows tumor with regions of high vascularization (perfusion inside the tumor is not effective) and necrosis.

3.II.8. **Organotypic slice culture**

P14-P16 BL6 littermate mice were decapitated and brains were removed and placed in ice-cold phosphate-buffered saline (PBS) under sterile conditions. The forebrain was dissected from the brainstem and glued (using cyanoacrylate glue) onto a metal block and cut in the coronal plane into 250 µm sections with a vibratome (Microm HM 650 V, Thermo Scientific, Waltham, MA, USA). The brain slices were transferred onto the 0.4µm polycarbonate membrane in the upper chamber of a transwell tissue insert (Falcon model 3090, Becton Dickinson), which was inserted into a 6-well-plate (Falcon model 3502, BectonDickinson). Thereafter, the brain slices were incubated in 1 ml of DMEM complete per well. After overnight equilibration of the

brain slices, the medium was exchanged to cultivation media and changed every second or third day.

One day after cutting the slices, 5000 cultured RCAS-PDGFb-RFP tumor cells in a volume of 0.1 µl were injected into the slices using a syringe (Hamilton, Reno, USA) mounted to a micromanipulator (Kopf, Tujunga, USA). An injection canal was formed that reached 150 µm deep into the 250 µm- thick slice. The needle was then retracted by 50 µm, leaving an injection cavity of approximately 50 µm. The cell suspension was slowly injected over 30 seconds and subsequently the syringe was slowly pulled out in 10 µm incremental steps over 30 seconds. To ensure identical experimental conditions, gliomas were always inoculated into the same area, 1 mm anterior of the ventricle. After 72 hours of the injection peptide treatment (TLQP-21 or TLQP-62, diluted in PBS) was added or PBS as control until the tumors completed 1 week of organotypic growth (medium was changed twice).

Tumor sizes were determined 7 days post-injection by fluorescence microscopy (Axiovert 135, Carl Zeiss, Jena, Germany) using a 5x objective and the fluorescent area was evaluated using threshold tool of Fiji ImageJ. Statistical significances were calculated applying a One-Way-ANOVA using GraphPad Prism 5.

3.II.9. **BrdU cell proliferation ELISA**

Three RCAS-derived tumor primary cell lines were dissociated with Accutase counted and ressuspended at a density of 50000 cells per ml in DMEM F12 complete with supplements. A total 100 µl of cell suspension were seeded in quintuplicate on Geltrex-coated 96 well plates. After 15 hours of incubation, medium containing different concentrations of mouse TLQP-21 or TLQP-62 (1 to 1000 nM) was added to the designated wells. Normal medium was used as baseline control. After 48 hours, BrdU cell proliferation ELISA (Roche) was applied according to the manufacturer's protocol.

3.II.10. **Immunohistofluorescence**

Tumor-bearing animals were sacrificed and perfused under deep anesthesia (0.1 mg/g ketamine and 0.02 mg/g xylazine) by intracardiac infusion of 0.1 M phosphate buffer followed by perfusion with 10% formalin. After perfusion, the brains were removed, post-fixed in 10% formalin for 24 hours, in a tissue processer (Leica, Wetzlar, Germany), paraffin-embedded, and cut into 5-µm sections. The sections were microwaved at 700 watts for 2 minutes and deparaffinized in Histo-Clear (Richard-Allan Scientific) and passed through graded alcohols. The next step was antigen retrieval with citric acid (Vector Laboratories) in a boiling-water bath for 20 min. After two washes in PBS and water followed by permeabilization in 0.2% Triton in 0.1 M PBS for 45 min, sections were incubated in 0.1 M PBS containing 2% BSA, 5% NDS, and 0.1% Triton for 1 h at room temperature for blocking. For single staining, sections were incubated with the following antibodies overnight at 4°C in PBS plus 1% BSA:

- Rabbit anti-VGF 1:2000
- Rabbit anti-Olig2 1:250
- Goat anti-VGF 1:100
- Goat anti-Iba1 1:500
- Mouse anti-GFAP 1:1000
- Rabbit anti-GFAP 1:1000

For immunofluorescence staining after primary antibody, the secondary antibodies conjugated to different fluor dyes at a dilution of 1:500 in PBS were applied for 2 hours:

- Cy3 anti-rabbit IgG
- Cy5 anti-goat IgG
- DyeLight 488 anti-mouse IgG
- DAPI for nuclear counterstaining

For quantification of Iba1/VGF/GFAP staining, five to ten images (20x or 40x) were taken from 5 different regions of tumor-sections (including tumor border and core) per mouse brain using DAPI staining as a reference. The positive areas and intensity were assessed using ImageJ threshold tool and color histogram respectively. In order to obtain a spot-dependent correlation of the markers and VGF the pictures from different brains were pooled together for analysis instead of using the average values. VGF and GFAP or Iba1 values were normalized by DAPI values obtained in each picture. The results obtained with Pearson r were analyzed with GraphPad Prism.

For evaluation of VGF and GFAP or Iba1 colocalization, confocal z-stacks were prepared from the stained slices using a Leica TCS SPE confocal microscope (Leica Microsystems, Wetzlar, Germany). Ten z-stacks (0.5 μm steps) were imaged in the tumor core and border. Images shown are 2D representatives of the z-stacks from maximum intensity projections made with the ImageJ software.

3.II.11. **Immunohistochemistry**

For immunohistochemical detection, an automated staining processor was used (Discovery, Ventana Medical Systems, Inc.). The protocols were previous established at the Molecular Cytology Core Facility at Memorial Sloan-Kettering Cancer Center and adapted by Dr. Dolores Hambardzumyan at the Cleveland Clinic, USA. Rabbit anti-VGF 1:2000 was used in tumor-bearing brain and control for qualitative comparison of expression intensity. 20x images were taken from the whole brain with a slide scanner (Leica SCN400) at the Lerner Research Institute at the Cleveland Clinic.

3.II.12. **Microglia and astrocytes neonatal primary cultures**

Glial cultures were prepared from whole brains of P0-P1 mice as described previously (Prinz et al., 1999). The full brains of 0 to 1-day old pups were removed and carefully freed of blood vessels and meninges. Brains were then washed 3 times with HBSS and treated (except for olfactory bulb and cerebellum) with trypsin (10 mg/ ml PBS) and DNase (0.5 mg / ml PBS) for 2 min. The reaction was stopped by the addition of 10 ml DMEM, supplemented with 10% FCS. After removing the excess of medium, tissue was dissociated with a fire-polished pipette and DMEM was added to 15 ml of total volume. Cells were then washed by centrifugation for 10 min, 1000 g at 4°C. Mixed glial cells were cultured for 9 to 12 days in DMEM, supplemented with 10% FCS, 2 mM L-glutamine and antibiotics (100 U/ml penicillin and 100 µg/ml streptomycin, PSG), with medium changes every third day. For further preparation of pure microglial cells, medium was changed to supplemented DMEM with 1/3 volume of conditioning medium from L929 fibroblasts. After 2-3 days first microglia was separated from the underlying astrocytic monolayer by gentle shaking of the flasks for 1 h at 37°C in a shaker-incubator (100 rpm). Addition of L929 conditioning medium ensured 3 consequent dissociations of microglia from the astrocytic layer with 2-3 days intervals. Cultures usually contained >95% microglial cells, identified by positive staining with Griffonia simplicifolia isolectin B4 (Sigma, Deisenhofen, Germany), a marker for microglia. Cultures were used for experiments 1 to 2 days after plating at 70% of density in DMEM complete.

Enriched astrocyte cultures were cultured with DMEM complete on poly-L-lysine (PLL)-coated 25 cm^2 flasks also at 37 °C in a humidified 5% CO_2 atmosphere. After approximately 15 days, after microglia shake-offs, cells were harvested for experiments or were trypsinized and re-plated for collection of conditioned medium. The astrocytes were used within 14-21 days from the preparation of the primary culture. For enhanced purity astrocytes cultures were treated with clodronate for elimination of microglial cells: after microglia shake-off cells were washed and treated with 4 ml of a solution containing 40ug/ml of clodronate salt in DMEM complete overnight. Cells

were transferred into a shaker-incubator (100 rpm), washed twice with PBS and medium was replace to DMEM complete without clodronate.

3.II.13. **Conditioned medium**

Conditioned medium (CM) from astrocytes (ACM), microglia (MCM) and RCAS-PDGFb tumor cells (GCM, control medium) was collected when cells reached 70-80% confluence at low passages. Culture medium was changed for F12 complete medium for 24 hours, using appropriated volume of medium. After conditioning, medium was collected and filtered in filters with pore size of 0.2 μm (Sigma-Aldrich) and stored in aliquots at -20°C until use or 1-2 months.

3.II.14. **Immunocytofluorescence**

RCAS-PDGFb tumor cells were grown for 24 hours on coverslips previously covered with Geltrex and treated with MCM, ACM or GCM for 48 hours. After that, cells were washed 3 times with PBS, fixed with 4% paraformaldehyde (4% PFA in PBS, pH 7.4) for 15 minutes at room temperature. Following the fixation, cells were washed with PBS and incubated with the Rabbit anti-VGF (1:2000) antibody overnight at 4°C in PBS plus 1% BSA. For immunofluorescence staining after primary antibody, the secondary antibodies conjugated to fluor dye at a dilution of 1:500 in PBS were applied for 2 hours and washed. Nuclear dye DAPI at the concentration 1μg/ml diluted in water was used for 15 minutes at room temperature in a dark chamber. Afterwards, cells were washed 3 times with PBS, mounted and left to dry for at least 1 day. 5 pictures from each coverslip were taken using Leica TCS SPE confocal microscope for each experiment.

3.II.15. **Quantitative reverse transcription polymerase chain reaction (RT-qPCR)**

Total RNA extraction from mouse microglia was performed with the RNeasy Kit (Qiagen, Düsseldorf, Germany) according to the manufacturer's instructions. RNA concentrations were measured with a Nanodrop 1000 spectrophotometer and stored at minus -80°C until further use. First strand cDNA synthesis was carried out using the SuperScript II reverse transcriptase (Invitrogen) using oligo-dT primers (Invitrogen) according to the manufacturer's instructions. cDNA samples were stored at -20°C until further use. Quantitative real-time PCR reactions were performed in a 7500 Fast Real-Time thermocycler using the SYBR Select Master Mix (Applied Biosystems) according to the manufacturer's instructions. cDNA input ranged between 1–5 ng/µl of total RNA transcribed into cDNA. Calculation of the relative expression was carried out using the ΔΔCt method with Actin as reference gene. All primers used are listed in **Table 8**. Primers for target genes were designed to recognize all validated mRNA splice variants of the gene, relying on the RefSeq sequences of the UCSC genome browser (http://genome.ucsc.edu/). The primer sequences were generated using the Primer- Blast tool (http://www.ncbi.nlm.nih.gov/tools/primer-blast/). Amplification of unintended targets was excluded by BLAST search (http://blast.ncbi.nlm.nih.gov/Blast.cgi). Statistical significance was tested using ANOVA followed by Tukey's post-hoc test performed using GraphPad Prism.

3.II.16. **Calcium Imaging**

For calcium imaging experiments, microglia cells were seeded at a density of 25,000 cells per glass coverslip and allowed to adhere to the glass for 3 hours. Cells were loaded with the calcium indicator Fluo 4 AM (5 µM in DMSO, dissolved in HEPES buffer) for 20-60 minutes at 37°C. The coverslip was then transferred to a chamber with constant, local perfusion of buffer with a speed of 120 µl/min through a

Perfusion Pencil (AutoMate Scientific, Berkeley, USA). After 1 minute, the TLQP-21 (100nM) was applied for 30 s, followed by a washout. After 7 minutes 1mM ATP was applied for 30 s as positive control. For experiments using the C3ARA (1μM) the substance was applied after washing the cells 1 minute with HEPES, 30 s before and after TLQP-21 (100nM) treatment, for a total of 90 s. The whole protocol lasted 11 minutes including the final washout. Fluo 4 AM was excited at 488 nm wavelength by a Polychrome II monochromator (Till photonics, Martinsried, Germany) and pictures were taken at a rate of 0.5 Hz by an inverted CCD camera. Images were acquired by CamWare v3.16 software (PCO, Kelheim, Germany). For analysis, cell somata were selected as regions of interest (ROI) and the mean relative fluorescent intensity (rFI) for each ROI and frame was determined with the program Imaging cells easily (own development) by myself or IGOR Pro by Marcus Semtner. The monochromator, the camera, the perfusion system and data acquisition were controlled by the TIDA software (HEKA, Lambrecht/Pfalz, Germany). Further analysis was performed with Excel. Only cells responding to the positive control were analyzed. Cells were classified as "responding" when the Ca^{2+} signal during the application of a given substance was elevated 2% or more compared to baseline levels (signal immediately before the application). Each cell trace of relative fluorescent intensity was checked manually for exclusion of false positives. HEPES was used to control unspecific cellular responses to the switch of perfusion pumps at the beginning of each experiment. The response rates of the treated groups with or without antagonist were compared with an unpaired t-test different. One-way ANOVA was used for comparing the different doses of TLQP-21 against the response rate for HEPES alone. All experiments were performed in quadruplicates from three independent cultures. Experiments with the antagonist were performed by the master student Josien Visser under my supervision and analyzed with the help of Dr. Marcus Semtner .

3.II.17. **Whole-cell patch-clamp recordings**

To test whether microglial cells display TLQP-21 membrane current activity after C3AR1 activation, we employed the whole-cell patch-clamp technique on neonatal microglia in vitro. The following intracellular solution was used containing (in mM): NaCl 130; MgCl2 2; CaCl2, 0.5; Na-ATP, 2; EGTA, 5; HEPES, 10; and sulforhodamine-101, 0.01 (SR101 - Sigma Aldrich, St. Louis, USA) with an osmolarity of 280-290 mOsm/L adjusted to a pH of 7.3 with KOH. Patch pipettes were pulled from borosilicate glasses and used with a resistance of 4-6 MOhm. Cells were plated on coverslips with a density of 4 to 5 x 10^5 cells. A conventional patch-clamp amplifier was used (EPC10, HEKA Lamprecht, Germany). After establishing whole-cell configuration we clamped the cell to a holding potential of -20 mV in voltage clamp mode and applied a series of de- and hyperpolarizing voltage steps ranging from -140 to 60 mV for 50 ms each with 10 mV increments. This protocol was repeated every 5 s to continuously monitor membrane currents upon substance application. A perfusion system (4 - 6 ml/min) was used for superfusion of the cells with HEPES. The peptide TLQP-21 was applied through the bath for 30 s. The C3AR1 antagonist SB290157 (C3ARA, 1μM) was applied during, 30 s before and after peptide administration. Whole-cell patch-clamp recordings were performed using an EPC 10 patch-clamp amplifier combined with TIDA software. To confirm intracellular access, a fluorescent dye was added to the pipette solution as described above. The capacitive transients of the whole-cell recordings were compensated by TIDA 5.24 software. The recordings were done and established by Stefan Wendt and by Josien Visser, final analysis was carried out by the three of us.

3.II.18. **Agarose spot assay**

The chemotactic effect of TLQP-21 on microglia migration was determined using the agarose spot assay, Boyden chamber assay and the scratch assay (Ku et al.,

2013). For the agarose spot assay, 0.1 g of low melting point agarose was dissolved in 20 ml of PBS to obtain a 0.5 % agarose solution. The agarose solution was heated until all agarose particles were dissolved, and subsequently cooled down to 40 °C. Four spots (each spot 10 µl, from a solution of 90 ul 0.5 % agarose mixed with 10 ul of peptide or PBS) per dish were placed onto 35 mm glass dishes (MatTek Corporation, MA, USA).The first peptide for all the dishes contained only PBS, the others contained different concentrations of the peptide. The dish was then cooled for 10 min at 4 °C to allow the agarose spots to solidify. One million diluted in 2 ml of DMEM with 10 % FCS without antibiotics were slowly added to the dishes and incubated at 37°C in 5% CO2. Medium with the same concentration of the peptide in the agarose spot was used for motility analysis in the absence of gradient. After 3 hours microglia under or inside the spot were counted. The values reported herein are the average of at least 10 independent dishes from a minimum of three independent microglia preparations. The number of cells in each spot was normalized to the average in control PBS spots (100%).

3.II.19. **Boyden chamber assay**

TLQP-21-induced chemotaxis was tested using a 48-well microchemotaxis Boyden chamber (Neuroprobe, Bethesda, USA). Upper and lower wells were separated by polycarbonate filter (8 µm pore size; Poretics, Livermore, USA). Microglial cells (2-5 × 10^4 cells) in 50 µl of serum-free DMEM medium were added to the upper compartment, while the lower wells contained peptide diluted in medium. Medium with the same concentration of the peptide in the lower well was added to the upper well with cells to assess motility in the absence of peptide gradient. Culture medium was used as a control. The chamber was incubated at 37 °C and 5 % CO_2 for 3 h. Cells remaining on the upper surface of the membrane were removed by wiping, and cells in the lower compartment were fixed in methanol for 5 min and subjected to Diff-Quik stain (Medion Grifols Diagnostics AG, Düdingen, Switzerland). The rate of microglial migration was calculated by counting cells in two fields of each well using a 10 ×

bright-field (phase 2 contrast) objective. The pictures were analyzed on ImageJ software using the color threshold contrast tool (selecting colors in the hue range of 150 (upper)-240 (lower), which are specific for the migrated cells stained in red-violet): the background area from the pores was subtracted for each experiment, then the area for one cell (averaged from at least 10 representative migrated cells) was calculated, for each experiment, as well. For each condition 40-120 fields in 10-30 wells were analyzed using cells from at least 3 independent microglia preparations. The number of cells in each field was normalized to the average in control condition (100%).

3.II.20. **Scratch wound-healing assay**

The scratch assay was performed as described previously with adaptations (Liang et al., 2007; Lively & Schlichter, 2013). Briefly, microglial cells were seeded at a density of 5×10^4 cells/dish in the glass-bottomed cell culture dish, and incubated at 37 °C under the 5 % CO_2 for 24 h. A scratch wound was created with a 10 µl pipette tip on the cell monolayer and the cells were washed with PBS. Thereafter, the cells were stimulated with TLQP-21-contaning media or PBS as a control for 3 hours. Pictures were taken in pre-marked areas of the dish at the moment of the scratch and 3 hours after. The pictures were analyzed on ImageJ software, marking the initial cell-free zone and counting the cells that migrated to that area 3 hours after treatment. The number of migrated cells was normalized to the average in control condition (100%). A minimum of 3 technical replicates from 3 individual cultures were used to calculate the mean migratory capacity of each cell culture condition.

3.II.21. **Flow cytometry based phagocytosis assay:**

Neonatal microglial cultures were plated 16-24 hours before the experiment in a concentration of 10^6 in 2 ml of DMEM complete in 35 mm uncoated culture dishes.

Fluoresbrite® Carboxylate Micropheres (BrightBlue, 4.5 μm) were coated with FCS for 30 min at RT, 1000 rpm. The beads were pulled down and resuspended in HBSS at a final concentration of $2x10^6$ beads/ml. Microglia were washed once with HBSS before 1 ml bead solution with different doses of TLQP-21 was applied. Medium was used as baseline control of phagocytosis. The cells were incubated with the beads for 30 minutes at 37 °C under the 5 % CO_2. Afterwards, they were harvested and washed once in HBSS for removal of non-internalized beads and resuspend in 250 ul of FACS buffer with 0.5 μl of Propidium Iodide (1.0 mg/ml solution in water) to stain dead cells. Stained cells were transferred to a BD LSRFortessa Flow cytometer (BD Bioscience) and data were analyzed using FlowJo v10 software (Tree Star, Ashland, USA). The data is presented as the percentage of cells with bead signal (phagocytic cells) normalized by untreated control (100%). Data was analyzed with R (R Core Team, 2015).

3.II.22. **ELISA (enzyme-linked immunosorbent assay)**

Microglia cells were plated on 24-well plates in a concentration of 10^6 cells per ml of medium for 24 hours. TLQP-21 or scrambled peptide were added to the medium. PBS was used as negative control and LPS as positive control. The cells were treated for 24 hours and the supernatant was collected, centrifuged (500 g 5 minutes) and stored in aliquots at – 20 °C. ELISA was performed following the kit instructions.

3.II.23. **Statistical analysis**

Statistical analysis was performed using GraphPad Prism 5 and Microsoft Excel 2007, unless stated otherwise. For analysis of TCGA patient survival statistical significances between high and low expression groups were calculated using the Log Rank (Mantel-Cox) test. Survival plots were generated and Kaplan-Meier curves were produced. For all other experiments, unless stated and specified otherwise, repeated

One-Way ANOVA followed by Tukey post-hoc test was used for comparison of three or more groups and paired analysis was done with paired two-tailed t-test. For analysis of microglia migration assays (agarose spot assay, Boyden chamber assay and the scratch assay) non-parametric One-Way ANOVA followed by Tukey post-hoc test was used. For correlation of VGF protein immunofluorescence staining with Iba1 and GFAP levels in vivo, Pearson r was used and significance was measured with two-tailed p-value. BrdU cell proliferation ELISA was analyzed with paired t-test. Column graphics display means and error bars indicate the standard error of the mean (SEM). Indicators for all significant results: *, $p<0.05$; **, $p<0.01$; ***, $p<0.001$

4. Results

I. VGF and GBM

4.I.1. Survival estimate of human GBM patients with differential VGF expression

Using the cBioPortal for Cancer Genomics we looked for VGF expression in different data sets of TCGA stratified according to its molecular signatures. First analysis shows an overview of VGF expression across all the data sets available from different types of cancer. The groups with number of samples larger than 80 were sorted according to VGF expression. It is possible to distinguish low grade gliomas (LGG) and GBM among the tumors with highest expression of VGF mRNA, GBM did not show significantly different median expression when compared with LLG by t-test (**Figure 14-A)**. Using the same samples VGF expression among the different molecular subtypes of GBM was analyzed. The proneural subtype had a significantly ($p< 0.0001$, ANOVA) higher VGF expression (showed as logarithmic Z-score in **Figure 14-B**) then the other subtypes with a mean Z-score of 0.64. In the different GBM subgroups it was possible to estimate the changes in the median survival of patients with GBM classified in high or low VGF expression, with the threshold set in relation to the median expression.**Figure 15** shows that when first looking at all GBM cases together, 134 low expressing VGF cases with a median survival of 14.89 months against 12.2 months of the 131 high expressing VGF cases were observed (Log-rank, Mantel-Cox test $p=0.0120$). The VGF effect on median survival was amplified when analyzing the subgroups individually and the proneural group showed the most significant difference in survival related to VGF expression: low expression was seen in 22 cases with a median survival 20 months against 11 months in the 47 patients with high VGF

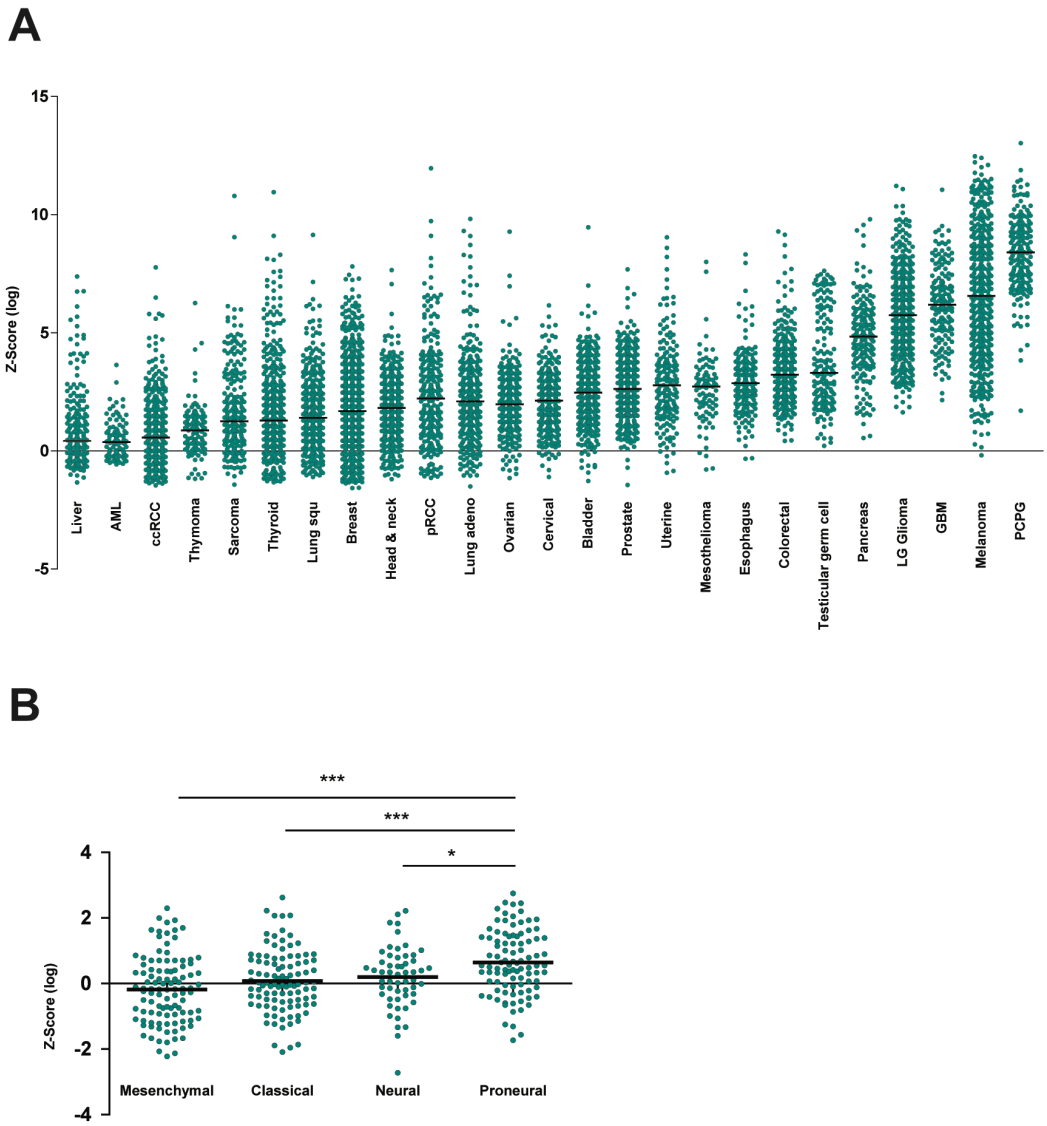

Figure 14: VGF expression in human cancer patients and different GBM subtypes

The Cancer Genome Atlas provisional microarray data sets available from the cBioPortal for Cancer Genomics were analyzed by VGF expression (displayed in Z-score log scale). (**A**) The different data sets available (with more than 80 cases) were sorted according to VGF median expression. GBM and low-grade gliomas are among the tumors with higher median VGF expression. (**B**) GBM cases were cluster into previously described molecular subtypes and Z-scores from GBM subtypes were obtained from the database, sorted by median VGF expression. ANOVA showed that the proneural molecular subtype has significantly higher VGF avarage expression. Abbreviations: acute myeloid leukemia (AML), clear cell renal cell carcinoma (ccRCC), lung squamous cell carcinoma (Lung squ), papillary renal cell carcinoma (pRCC), lung adenocarcinoma (Lung adeno), pheochromocytoma and paraganglioma (PCPG).

expression (Log-rank (Mantel-Cox) Test, p=0.0418). The difference was larger in the few cases with G-CIMP: 6 cases of low expression with median survival of 46.98 months and 7 cases of high VGF with 17.7 months (not enough samples for trustful analysis; p=0.2913). The mesenchymal patients had also significantly different survival

curves (p=0.0411) but there was a larger number of cases with low VGF expression (n=49, 13.93 months) then high VGF (n=26 cases, 10.43 months), therefore for all GBM cases the numbers of high and low VGF expression cases are equaled out and the effect on survival is diluted, as a result of the lack of difference in the cases of classical (p=0.6247) and neural (**Figure 15**, p=0.5253) GBM.

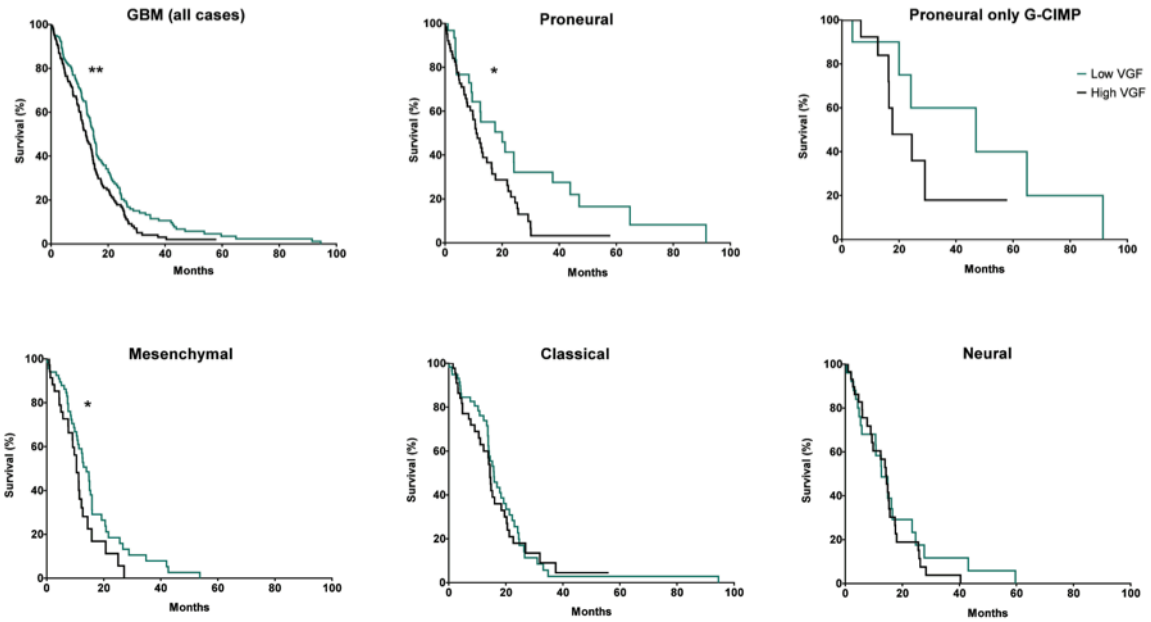

Figure 15: Survival estimates from human GBM subtypes according to VGF expression.

It was possible to estimate the changes in the median survival of patients with GBM classified in high or low VGF expression, with the threshold set in relation to the median expression, in the different GBM subgroups. 265 GBM cases were analyzed: 134 low expressing VGF cases with a median survival of 14.89 months against 12.2 months of the 131 high expressing VGF cases (p=0.0120). Proneural low expression was seen in 22 cases with a median survival of 20 months against 11 months in the 47 patients with high VGF expression (p=0.0418). The mesenchymal low expression was seen in 49 cases with a median survival of 13.93 months against 10.43 months in the 26 patients with high VGF expression (p=0.0411). In classical and neural cases VGF differential expression did not affect the patients survival (p=0.6247, p=0.5253; respectively). Log-rank, Mantel-Cox test was applied for statistical analysis.

4.I.2. **VGF protein and mRNA is expressed by glioma cells**

Immunohistochemistry revealed that VGF was spread throughout large areas of PDGFb-derived mouse glioblastoma, with very strong intracellular staining (not quantified). Hippocampus from adult wild-type, was used as comparison and positive control, because it was the region with the highest expression observed (**Figures 16-A, B**). As seen in further immunofluorescence assays (**Figures 16-C-E**), VGF was predominantly expressed in Olig2+ cells which is a transcription factor expressed in PDGFb-induced tumor cells, not present in proneural-associated cells (Katz et al., 2012). The tumor tissue contained great infiltration of Iba1 and GFAP cells. Microglia/macrophage cells (identified by Iba1) (**Figure 16-E**) or astrocytes (expressing GFAP) (**Figure 16-D**) coexpressing VGF were not found using slice screening with confocal microscopy.

Using two different transgenic mice, *CX3CR1*$^{GPF/wt}$*/CCR2*$^{RPF/wt}$ and *GFAP*$^{GFP/wt}$, microglia, monocytes/ infiltrating macrophages and astrocytes were isolated with FACS from naïve forebrain or tumor tissues. The mRNA of the naïve and tumor-associated cells was analyzed by RT-qPCR using primers designed for mouse VGF and compared with the mRNA from matching sorted tumor cells (RCAS-PDGFb^{RFP+}). Microglial cells were sorted with FACS as CX3CR1-positive /CCR2-negative cells and distinguished from the infiltrating monocytes by the expression of CCR2. Using the Gfap$^{GPF/+}$ mice the astrocytes (GFP+) were sorted in the same fashion **Figure 16-F** shows the levels of VGF mRNA expressed in fold change to the tumor cells. The statistical significance was determined using one-way ANOVA followed by Tukey. RCAS-tumor cells were significantly different than all populations analyzed ($p < 0.0001$). The results show that in the tumor environment the tumor cells are the major source of VGF.

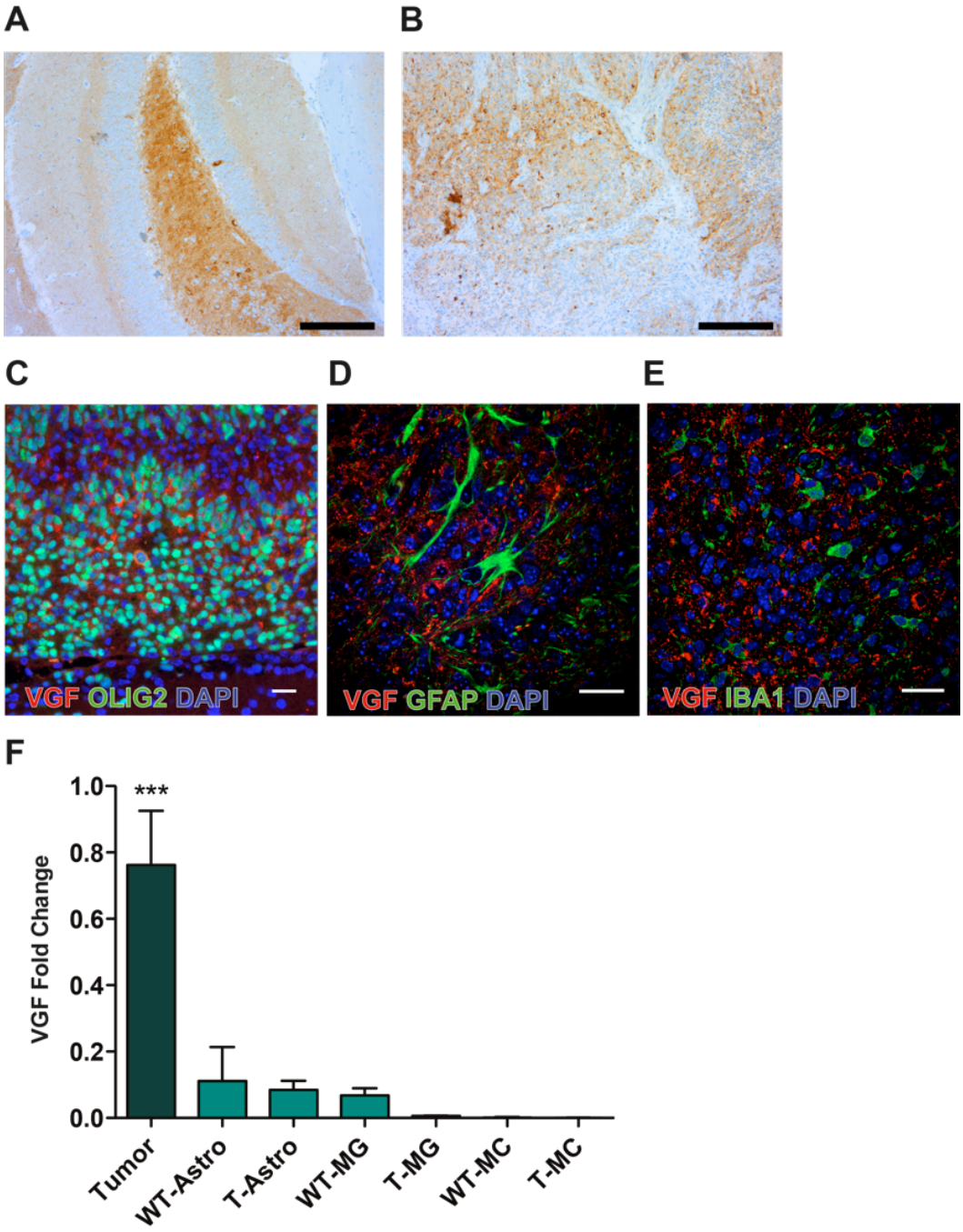

Figure 16 : VGF is expressed by PDGFb-GBM cells.

(A-B) Immunohistochemistry of mouse brain (**A**-Wild-type hippocampus; **B**- PDGFb-GBM tumor core) with polyclonal anti-VGF (C-terminal). Scale bars: 200 µm. (**C-E**) Immunofluorescence of PDGFb-GBM tumors. Olig2 was used as a marker of tumor nuclei, GFAP shows tumor-associated astrocytes and Iba1 tumor-associated microglia and macrophages. Scale bars: 25 µm. (**D**,**E**) Images are 2D representations (maximum intensity projections) of the z-stacks (10x 0.5 µm). (**F**) Tumor cells (n=4) and tumor-associated (T) astrocytes (Astro), microglia (MG) and monocytes (MC) were sorted from PDGFb-GBM. Wild-type (WT) mouse brains were used for sorting naïve cells. One-way ANOVA was used to compare the expression. Tumor n=4; WT-Astro n=5; T-Astro n=14; WT-MG n=3; T-MG n=3; WT-MC n=3; T-MC n=3.

.

4.I.3. **VGF knockout mice show better survival**

For generation of tumors lacking VGF expression, floxed VGF mice were first crossed with mice carrying Cre under the control of the human GFAP gene (hGFAP-cre/VGF^{flpflox}) and later crossed with *Ntv-a*/*Ink4a/Arf*$^{-/-}$ mice which when infected with the RCAS-PDGFb virus produced proneural-like GBM tumors. 10 wild-type (VGF WT, not floxed) mice and 10 knockout (VGF KO, floxed) were injected with DF-1-RCAS-PDGFb and the median survivals were compared (**Figure 17**). VGF KO bearing tumor mice showed a median survival of 95 days compared to 54 of VGF WT tumor mice (p=0.018).

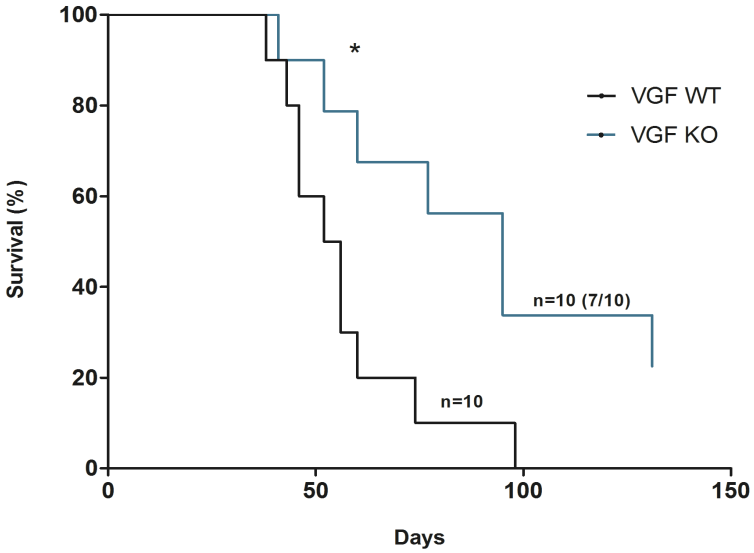

Figure 17: VGF knockout mice have better survival.

10 mice VGF wild-type (WT) and 10 VGF knockouts hGFAP-cre/VGF^{flpflox}/*Ntv-a*/*Ink4a/Arf*$^{-/-}$ (KO) were stereotactically injected with the virus packing cells for tumor induction and the survival curves were analyzed with Log-rank, Mantel-Cox test.

4.I.4. **Tumor-associated microglia and astrocytes affect VGF expression by the tumor cells.**

For in vitro assay, RCAS cell cultures were used.After inducing the tumor and extracting from the brains, the PDGFb-induced tumors were cultured as tumorspheres in the absence of serum. mRNA was extracted from the cells immediately after isolation (fresh tumor, normal microenvironment) and subsequently at passages 1, 2 and 5 and VGF mRNA was analyzed by RT-qPCR. Surprisingly, a substantial and significant decrease in VGF expression was observed with time of culture (**Figure 18-A**: ANOVA followed by Tukey p=0.0001; P0 RQ of 100%, P1 reduced to 14.59%, P2 3.65% and at P5 2.406% of P0; n=5). The major difference of the in vivo and in vitro tumor microenvironment is the loss of the tumor-associated cellular compartment. Considering that, we measured in the same samples the amount of GFAP and CX3CR1 mRNA, to assess whether a loss of VGF would also correlate with a loss of tumor-associated cells. GFAP mRNA levels were reduced in 90% after culturing the isolated tumor at P1, at P2 the levels increased to 22.45% in relation to P0, which could be caused by effects of cell culture on astrocytes reactiveness, and at P5 the levels were further reduced to 11.20% (**Figure 18-B** p=0.002; n=3). CX3CR1 levels drastically dropped to 4.25% of the fresh tumor at P1, 3.87% at P2 and 3.08 at P5 (**Figure 18-C** p< 0.0001, n=3). With the use of serum-free medium the tumor cells are grown in suspension and the parenchymal cells are probably lost during the selection via *Anoikis.* Indeed, the qPCR results show that the loss of astrocytes and microglia/macrophages is accompanied by VGF loss of expression or vice versa.

To investigate if the presence of microglia and astrocytes influences VGF expression in glioma, considering they are not the source of VGF mRNA in the tumor (**Figure 16-F**), we treated the cultured cells (with more than 5 passages) with filtered astrocyte or microglia condition medium (ACM/MCM, 24 hours conditioned). The expression of VGF was partially rescued when treating the tumor cells for 48 hours with ACM, but not significantly different from control glioma medium (GCM): GCM % of relative expression (RQ) was 6.37 ± 1.8 of ACM treated cells in relation to control. The rescue was significant with MCM, % RQ of 11.48 ± 4.9 (p=0.04, n=5), the levels

rescued were similar of those of tumor cells at passage 1 (**Figure 18-A**). Using the Geltrex matrix to promote tumorspheres adherence on coverslips we performed immunofluorescence staining after treating the tumor cells with condition medium for 48 h and with the ImageJ threshold plug-in we assessed stained area of VGF staining, normalized for the cell number with DAPI. MCM increased the expression of VGF protein in 5x compared to control (p=0.0473, n=3) while astrocytes had an RQ around 1 to control.

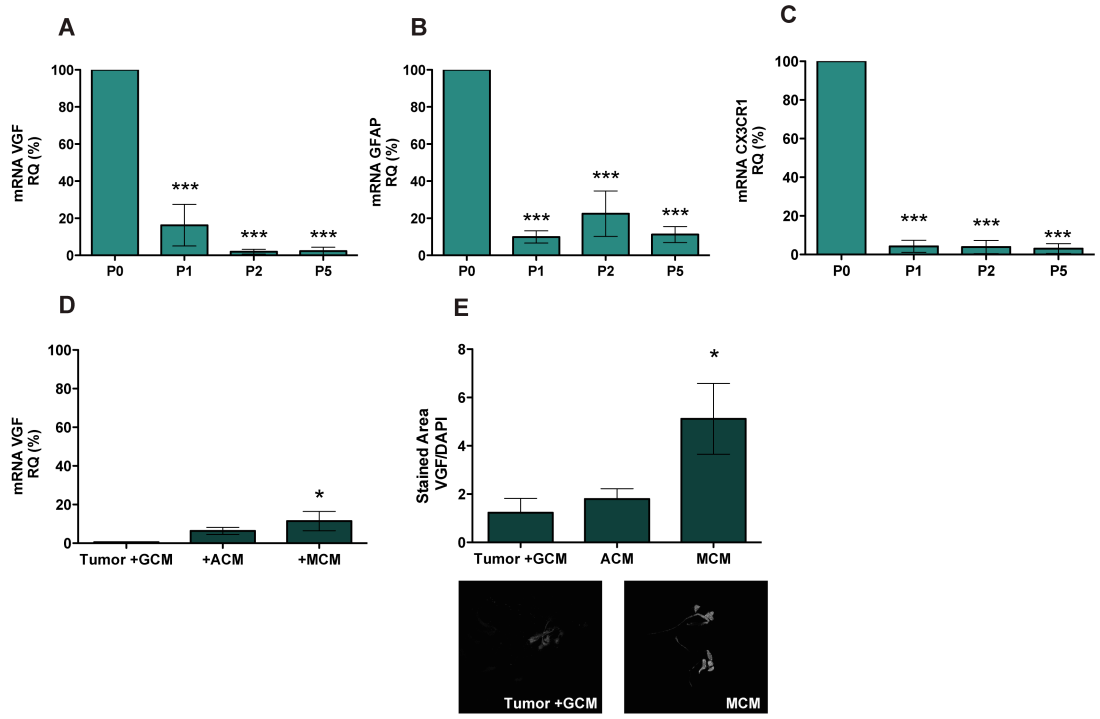

Figure 18: Loss of VGF mRNA and glial markers in vitro and rescue with MCM treatment.

(**A-C**) PDGFb-induced tumors were culture in serum-free medium and analyzed for VGF, GFAP and CX3CR1 mRNA levels with RT-qPCR at passage 0 (P0), 1, 2 and 5. Glial marker reduction indicates loss of cellular microenvironment. Graphics show % of relative quantification (RQ) to P0. Bars represent mean ± standard error of mean (SEM), stars represent one-way Anova analysis. (**A**), n=5; (**B, C**) n=3. (**D**) VGF mRNA levels of P5 tumor cells treated with conditioned medium from glioma (GCM, control), neonatal cultured astrocytes (ACM) and microglia (MCM) for 48 hours (n=5). (**E**) Immunofluorescence with VGF polyclonal of P5 tumor cells treated with GCM, ACM and MCM for 48 hours. Below the graphic representative images (20x) of the VGF staining in isolated cells (n=3).

4.I.5. **VGF protein expression correlates with Iba1 but not GFAP in vivo**

VGF expression varies not only from every tumor but also in different location of a same tumor. If the glial cells are influencing the VGF expression of the tumor cells, it is possible that levels of VGF in different samples and also different regions from a sample could be correlated with levels of glia infiltration and activation. To test this hypothesis an immufluorescence assay was performed on paraffin sections of 4 different mouse brains bearing PDGFb-induced tumors, which were stained for VGF, GFAP or Iba1 and normalized by DAPI. The correlation of Iba1 with VGF stained area per microphotography had a Pearson's r of 0.43 and R^2 of 0.188 (n=20 microphotographies from 4 different tumors; p = 0.056, **Figure 19-A**). Iba1 area stained had a Pearson's r of 0.59 and R^2 of 0.35 (n=14; P = 0.026, **Figure 19-B**), showing a positive correlation with VGF protein expression. Therefore, tumor areas with high VGF staining were areas with highly activated microglia or macrophages (or high microglia invasion), which could indicate that the presence of these cells influence the tumor-derived VGF production or that high levels of VGF attract microglia or macrophages. A significant correlation with GFAP was not observed.

4.I.6. **VGF-derived peptide influences tumor cells proliferation**

To understand why is VGF affecting the survival of proneural GBM patients we first checked for VGF influence on cell proliferation, using the in vitro BrdU-ELISA assay as readout. Primary tumorspheres (passage <5) were dissociated and plated in a confluence of 5000 cells per well (96 well plate), 7 wells per group. Geltrex (GIBCO) in a concentration of 0.1 mg/ml was used to coat the plate and promote adhesion of the cells in the absence of serum. The cells were treated for 48 hours with two VGF-derived C-terminal peptides with known relevant biological activity. TLQP-21 and TLQP-62 (BACHEM) were diluted with PBS and used in serial dilutions ranging from 1 nM to

1uM. A BrdU ELISA Kit (ROCHE) was used to measure the effects of the peptide treatment on cellular proliferation. **Figure 20-A** shows that 10 nM of TLQP-21 significantly increased the incorporation of BrdU by 17.3% compared to non-treated control (P =0.0010, n=3 paired t test) and 100 nM of TLQP-62 resulted in a significant 15% increase in BrdU incorporation (p=0.0088, n=3). Both treatments present bell-shaped dose-curves indicating sensitization of the corresponding receptor to higher doses of treatment.

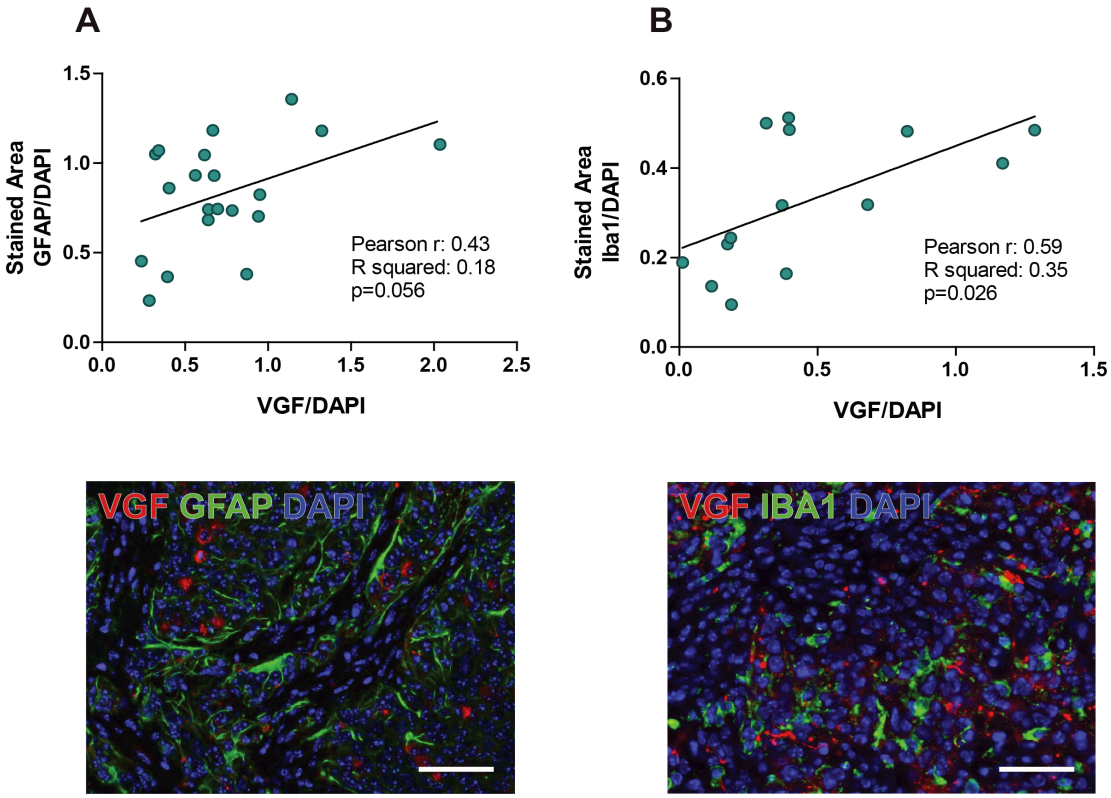

Figure 19: Correlation of intratumoral VGF protein levels with GFAP and Iba1.

PDGFb-induced tumors were fixed and stained for VGF and GFAP (**A**) or Iba1 (**B**). Several random regions of 4 different tumors were photographed and the stained areas of VGF were correlated with GFAP or Iba1 using the Pearson's r and R^2.Scale bars at the representative pictures: 50 µm.

To investigate if the increase in proliferation could also reflect differences in tumor growth, the RCAS-PDGFb-RFP tumorspheres at low passage were injected in organotypic brain slices cultures from 16 days old BL6 mice. Different cell cultures were inject in 6 independent biological replicates 24 hours after the establishment of the culture. After 72 hours of resting, the first treatment of either TLQP-21 10 nM or

TLQP-62 100 nM was added to the cultivation medium at the bottom of the insert in six well plates. The treatment was repeated every second day. Pictures of the RFP tumors were made with an inverted fluorescence microscope seven days after the start of the treatment. The pictures were analyzed with the software ImageJ and the areas were measured with the use of contrast with the threshold analytic tool. The calculations were made given the ratio of tumor area of day 7 in relation to day 0, before treatment. TLQP-21 10 µM significantly increase the tumor area in relation to control after seven days of treatment: mean control of 1.7 ± 0.16 and TLQP-21 10 nM 2.74 ± 0.36 n=11-12, p=0.02. This result is supported by the increased BrdU uptake (**Figure 20-B, C**). TLQP-62 did not significantly affected tumor size, reflecting its lower increase in proliferation in relation to TLQP-21.

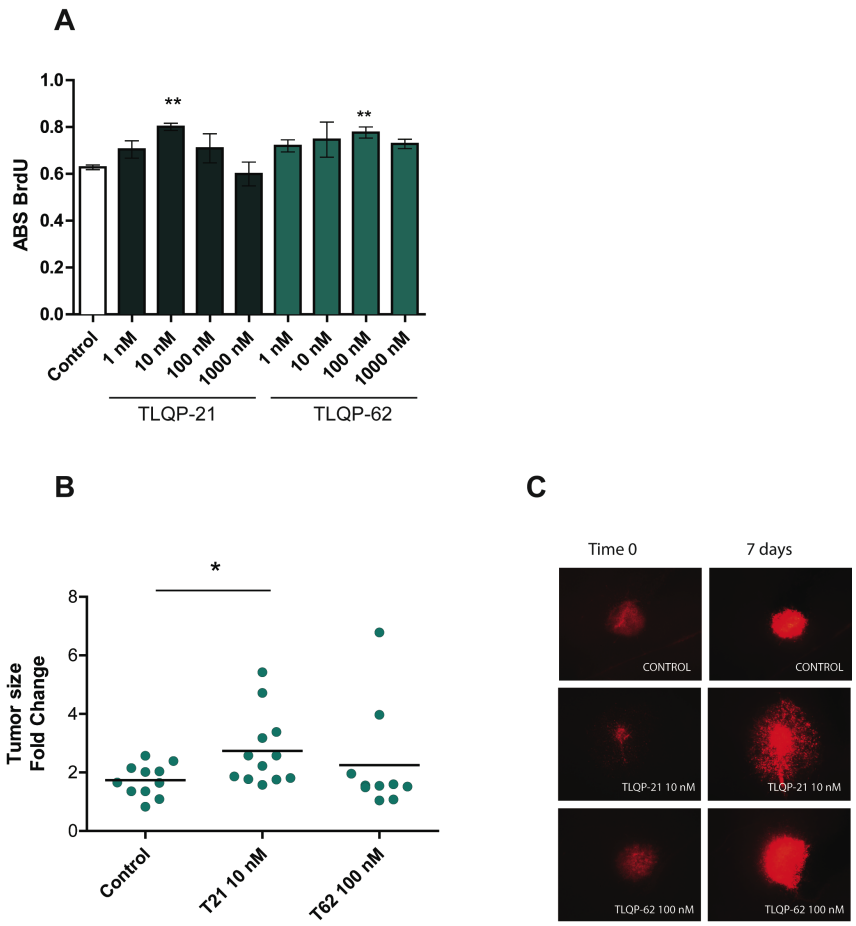

Figure 20: VGF-derived peptides increase PDGFb-derived tumor cells proliferation.

(**A**) Proliferation of cultured primary RCAS-tumor cells was determined after treatment with different doses of the VGF-derived peptides TLQP-21 and TLQP-62 for 48 hours on 96 well plates coated with Geltrex®. The

incorporation of BrdU was analyzed using an ELISA kit (ROCHE). The graphic display BrdU absorbance (ABS). 10 nM of TLQP-21 increased 17.3% the incorporation of BrdU by 17.3% compared to non-treated control (p =0.0010, n=3 paired t test) and 100 nM of TLQP-62 increased by 15% (p= 0.0088, n=3). (**B**) Injection of RCAS-RFP tumor cells on GFAP-GFP organotypic cultures treated with VGF-derived peptides. The results are expressed by the fold change of the average threshold RFP area from different slices of each brain at day 7 to day 0 before treatment. Mean control of 1.7 ± 0.16 and TLQP-21 10 nM 2.74 ± 0.36 n=11-12, p= 0.02. (**C**) Example of the images taken for the analysis at day 7 for each group of treatment, 5x magnification.

II. VGF and Microglia

4.II.1. Application of TLQP-21 induces outward rectifying potassium currents in microglia

To investigate if TLQP-21 induces membrane currents in microglia cells and characterize the TLQP-21 receptors responsible for this activation, cultured microglia were patched in voltage clamp mode and a series of de- and hyperpolarizing steps were applied repeatedly every 5 s (see Methods). TLQP-21 and ATP (as positive control) were applied via the bath perfusion system. Both TLQP-21 (100nM) and ATP (1mM) induced outward membrane currents in microglial cells, displayed for representative recordings in **Figure 21-A**. Note that ATP induced an additional inward response. Current voltage relationships are both linear at voltages positive to the reversal potential (**Figure 21-B**) and the outward kinetics for TLQP-21 and ATP induced currents where both fast opening without inactivation (**Figure 21-C**). We used three concentrations of TLQP-21 (1, 10 and 100 nM) to test whether the induced currents are dose dependent with a wash-out time of 15 min. In only 13% of the cells a response to 1 nM was measured whereas 47 % responded to 10 nM and even 93 % to 100 nM TLQP-21 (**Figure 21-D**, n = 15). Averaged current-voltage relationships are shown in **Figure 21-E** with maximum amplitudes at 60 mV membrane potentials (1 nM: 0.97 ± 0.24 (n = 2); 10 nM: 1.71 ± 0.57 (n = 7); 100 nM: 5.35 ± 1.8 pA/pF (n = 14) and reversal potentials close to the potassium equilibrium potential (~-80 mV).

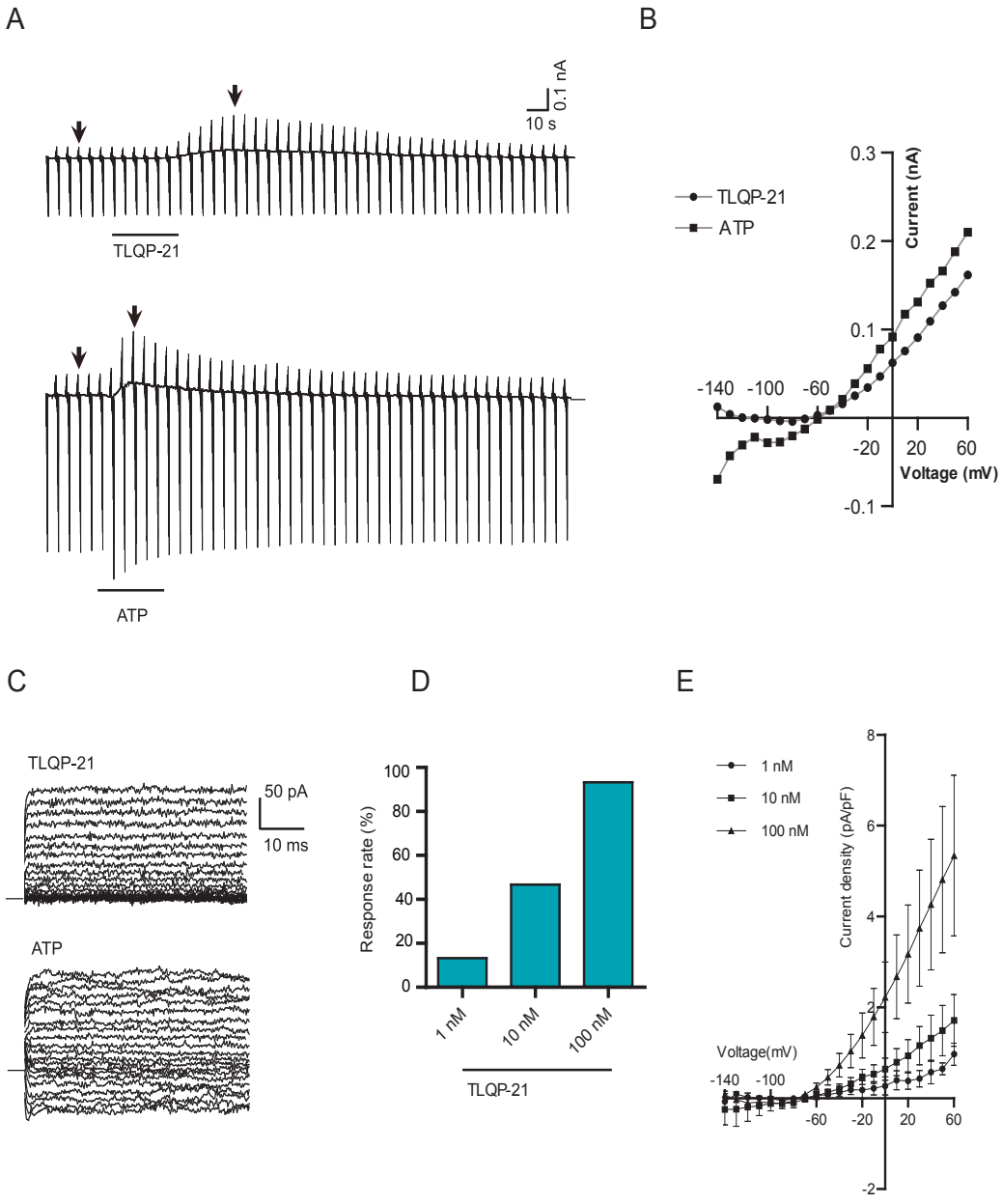

Figure 21: Application of TLQP-21 induces outward rectifying potassium currents in microglia.

(**A**): Example recordings for TLQP-21 (100 nM) and ATP induced membrane currents using repeated de- and hyperpolarizing voltage steps with a holding potential of -20 mV. (**B**): Current-voltage relationships with baseline substracted (indicated by arrows) of the TLQP-21 and ATP induced example responses are shown with similar outward currents with an additional inward current which was only recorded after ATP applications. (**C**) Kinetics of both responses are shown with a fast rising and non-inactivating channel kinetics for TLQP-21 and ATP induced currents. (**D**) Response rate for three different TLQP-21 concentrations (1, 10, 100 nM). (**E**) Averaged current voltage relationships for 1, 10 and 100 nM TLQP-21 induced currents are shown.

4.II.2. **TLQP-21-induced membrane currents in microglia are blocked by C3AR1 antagonist partially rescuing ATP responses**

To study whether the TLQP-21-induced membrane currents acted via the C3AR1 receptor, the antagonist SB290157 (named C3ARA,1μM) together with TLQP-21 (100nM) was applied to the patched cell, which was exposed to the same voltage steps protocol as previously described. ATP (1mM) was again administered as positive control, following TLQP-21 application. **Figure 22** illustrates representative recordings of this application procedure. From the 9 experiments, normal ATP response was observed in only 2 cells (**Figure 22-A**). Most of the cells had altered or absent response to ATP (77 %, n = 7, **Figure 22-B**), whereas a single ATP application always induces current responses in microglia (n = 7, **Figure 21-A**). When pre-treating the cells with C3ARA, it could be observed that the previously TLQP-21 induced outward currents are not preserved (87.5%, n=8). Regarding the ATP response, as can be observed in **Figure 22-C**, it seems that both inward and outward currents are present when TLQP-21 is blocked by the presence of the antagonist. Only in one cell a small TLQP-21 response was detected with the antagonist (12.5%, n=1, **Figure 22-D**). In this trace a maximum current density at a 60mV membrane potential of 1.32 pA/pF was observed, which is smaller than the previously described current density of 5.35 ± 1.8 pA/pF after 100nM TLQP-21 application. **Figure 22-E** depicts the conductance of the outward currents from 0 till 60 mV. Since most of the cells that were exposed to the C3ARA did not show a current increase, the average time between TLQP-21 application and peak response was established. This time point was used in order to calculate current-voltage relationships from the recordings in which microglia were treated with C3ARA. From **Figure 22-E** it can be observed that the TLQP-21 with C3ARA conductance (mean of 0.002 ± 0.004**,** n=8) is significantly reduced (P = 0.0117) when comparing to TLQP-21 100nM alone (mean of 0.096 ± 0.03, n=9). Therefore, the results show that the outward currents induced by TLQP-21 in microglia occur via C3AR1 signaling and that TLQP-21 and ATP induce similar intracellular pathways, which leads to potassium currents.

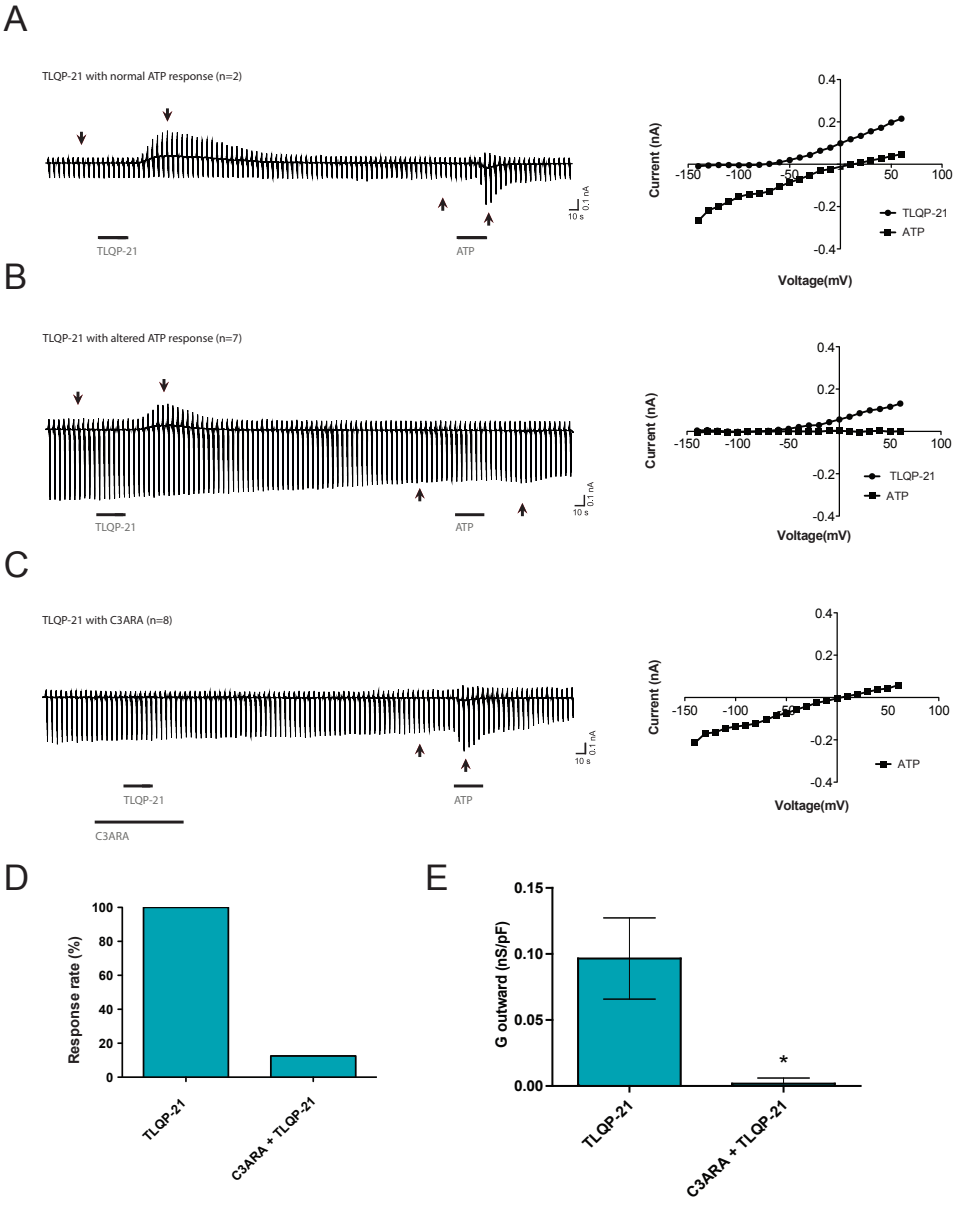

Figure 22: Application of C3ARA blocks TLQP-21-induced outward rectifying potassium currents, rescuing ATP response.

(**A-C**): Example recordings for TLQP-21 (100 nM) followed by ATP (1 mM) induced membrane currents using repeated de- and hyperpolarizing voltage steps with a holding potential of -20 mV. Current-voltage relationships with baseline substracted (indicated by arrows) of the TLQP-21 and ATP responses are shown on the right side of the corresponding trace. Examples show TLQP-21 response followed by normal ATP currents (**A**), altered ATP response (**B**) which were rescued when TLQP-21 currents were blocked with C3ARA (**C**). (**D**) Response rate for TLQP-21 (100 nM) with or without C3ARA (1 µM). (**E**) Specific outward conductance between 0 and 60 mV for TLQP-21 (100 nM) with or without C3ARA (1 µM).

4.II.3. **TLQP-21 induced intracellular calcium elevation is blocked by the C3AR1 antagonist.**

Chen et al. (2013) found a dose-dependent increase of percentage rat cultured bone marrow-derived primary macrophages responding with calcium elevations after TLQP-21 stimulation. Moreover, Chen and his colleagues observed that a 100 nM TLQP-21 application caused an intracellular Ca^{2+}-increase in 100% of the cells and that this response occurred via gC1qR. We tested whether this response pattern could be replicated in neonatal microglia from mice, since in another study using hamster ovary cells, a dose-dependent calcium signal increase could be observed, however, this effect was via C3AR1 and required ATP-priming, therefore it possibly acts upon a different intracellular pathway. We used two doses of the peptide (10 and 100 nM), followed by a washout and, thereafter, positive control application. Furthermore, we wanted to investigate whether the effect in microglia was mediated via C3AR1, therefore we also applied TLQP-21 together with the receptor antagonist. As **Figure 23** indicates, ANOVA followed by post hoc comparisons indicated that the mean percentage of cells responding to TLQP-21 10 nM had a mean of 66.89% ($p<0.0001$ to control HEPES, 16.48%,) and TLQP-21 100 nM had a mean of 90.18% ($p<0.0001$ to control HEPES). However, the condition with both TLQP-21 and antagonist (23.25%, $p>0.05$) did not significantly differ from control. The results show that the dose-dependent cellular response to TLQP-21 observed by Chen et al., (2013) could be reproduced in neonatal microglia and that this effect can be mediated by binding of TLQP-21 to the C3AR1 receptor.

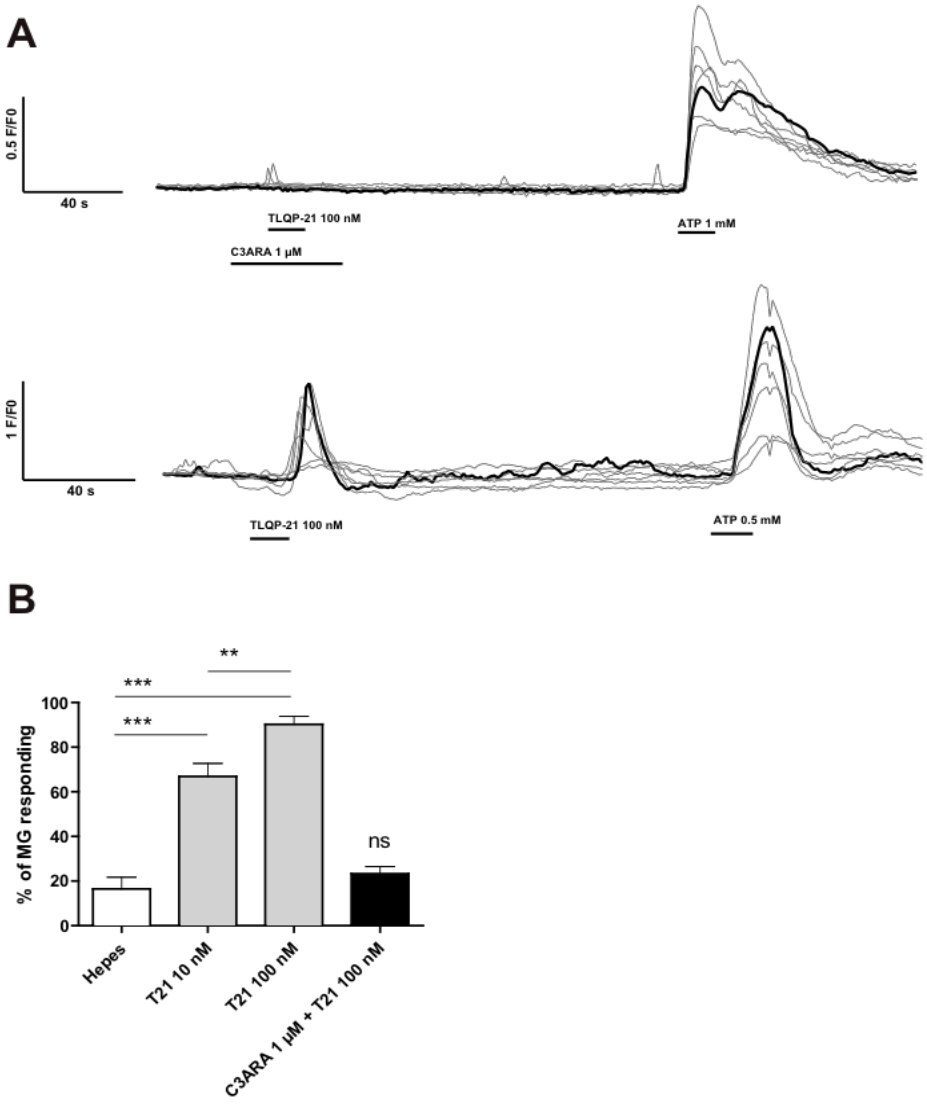

Figure 23: TLQP-21 induced intracellular calcium increase is blocked by the C3ARA.

Example traces of TLQP-21 (T21) applied to microglia cells with (**A-up**) or without C3ARA (**A-down**) are shown. ATP was used as control. (**B**) The % of cells responding to TLQP-21 admnistration was not different from control (Hepes), suggesting that C3AR1 is mediating TLQP-21 in microglia cells. Number of experiments for treated groups varied from 12-15 and for control 5.

4.II.4. **VGF-derived TLQP-21 promotes microglia migration and motility**

Different signals control microglia activation and function in the diseased brain. Microglia motility and chemotaxis are essential for monitoring the brain and dislocating towards injured areas. To assess whether VGF-induced signaling controls microglia motility and migration three assays were used. Microglial motility was first evaluated using the agarose spot assay. Agarose was mixed with TLQP-21 to create a gradient outwards the agarose spot at different concentrations. After 3 hours of incubations the cells that migrated to the inside of the agarose area were counted: 1 nM of the peptide increased the percentage of migration (in relation to control) to 239.6, 10 nM to 349.3 and 100 nM to 244%, the final result displaying a bell shape (ANOVA, p = 0.0008, 15-23 spots from four independent biological replicates) as seen in **Figure 24**. When adding TLQP-21 100 nM not only to the agarose spot but also to the medium, removing the gradient of peptide the mean percentage of migrating cell towards the spot

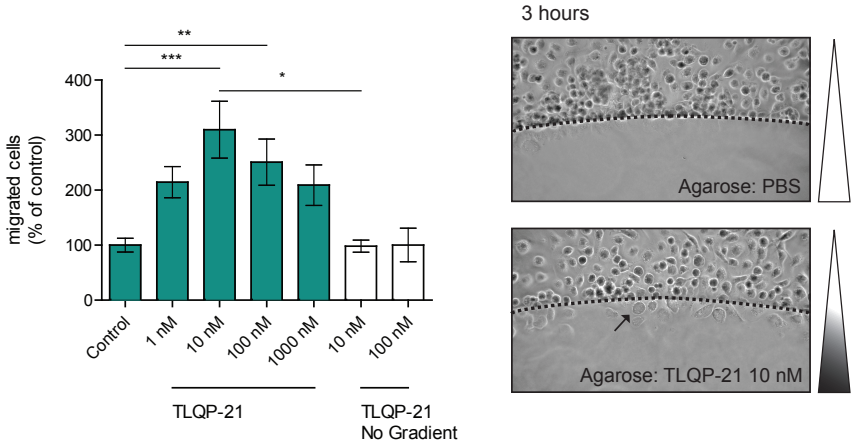

Figure 24: Effect of TLQP-21 on microglial migration in the agarose spot assay.

Microglia were plated on 35-mm cover slips with spots containing PBS or a TLQP-21. Agarose spot assay without peptide shows low microglial invasion after 3 h incubation. Microglia cells migrate towards gradient of TLQP-21, showing significant differences from control and no gradient control (peptide added in the spot and the surrounding medium at the same concentration). Bars represent the mean ± SEM. At the right side are representative pictures (100x) showing control (PBS) and TLQP-21-containing agarose spots. Dashed lines show agarose borders.

was 112.3% which was not significantly different from control. This number suggests that mostly of the observed migration is due to chemotaxis and not motility.

The scratch wound assay was performed to verify if adding TLQP-21 to the culture medium resulted in an altered microglia migration towards the less populated areas compared to control, as a result of cellular motility. At 3 hours the number of migrating cells in % of control did not significantly increase when TLQP-21 was applied: 1 nM altered the mean migration to 112 ± 65% of control, 10 nM to 132 ± 111% 100 nM to 154 ± 46 and 1000 nM to 116 ± 61% of control (**Figure 25**).

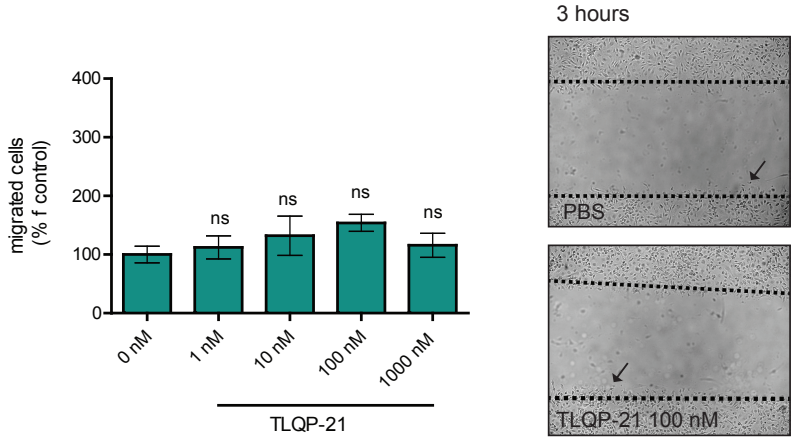

Figure 25: TLQP-21 does not induce invasion in the scratch assay.

The scratch was implemented in a layer of microglial cells, and migrating cells into the initial scratched area were analyzed after incubation for 3 h. Number of cells in the scratched zone relative to the control is expressed as mean ± SEM (n=9/group). ANOVA did not show significant differences in the treated groups vs. control. Representative pictures (100x) at 3 h after scratching of control (PBS) and treatment with TLQP-21 are shown at the right side of the image, dashed lines delineate the initial scratched area and arrows point at examples of migrated cells used for couting. A minimum of 3 technical replicates from 3 individual cultures were used to calculate the mean migratory capacity of each cell culture condition.

To better assess the effects of TLQP-21 on motility and chemotaxis individually the Boyden chamber assay was used. TLQP-21 at 1, 10, 100 and 1000 nM was added only in the bottom (positive gradient) of the chamber or also in the top (no gradient). The percentage of migrated cells to the bottom chamber through a membrane with 8 µm pores was calculated related to the untreated control. TLQP-21 100 nM increased the percentage of migration to 303 ± 47% in relation to control (**Figure 26-A**,

N=4, p = 0.0006, ANOVA). Increase in mean percentage as seen in other doses was not significant in the post hoc paired test and the resulting curve presented a bell shape as in the spot assay, although the peak in the Boyden chamber assay was higher at 100 μM instead of 10 μM as in the spot assay. No gradient did not alter the number of migrated cells from control in any concentration after 3 hours, reflecting a specific effect on chemotaxis specifically and not random motility (p=0.81). Scrambled peptide at 100 nM did not altered the migration of microglia in any gradient after 3 hours of assay (**Figure 26-B**), p=0.60.

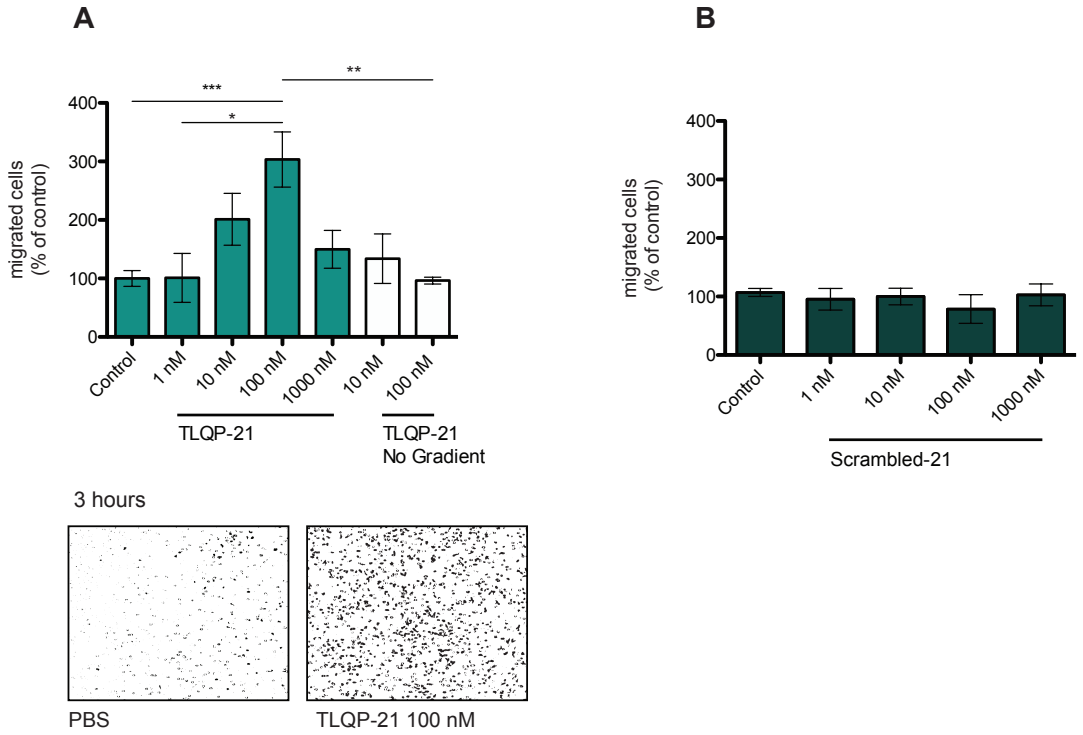

Figure 26: TLQP-21 induces chemotactic activity in the Boyden Chamber.

(**A**) Cells crossing the polycarbonate membrane (8 μm pore size) into the TLQP-21-containing lower chamber were stained by Diff-quick and were displayed in light microscopic images, later processed with ImageJ for counting. The relative increase in cell numbers compared to the PBS control is shown in a dose-dependent relationship. Boyden chamber with the peptide in the upper and lower chambers in equal concentrations did not induce chemotaxis or motility. Representative pictures (100x) from the fixed membranes used for analysis after ImageJ editing show stained migrated microglia (8-bit, high-contrast image). (**B**) Scrambled peptide did not induce an increase in migratory activity of microglia.

4.II.5. **VGF-derived peptide promotes microglia phagocytosis in vitro**

Microglia act in both physiological and pathological conditions as the brain macrophages. After demonstrating that they respond to TLQP-21 gradients and migrate towards it we assessed the effect of TLQP-21 on neonatal cultured microglia phagocytosis using a flow cytometry based phagocytosis assay. Cultured microglia were incubated for 30 minutes with a solution of FCS coated fluorescence beads in HBSS in the presence of different doses of TLQP-21. **Figure 27-C** shows the gating strategy used to identify living microglia and the bead fluorescence the analysis is based on. 1000 nM of TLQP-21 induced a significant increase of 19 % of mean phagocytic cells compared to untreated control, (**Figure 27-A, B** $p = 0.02$, $n=7$, ANOVA**)** suggesting a positive effect of TLQP-21 on microglial phagocytosis.

4.II.6. **TLQP-21 does not affect cytokine release in microglia**

Microglia is a key player in the modulation of inflammatory processes, acting through the release of pro- and anti-inflammatory cytokines. To check if VGF participates in such processes microglia were treated with TLQP-21 or scrambled and with ATP or LPS as control treatment for 12 and 24 hours. The release of cytokines into the culture medium was measured with ELISA multiplex. IL1-beta, IL6, TNF-alpha and CCL2 were analyzed after the treatment (**Figure 28-A**). IL1-beta was increased significant in relation to control after 12 hours of stimulation ($+1.6 \pm 0.46$ pg/ml) (t-test, $p=0.0135$, $n=5$). ELISA simplex was used as validation (**Figure 28-B**), but detection range was different than that from the multiplex, not reaching the necessary detection threshold to confirm the IL1-beta secretion differences observed with the multiplex assay. IL-6, CCL2 and TNF-alpha were not altered by 100 nM TLQP treatment. Overall, the results indicate that TLQP-21 does not acutely affect the release of the four measured cytokines.

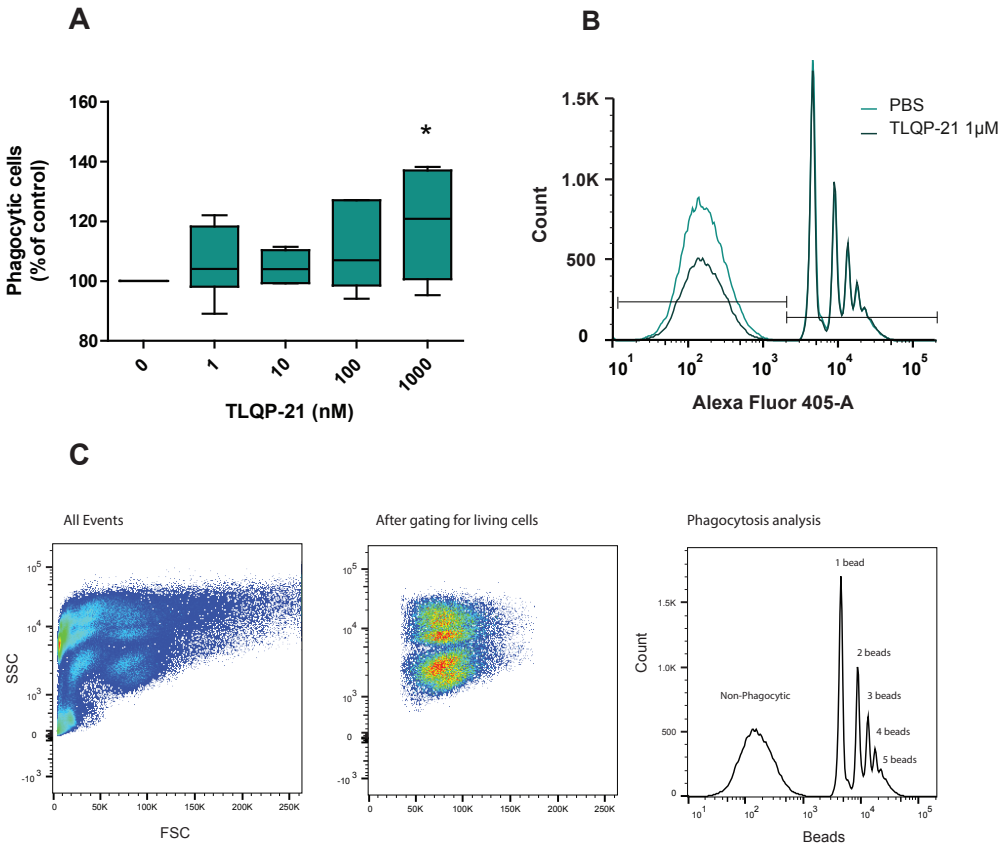

Figure 27: TLQP-21-induced phagocytosis

Neonatal mouse microglia were incubated with FCS-coated Fluoresbrite® Carboxylate Microspheres (BrightBlue, 4.5 µm beads) diluted in HBSS with TLQP-21 for 30 minutes at 37 °C. Afterwards, they were harvested, washed, stained with propidium iodide and analyzed in a flow cytometer. (**A**) TLQP-21 induces an increase of 19% of phagocytic cells at 1000 nM, p=0.02. The data is presented as the percentage of cells with bead signal (phagocytic cells) normalized by untreated control (100%), graphic represents box plot (Tukey method), ANOVA was used for statistics (n=7). (**B**) Representative imagine from the results were analyzed with FlowJo after gating for living cells excluding debris, duplets and cells stained for propidium iodide (**C**).

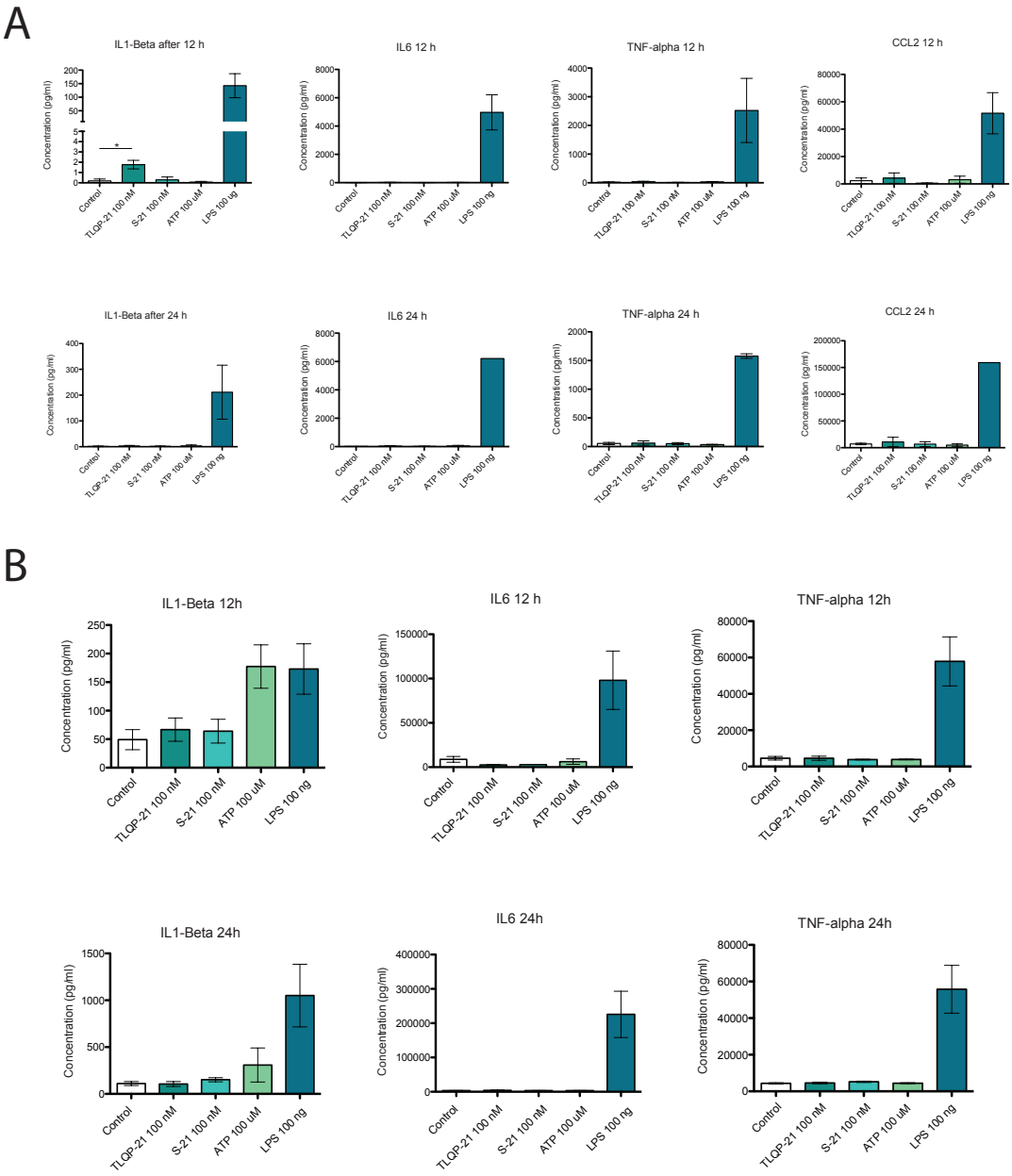

Figure 28: Cytokine release by microglia cells is not affected by TLQP-21 treatment

Microglia were treated for 12 or 24 hours with TLQP-21, scrambled-21, ATP (negative control) and LPS (positive control) and the conditioned medium was collected and analyzed with (**A**) ELISA multiplex immunoassay for IL1-beta, IL6, TNF-alpha and CCL2 simultaneously. IL1-beta was slightly increased after 12 hours of TLQP-21 but not scrambled treatment (t-test $p<0.05$, $n=5$). Samples that were out of the detection thresholds were taken as zero (for below the limit) or as the maximum detectable concentration established by the provider (for samples above the limit). (**B**) The same samples were reanalyzed with ELISA simplex for IL1-beta, IL6 and TNF-alpha. No significative difference was observed.

5. Discussion

I. The role of VGF in the glioma microenvironment

Recent technological advances (i.e. high throughput screening and sequencing) have allowed researchers to explore the molecular differences between tumor types including brain tumors on a personal level (Masui et al., 2016). Such tools made it possible to identify molecular targets that are relevant for specific subtypes of tumors. Therefore, it is important to increase knowledge about how these targets work, are regulated and how their regulation impacts a specific set of tumors.

When information from many targets is gathered it is possible to better see the molecular puzzled landscape that has so far hampered advances in brain tumor therapy. Because cancer cells are not only connected to their microenvironment (invading cells, molecules and associated matrix) but they together constitute the tumor entity. Unraveling their communication and interactions is essential for achieving personalized therapy.

We here report VGF as a new target to be expressed by proneural GBM tumor cells and to participate in the crosstalk between tumor cells and their microenvironment, finally modulating tumor growth and patient survival. Specifically, VGF expression was dependent on tumor-associated microglia cells and VGF-derived peptide treatment affected neonatal mouse microglia functions in vitro, such as migration and phagocytosis. Investigation on VGF functions is relatively recent (**Table 1**) and although it has been extensively studied in regards to its effects on energy balance and metabolism, its role on neural cellular functions is still not fully elucidated. Even less is known about VGF participation in the cancer pathology, highlighting the potential of further research.

5.I.1. **VGF is highly expressed by gliomas**

Although VGF expression has already been reported in different cancers, including neuroblastomas (Rossi et al., 1992; Rozek et al., 2013), breast cancer (Annaratone et al., 2014), lung cancer (Matsumoto et al., 2010), insulinoma, gastrointestinal cancers, parathyroid adenoma, medullary thyroid, parathyroid adenoma, pheochromocytoma and pituitary cancer (Rindi et al, 2007), little is known about its expression regulation and tumoral functions. Furthermore, to our knowledge, until now there were no reports about VGF in primary brain cancers.

In pursuance of having a clear overview of VGF expression across different tumors, an analysis was performed of different datasets from TCGA available at the cBioPortal revealing the variable VGF expression across different. Pheochromocytoma and paraganglioma were the tumors with highest VGF mRNA expression. The pheochromocytoma cell line has been the first model chosen to study VGF regulation after NGF stimulation (Levi et al., 1985). These are neuroendocrine tumors of the medulla of the adrenal glands, which normally express high amounts of VGF and the derived peptides are carefully regulated (D'Amato et al., 2008). Melanomas present very high VGF expression as well. Recent genomic profiling revealed that gain of 12q chromosomal regions including genes for VGF and GDNF are common in the invasive and metastatic melanomas, therefore these genes could play a role in invasion of these tumors (Koroknai et al., 2016).

GBM and LGG were the third and forth tumor classes with highest median VGF mRNA expression. Findings on glioma origin point out that cancer stem cells are probably originally derived from the transformation of neural stem cells, therefore it is likely that the tumor conserve many of the pathways that maintain all the aspects necessary for cell propagation, stemness and survival (Sassi et al., 2012; Toledo et al., 2015). As VGF has been already shown to control neural stem cell proliferation (Thakker-Varia et al., 2007) and neural cell survival (Severini et al., 2008; Shimazawa et al., 2010), it is possible that brain tumors maintain VGF expression for their benefit, not only for proliferation and cell survival, but also possibly for controlling of the

energy balance and cellular metabolism, functions that VGF effectively maintain in physiology (Levi et al., 2004; Bartolomucci et al., 2011).

Glioblastoma tumors are highly heterogeneous regarding their molecular profiles and clinical manifestations (Verhaak et al., 2010). VGF expression in GBM seems to reflect this fact in our analysis, showing variable expression among the different molecular subtypes but significantly higher median expression in the proneural subtype. Interestingly, proneural GBM seems to be derived from neoplastic transformation of OPC (Liu et al., 2011; Galvão et al., 2014) and these cells naturally show high VGF expression associated with the stemness maintenance, because VGF expression is lost during oligodendrocytic differentiation (Ferri et al., 2011). Other tumors that showed low VGF mRNA expression, such as hepatocellular carcinoma and acute myeloid leukemia are derived from cells that lack VGF expression (hepatocytes and hematopoietic progenitors, respectively). In summary, although VGF expression in tumors can be explained by mimicking genetic profile from the parental tissues/cells, the well-known tumor heterogeneity dictates the variable VGF expression. It has also been suggested that VGF expression in neuroendocrine tumors is activated during the neoplastic transformation, being associated with the acquired proliferation of cancer cells (Rindi et al., 2007).

We confirmed VGF expression in GBM in a mouse model of proneural GBM arising from the PDGFb-induced transformation of neural progenitors. We observed the expression first at the mRNA level, using qPCR as readout from sorted tumor cells and tumor-associated microglia and astrocytes. We compared the mRNA levels in all the groups, also including microglia and astrocytes from naïve brain and the tumor cells had a much higher relative expression of VGF mRNA. Astrocytes and microglia did not upregulated VGF expression when associated with tumors. We also confirmed VGF expression with confocal microscopy and immunohistochemistry, which revealed a widespread VGF expression in multiple regions of the tumor mainly in tumor cells or in the extracellular space. A previous study on genetic profile of sorted astrocytes from LGG and PDGFb-induced mouse GBMlike tumor revealed an 4 fold increase in VGF mRNA in astrocytes associated with GBM-like tumors in relation to LGG-associated astrocytes (Katz et al., 2012). Although we detected VGF mRNA in tumor-associated astrocytes from our samples, we never observed VGF C-terminal staining in astrocytes

associated with tumors nor in the naïve brain (not shown). Furthermore, the VGF mRNA levels in the transformed cells were much higher than in the astrocytes, therefore although astrocytes might express VGF mRNA, they are not the main source of the VGF protein, since VGF can be uniquely processed and translated in different cell types (D'Amato et al., 2008).

5.I.2. **VGF gene can predict survival in proneural glioma and affects tumor cell proliferation.**

Analysis of Kaplan Meier curves for VGF expression in each subtype, revealed that the fluctuations of VGF mRNA levels observed in these groups are correlated with the clinical outcome of the respective patients, showing that high levels of VGF by the tumors predicted shorter survival in the proneural subtype and lesser extend in the mesenchymal as well. The data indicates that VGF expression is beneficial for the glioma cells. To better explore this hypothesis we developed a GEM (using Cre-Lox) which develops tumors lacking the VGF gene (VGF KO). The floxed VGF gene is also lacking in the tumor microenvironment, as a result of using a GFAP-Cre driver, which causes recombination of on all of the GFAP-derived neural cells (only absent in microglia, during CNS development). Both VGF KO and WT were injected with the virus to induce a GBM-like tumor and the average mouse survival was compared, showing that VGF KO tumor-bearing mice survive double the time of the VGF WT tumor-bearing mice littermates. Interestingly, the outcome reflected the survival of the human proneural patients stratified in VGF high and low expression, confirming the VGF is advantageous for the tumor growth.

Indeed, when WT tumor cells were cultured and treated with VGF-derived C-terminal peptides TQLP-21 and TLQP-62 for 48 h, they increased their proliferation to more than 15% each in relation to non-treated.. An increase in cancer proliferation might be sufficient to explain the decrease in survival if the tumors are actually growing faster and larger in size. We supported this hypothesis, making use of organotypic

mouse brain slices for ex vivo culture of primary proneural glioma cells. After 7 days in culture TLQP-21, but not TLQP-62-treated cells display larger tumor areas than control.

Two studies have already explored the role of VGF in cancer proliferation, one in ovarian cancer (Brait et al., 2013) found that the tumor cells usually have VGF silenced by promoter hypermethylation and once the expression is forced with overexpression plasmids, in vitro colony formation is reduced. Interestingly, VGF methylation alone was sufficient to predict better survival for human patients of ovarian cancer, but unfortunately the effect of VGF expression itself on survival was not assessed. The second study, from the same group, was in urothelial cell carcinoma (Hayashi et al., 2014) and it was carried out in a similar way as the first one: they found increased VGF promoter hypermethylation in 20 tissue samples compared to control tissue, they forced VGF expression in commercial bladder cancer cell lines and observed a reduction in the colony formation and also metabolic cell state measured by MTT-assay, alleging there was a decrease in proliferation. The VGF expression in both studies was evaluated only by qPCR and therefore the presence of the protein is unknown. This is very important, because VGF regulation and secretion depends on multiple factors, therefore discrepancy between mRNA and protein levels is not an unexpected fact (Possenti et al., 1989; Levi et al., 2004), and therefore overexpressing VGF in a cell type that usually does not express it does not guarantee its further processing. Besides this, the methodology used by the authors to assess cellular proliferation is very rudimentary, as the colony assay actually assesses cellular survival (Rafehi et al., 2011) and MTT-assay results should not be translated to glioma cell proliferation or cytotoxicity, because it measures cellular metabolism only (Jo et al, 2015) especially when assessing the effects of targets, like VGF, which is known to affect cellular metabolism. Overall, if VGF dampens in vitro proliferation of bladder and ovarian cancers, that means that are differences in the VGF regulation and function in tumors which normally have low VGF expression in comparison to tumor with higher VGF expression, such as for GBM, considering the data herein presented. This is possible based on differential processing of VGF, since VGF-derived peptides can have opposite biological functions in a specific context, as seen by opposite effects of TLQP-21 and TLQP-62 in memory formation (Lin et al., 2015) and of TLQP-21 alone in comparison with the whole VGF precursor in energy expenditure regulation

(Bartolomucci et al., 2006). Therefore, differential VGF processing might dictate its effects on the course of the cancer pathology. In our study we found TLQP-21 to be sufficient to increase tumor cell proliferation in vitro and ex vivo. Because TLQP-62 only had an effect in vitro, the effects of TLQP-21 in tumors grown in organotypic slices might also be associated with a crosstalk with the tumor-associated parenchymal cells, which TQLP-62 may not participate in.

Taken together, these results make VGF a promising target for glioma therapy, more specifically for proneural GBM patients. Nevertheless, more studies should be carried out considering the impact on GBM proliferation and in vivo growth of other VGF-derived peptides. The involvement of VGF in other GBM subtypes should be assessed as well; it would not be surprising to learn that VGF has a different action in a different GBM molecular subtype. We hope that new studies will further analyze the impact of VGF-based therapy on other animal models and in the future on human GBM patients.

5.I.3. **Microglia and glioma crosstalks**

Tumors depend on their niche to successfully thrive. Their collaboration is intricate and can affect different aspects of the tumor signaling. In most types of GBM TAM comprise the most frequent non-transformed cell population in the tumor bulk (Charles et al., 2011), but many studies still need to be done to uncover all clinically relevant molecular communications between the tumor cells and the TAM. Our group has been studying such interactions carefully and some of the findings include the secretion of chemokines, such as GDNF (Ku et al., 2013), by glioma cells that recruit TAM, involvement of toll-like receptors in the recruitment and activation of microglia (Vinnakota et al., 2013; Hu et al., 2014) activation of TAM into a specific molecular state that is beneficial for the glioma cells (Szulzewsky et al., 2015) and finally increased tumor invasion and progress, by activation and processing of MMP dependent on TAM (Markovic et al., 2009; Vinnakota et al., 2013; Hu et al., 2014; Hu et al., 2015).

In this study we propose VGF as a new player in the TAM-cancer crosstalk, showing that levels of VGF and Iba-1 correlate in different tumor areas from mouse GBM. This correlation could occur by accumulation of TAM in tumor regions rich on VGF, meaning that VGF could be a chemoattractant, and/or microglia cells secrete factors that stimulate VGF expression/processing by glioma cells. We tested both possibilities separately. First, loss of microglia markers in vitro correlates with loss of VGF expression and the mRNA and protein expression were partially rescued upon treatment of primary GBM proneural cell lines with MCM for 48 hours, indicating that microglia can regulate VGF mRNA and protein expression by tumor cells. Some of the microglia-derived signals that trigger VGF expression might include EGF, since TAM were already shown to secrete it affecting glioma migration (Coniglio et al., 2012) and several studies reported EGF regulating VGF expression (Ferri & Possenti, 1996). Also IL-6 can increase VGF mRNA (Ferri & Possenti, 1996) and our group recently showed that IL-6 is secreted from TAM when activated by cancer stem cells (a Dzaye et al., 2016). Other neutrophins such as NGF and BDNF are known to be more secreted by microglia cells after LPS stimulation (Nakajima et al., 2001) and they can also regulate VGF (Levi et al., 1985; Thakker-Varia et al., 2007; Lin et al., 2015), thus it would be interesting to check if this also happens in the tumor microenvironment.

The astrocyte marker GFAP did not correlated in tumor regions with VGF although loss of VGF in vitro also correlated with loss of the GFAP marker.Since ACM did not upregulate VGF expression in GBM cells we conclude that tumor cells depend on microglia, but not astrocyte signals for VGF expression.

5.I.4. **VGF-derived TLQP-21 peptide is a chemoattractant for microglia**

To test the second hypothesis that VGF is able to recruit microglia to the glioma bulk, causing a correlation of the protein levels of VGF and Iba1 in vivo, giving that glioma cells produce large amounts of VGF C-terminal peptides (**Figure 16-B, C**) mouse neonatal microglia cultures were used for in vitro experiments using the C-

terminal peptide TLQP-21 as chemoattractant. TLQP-21 was chosen considering that microglia express both receptors described for it: C3AR1 and gC1qR (Hannedouche et al., 2013; Chen et al., 2013; Cero et al., 2014), both belonging to the complement system receptor family, which regulates many of microglia biological functions (Zabel & Kirsch, 2013).

For assessment of migration and chemotaxis two assays were used: the Boyden Chamber and agarose spot assay. Both had very consistent results, showing increased migratory activity of microglia towards TLQP-21 gradients with peak on 10 nM for agarose assay and 100 nM for Boyden Chamber and further reduction of the migration in higher concentrations. The difference in the peaks can be explained by the differences in the diffusion of the peptide in the two systems, TLQP-21 probably diffuses slowly in the chamber compared to the open agarose spot. Removing the gradient and only treating microglia with the peptide canceled the cell migration in both assays, meaning that the phenomena observed was a consequence of chemotaxis and not general motility. In addition scrambled peptide was used in the same concentration as control in the Boyden Chamber assay and scrambled gradients did not attracted microglia cells, conferring the effects specificity to TLQP-21 receptor signaling. To exclude the effect of cellular motility on the results observed the scratch wound assay was also performed and the results corroborated the previous findings, as we did not observe an increase in microglia migration. Our results in neonatal microglia also confirmed the TLQP-21-induced effects in RAW264.7 in vitro migration, a mouse monocytic cell line, which also express C3AR1 (Hannedouche et al., 2013). Migration was inhibited when the selective C3AR1 antagonist SB290157 was applied together with TLQP-21. The authors also propose a very interesting hypothesis based on similar results that C3a and TLQP-21 showed: that TLQP-21 has evolved to allow the chemotactic function of C3AR1 in the absence of the activation of the complete complement cascade (referring to all the biochemical steps necessary for production of the C3a factor) (Hannedouche et al., 2013).

5.I.5. **TLQP-21 can increase microglia in vitro phagocytosis but does not affect cytokine release**

The complement system participates in the signaling of many biological functions of microglia cells in physiological and pathological processes including phagocytosis (i.e. of apoptotic debris or synapses) and cytokine release (for modulation of inflammation) (Harry, 2013). In gliomas microglia phagocytosis seems to play the role of scavengers (Penfield, 1925; Hussain et al., 2006; Nickles et al., 2008; Kopatz et al., 2013), processing dead cells, including the apoptotic glioma cells, and opening space for the tumor to grow. On the other hand, this innate response from microglia can also be cytotoxic for the tumor cells and could be used for hampering the tumor growth (Hussain et al., 2006; Kopatz et al., 2013). Unfortunately, besides the large presence of TAM in the GBM bulk, not many studies have evaluated the impact of microglia phagocytosis for the tumor progression, therefore we focused only on assessing whether acute treatment of microglia with TLQP-21 could trigger or decrease bead phagocytosis by these cells, outside the tumor context. For this purpose we used neonatal microglia cultures as a model and cytometry as readout. Concomitant treatment of microglia with beads and TLQP-21 for 30 min caused a significant increase in the number of phagocytic cells, meaning that TLQP-21 receptor, C3AR1, downstream signaling pathways crosstalk with the complex actin polymerization pathways involved in the engulfment of solid particles, such as DAP12-associated signaling (Kopatz et al., 2013). Interestingly, C3AR has been recently shown for the first time to modulate microglia phagocytosis in a mouse model of Alzheimer's Disease (Lian et al., 2016). In this model C3a increased bead phagocytosis after 1 h incubation, but decreased if incubated with microglia 24 h before the incubation with the beads. The C3AR antagonist SB290157 inhibited the C3a-mediated decrease in phagocytosis.. In our model the receptor, when activated by TLQP-21, also increased the percentage of phagocytic cells, but we did not tested longer treatment with beads and peptide, first because it would increase the phagocytosis to plateau, hiding the differences between control and treated and second, because we did not aimed on investigating long-term effects of TLQP-21 involving

protein expression, but rather the acute effects of the peptide on phagocytosis. Therefore, we are the first study to show that microglia cells can acutely respond to TLQP-21 with increased phagocytic activity. Now it remains to be explored how other VGF-derived peptides can affect TAM-phagocytosis in gliomas models.

The release of cytokines from TAM has been extensively studied and correlated with the M1 or M2 states of polarization of microglia and macrophages (Hambardzumyan et al., 2015), but so far nothing is known about a potential action of VGF in modulating cytokines secretion from microglia cells. To simply answer this question we treated neonatal microglia cultures 12 and 24 hours with TLQP-21 or scrambled and analyzed the release of IL1-beta, IL6, TNF-alpha and CCL2 with ELISA. IL6, TNF-alpha and CCL2 were unaltered, but although a small increase in IL1-beta production after treatment with TLQP-21 was observed with multiplex ELISA this was not confirmed with ELISA simplex, possibly due to its limited detection ranges, indicating that the modulation of cytokine response does not involve TLQP-21-associated signaling.

Other studies showed nonetheless that C3AR signaling can modulate chemokine release in other cell types: one study using C3a as a ligand in dendritic cells showed that C3AR can modulate TNF-alpha, TNF-gamma and IL-10 release in vitro via P38 inhibition (Li et al., 2009). Since treatment of BV-2 microglial cells with the VGF-derived peptide LQEQ-19 resulted in increased P38 phosphorylation (Riedl et al., 2009), it might be that VGF processing and final concentration of the secreted peptide at the milieu is also essential for the final outcome regarding VGF effect on microglia signaling, considering that the different peptides might have opposite actions. Another study (Ingersoll et al., 2010) in BV-2 microglia cell line showed that CCL4 secretion is increased after 72 h of C3a stimulation via Erk1/2 MAPK pathway, indicating that TLQP-21 receptor C3AR1 could still be involved in the regulation of chemokines. In conclusion, more studies regarding VGF-derived peptides receptors are necessary in order to better understand VGF's full impact on the cytokine and chemokine production control in microglia cells. Other studies including treatment of microglia cells with different VGF-derived peptides will provide better insight of VGF's role on microglia biological activities, including their innate functions as phagocytic, cytotoxic and immunomodulatory cells, also in the glioma microenvironment.

II. Characterization of the TLQP-21 response in mouse microglia

5.II.1. TLQP-21-induced potassium currents and calcium signal in microglia cell is dependent on C3AR1 and can alter ATP response.

Previous studies have shown a dose-dependent cells responding with calcium elevations to TLQP-21 in macrophages and 100nM TLQP-21 application caused an intracellular calcium response in 100% of cultured brain microglia (Chen, et al., 2013). In addition, in CHO-K1 cells, which are hamster ovary cells, a dose-dependent calcium signal increase could be observed, however, this effect required ATP-priming (Hanndouche, et al., 2013). In this study, we used calcium-imaging and electrophysiological tools to further investigate the influence of VGF-derived TLQP-21 presentation to microglia. Our results indicate that TLQP-21 application to cultured microglia increases outward rectifying potassium currents in a dose-dependent manner. Similarly, enhancing TLQP-21 administration doses increases the percentage of cells responding with an intracellular calcium-concentration elevation.

Two TLQP-21 receptors have been described in previous literature. First, the globular heads of the C1q receptor, gC1qR, has been identified as binding protein for TLQP-21 by combining chemical crosslinking with mass spectrometry analysis. Moreover, western blot analysis indicated that both microglia and macrophages express gC1qR. Subsequently, siRNA was used to silence gC1qR expression in macrophages. Exposing macrophages to these siRNAs resulted in a reduced macrophage percentage reacting to TLQP-21 by calcium concentration increases (Chen, et al., 2013). Second, complement C3a-receptor-1 (C3AR1) has been associated with TLQP-21. It was observed that applying the C3AR1 antagonist, SB290157 or C3ARA, resulted in the highest reduction of the calcium response after ATP priming. Furthermore, these finding were replicated by using siRNAs against C3AR1 (Hanndouche, et al., 2013). In addition, photoaffinity labeling and β-arrestin assays indicated that TLQP-21 binds to

C3AR1 in 3T3L1 and CHO cells. However, in these cells a second binding site was not observed, which could contradict the previous described effects of TLQP-21 binding to gC1qR, at least in the described cell lines. Moreover, it seems that TLQP-21 in solution is disordered, but binding of the peptide to C3AR1 induces as folding-upon binding resulting in a α-helical conformation (Cero, et al., 2014).

In order to investigate whether the C3AR1 receptor is responsible for the TLQP-21 induced intracellular calcium and electrophysiological responses in microglia, we carried out experiments which involved combining TLQP-21 application with the receptor antagonist C3ARA. Similar to the former research on hamster ovary cells, the TLQP-21-induced increase of calcium elevations were not observed when C3AR1 was blocked in mouse microglia. Moreover, the observed outwardly rectifying potassium currents were completely diminished in almost all microglia. In conclusion, our results indicate that the C3AR1 is involved in the cellular physiological changes of microglia after TLQP-21 application.

Since in ovarian cells, ATP priming is necessary in order to get the TLQP-21 induced calcium elevations, it appears that C3AR1 is not a G_q-coupled receptor. Additionally, after pertussis toxin (PTX) application this effect was not apparent anymore for both TLQP-21 and C3a, which suggest that the receptor is either G_{i-} or G_o-coupled (Möller et al., 1997; Hanndouche, et al., 2013). Moreover, cAMP or inositol phosphate accumulation could not be detected in this signalling pathway, which rules out the involvement of $G_s/G_{i,}$ and G_q-coupled receptors. These observations led to the implication that the TLQP-21 mediated effects are G_o-coupled (Hanndouche, et al., 2013), although C3a single responses in microglia are independent on extracelullar calcium (Möller et al., 1997) and possible also TLQP-21 (Chen, et al., 2013). In microglia this ATP priming is not needed, which suggests that C3AR1 GPC could be different in glia cells, since the involvement of another receptor is not probable due to the high efficiency of C3ARA on blocking TLQP-21 responses. Therefore, future studies need to investigate the signaling pathways behind these effects and also if exists a common pathway for the calcium elevations and potassium currents and if these responses are regulating biological functions.

A remarkable finding in this research was the reduction of the ATP response after TLQP-21 application and the rescue of this reaction after C3AR1 antagonist

application. These findings suggest that TLQP-21 and ATP act upon similar pathways. It would be interesting to investigate how long this ATP alteration after TLQP-21 stimulation is maintained and whether this is mediated via the PLC-pathway. Furthermore, microglia migrates towards extracellular ATP, which is mediated by $G_{i/o}$ coupled receptors (Honda, et al., 2001). Another interesting study would be to investigate whether this TLQP-21 mediated reduction of the ATP response reduces microglial migration towards ATP and if this could be also achieved with C3a treatment.

Based on the findings here reported a model for VGF's role in the glioma-microglia communication is proposed:

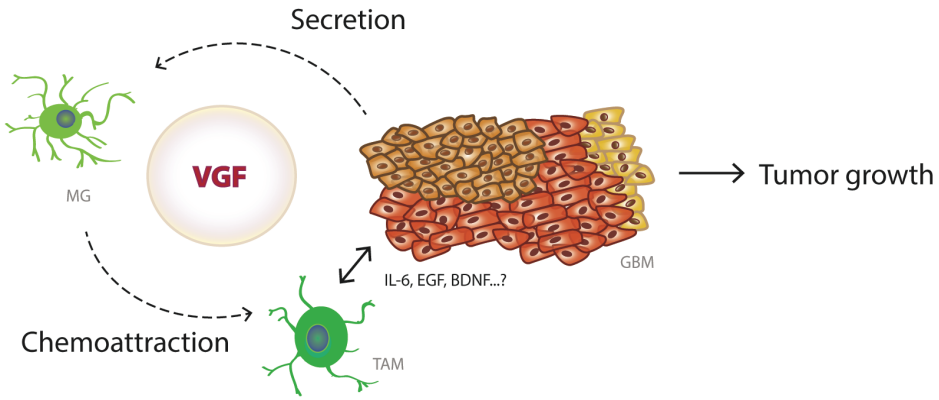

Figure 29: Model proposed for VGF's role in the glioblastoma microenvironment.

VGF expression was shown to affect survival in human GBM patients. Glioma cells highly express VGF. We propose a positive feedback loop as VGF being secreted from the tumor and attracting microglia cells (MG), which in turn trigger an increase in VGF expression by the GBM cells, possibly by secretion of VGF-producer factos such as IL-6, EGF or BNDF and thus potentiate their invasiveness and proliferation. Indeed, treatment of GBM cultures with VGF-derived peptides increased the proliferation of tumor cells. In vitro assays with VGF-derived peptide TLQP-21 confirmed that it is a potent chemoattractant for MG cells and increases MG phagocytosis.

6. OUTLOOK

In this work VGF expression by tumor cells was shown to affect survival in human GBM patients and knockout of the VGF gene in a corresponding mouse model showed a similar effect. Further investigation of the knockout tumors will be carried on to assess if the absence of VGF reduces the attraction of microglia and macrophages into the tumor, extending the present findings that VGF is a chemoattractant also in tumor-associated cells, adding evidence for a positive feedback loop between tumor and microglia. Another experiment that could be used to show that VGF expression depends on microglia cells is the ex vivo culture of glioma primary cells in organotypic brain slices depleted for microglia with clodronate (Feng et al., 2015). In the absence of these cells it would be expected that VGF expression by the glioma would be reduced over time. Also, it could be tested if forcing VGF expression by the tumor cells with activation plasmids would decrease the effect of microglia depletion on tumor size. In addition, this model is helpful for investigating the signals secreted by microglia which could trigger VGF expression by the tumor.

The VGF knockout tumors can be used as a tool for investigating pathways associated with VGF signaling. In this regards it is interesting to analyze possible alterations in metabolic pathways involved with glucose metabolism in tumor cells, which VGF coordinates in physiological processes. Based on the knowledge that brain tumor cells have abnormal glucose metabolism associated with oncogenesis (Ríos et al., 2013), it would not be surprising to find out that VGF is involved in such metabolic aberrations, resulting in increased proliferation of glioma cells.

VGF affects survival of neural cells and confers protection against apoptosis during neural development (Severini et al., 2008; Shimazawa et al., 2010). Using primary glioblastoma cultures from different molecular subtypes as a screening platform, it could be tested whether treating these cells with chemotherapeutic agents would result in different outcomes regarding cell death or senescence that could be correlated with VGF expression by the parental tumors. If tumor cells with higher VGF expression also display lower apoptotic rates, for example, it could be tested if treating

the cells lines with lower VGF expression with VGF-derived peptides, or forcing VGF expression with plasmids would result in protection against cell death induced by chemotherapeutic agents, such as temozolomide.

Taken together, the results make VGF a promising target for glioma therapy, more specifically for proneural GBM patients. Nevertheless, more studies should be carried out considering the impact on GBM proliferation and in vivo growth of other VGF-derived peptides. The involvement of VGF in other GBM subtypes should be assessed as well; it would not be surprising to learn that VGF has a different action in a different GBM molecular subtype. We hope that new studies will further analyze the impact of VGF-based therapy on other animal models and in the future on human GBM patients.

Regarding the effects of TLQP-21 in microglia biological functions it remains to be explored how TLQP-21 (and also other VGF-derived peptides) regulates phagocytosis in a glioma model. This would also help identify differences of chronic and acute exposure of microglia to VGF in phagocytosis or cytokine release. The pathways mediating these responses also need to be uncovered. It is possible that MAPKs are involved in TLQP-21 signaling in microglia. In respect to the electrophysiological properties of TLQP-21 response in microglia it remains to be assessed how potassium channels regulate microglia migration and phagocytosis, for example, and also if there is a correlation of the outwards currents induced by TLQP-21 with the increase in cytoplasmatic calcium concentrations. This could be achieved by performing simultaneous calcium imaging and patch-clamp using phospholipase c inhibitors. As this study also showed that TLQP-21 could alter ATP-related inward and outward currents it would be interesting to investigate whether pre-treatment of microglia cells with TLQP-21 could abolish ATP-induced cellular motility and chemotaxis.

7. Summary

VGF is a neuropeptide precursor that regulates several aspects of brain function and many other endocrine processes involved in metabolism. Accordingly, the dysregulation of the different VGF-derived peptides has been associated with many metabolic and neurological disorders. In this regards VGF has been also proposed as a biomarker for secretory cancers, but the literature in this topic is still scarce. Glioblastomas are very malignant brain tumors that have different molecular subtypes, which present different clinical behavior. Factors involved in the communication of the tumor cells with their associated microenvironment can be target for tumor therapy as they are essential for dictating the course of the pathology. Microglia cells were already shown to express VGF-derived peptide TLQP-21 receptors, but little is known about how they respond to it and what are the effects of the activation of these receptors on their biological innate functions.

This work showed for the first time VGF and its C-terminal peptides involvement in the glioma pathology, affecting the tumor cellular proliferation which could be associated with decreased survival of human patients, as it was demonstrated by TCGA dataset analysis that high VGF expression in GBM predicts poor survival. This data was confirmed in a mouse model of GBM lacking VGF, which resulted in a drastic increase in median survival compared to wild-types. In the wild-type mouse model high expression VGF was confirmed in both mRNA and protein levels. Furthermore, regions of the tumor with higher levels of VGF presented also higher infiltration or activation of microglia/macrophages, indicating the VGF could participate in the crosstalk between TAM and tumor cells.

It was demonstrated that in culture tumor cells lose VGF expression, which is probably due to the loss of microglia cells, which do not survive in serum-free cultures. Treating the GBM primary cultures with neonatal microglia-conditioned medium was sufficient to partially recover VGF expression, indicating that these cells indeed regulate VGF expression by the tumor cells. It was therefore proposed a positive feedback loop as VGF being secreted from the tumor and attracting microglia cells

(MG), which in turn trigger an increase in VGF expression by the GBM cells, possibly by secretion of VGF-producer factors such as IL-6, EGF or BNDF (according to the literature) and thus potentiate their invasiveness and proliferation.

In vitro assays with VGF-derived peptide TLQP-21 confirmed that it is a potent chemoattractant for MG cells and increases MG phagocytosis. TLQP-21 nevertheless, did not efficiently alter the immunomodulatory capacities of microglia cells measured by the secretion of IL1-beta, IL6, TNF-alpha and CCL2 cytokines and chemokines.

We sought to further characterize TLQP-21 response in microglia cells and therefore we performed whole-cell patch clamp during TLQP-21 treatment. We observed the presence of outward rectifying potassium currents, which reduced following ATP response, indicating a crosstalk with the ATP-associated signaling. The response was blocked by C3AR1 antagonist showing that this receptor mediates TLQP-21 currents. Stimulation of microglia with TLQP-21 also increased intracellular calcium concentration and this was also blocked by the C3AR1 antagonist. Therefore in microglia cells the biological effects of TLQP-21 are mediated by C3AR1. Is possible that both the calcium signaling and potassium currents are related and involved in microglia innate functions.

Further investigation on its multiple biological functions and many derived peptides and receptor will help clarifying the questions were here left opened. Overall the results make VGF a promising target for glioma therapy, more specifically for proneural GBM patients. We hope that new studies will further analyze the impact of VGF-based therapy on other animal models and in the future on human GBM patients.

8. Zusammenfassung

VGF ist ein Neuropeptid-Vorläufer, der am Stoffwechsel beteiligt ist und verschiedene Aspekte der Gehirnfunktion und viele andere endokrine Prozesse reguliert. Dementsprechend kann die Fehlregulation der verschiedenen VGF-abgeleiteten Peptide mit vielen metabolischen und neurologischen Störungen in Verbindung gebracht werden. In diesem Zusammenhang wurde VGF für sekretorischen Krebs auch als Biomarker vorgeschlagen, aber die Literatur zu diesem Thema ist nach wie vor spärlich. Glioblastome sind sehr bösartige Hirntumoren mit verschiedenen molekularen Subtypen und verschiedene klinischen Ausprägungen. Faktoren die an der Kommunikation zwischen Tumorzellen und den Zellen ihrer jeweiligen Mikroumgebung beteiligt sind, können für die Tumortherapie wichtige und neue Ziele darstellen. Es wurde bereits gezeigt, dass Mikroglia-Zellen Rezeptoren für das VGF-abgeleitete Peptid TLQP-21 exprimieren, aber es ist wenig darüber bekannt, wie sie darauf reagieren und welche die Wirkungen die Aktivierung dieser Rezeptoren auf die biologischen Funktionen dieser Zellen hat.

Diese Arbeit zeigt zum ersten Mal die Beteiligung von VGF und seine C-terminalen Peptide in der Gliome Pathologie. Wir zeigen, dass VGF die Tumorzellproliferation beeinflusst, die mit einer verringerten Überleben von Gliome Patienten in Verbindung gebracht werden könnten. Mit Hilfe der TCGA Datensatzes Analyse haben wir gezeigt, dass Patienten mit hoher VGF-Expression schneller sterben als Patienten mit geringer VGF-Expression. Diese Daten wurden in einem Mausmodell eines VGF knock out Tumors bestätigt , da die Mäuse mit dem VGF knock out Tumor länger überlebten als die Tiere mit einem wildtyp Tumor. Die Mäuse mit wildtyp Tumor zeigten eine hohe Expression von VGF auf mRNA und Protein-Ebene. Regionen des Tumors mit einem höheren VGF zeigten auch eine höhere Anzahl von Mikroglia / Makrophagen.

Es wurde gezeigt, dass frisch isolierte Tumorzellen mit fortschreitender Zeit in Kultur VGF-Expression verlieren, was wahrscheinlich auf den Verlust von Mikroglia-Zellen zurückzuführen ist, die in serumfreien Kulturen nicht überleben.

Behandelten wir die Tumor Primärkulturen mit neontal Mikroglia-konditionierte Medium wurde die VGF-Expression teilweise wieder hergestellt. Wir schlagen daher vor, dass VGF über eine positive Rückkopplungsschleife aus dem Tumor sezerniert wird und die Mikroglia-Zellen (MG) vom Tumor über VGF angezogen werden, was wiederum eine Erhöhung der VGF-Expression durch den GBM Zellen auslöst, die ihrerseits durch Sekretion von VGF-produzierenden Faktoren wie IL-6 , EGF oder BNDF (entsprechend der Literatur) die Invasivität und Proliferation des Tumors potenzieren.

In-vitro-Assays mit dem VGF-abgeleitetes Peptid TLQP-21 bestätigen, dass es ein potentes Chemoattraktant für MG-Zellen und erhöht MG Phagozytose ist. Andererseits verändert TLQP-21 die Sekretion von IL1-beta, IL-6, TNF-alpha und CCL2 durch Mikroglia nicht .

Whole-cell Patch-Clamp Studien mit TLQP-21-führten zu nach außen gerichteten Kaliumströme, die die folgenden ATP Reaktion reduzierten und somit eine Beteiligung an ATP-assoziierten Signalwegen nahe legen. Die Reaktion wurde durch C3AR1 Antagonist blockiert, was zeigt, dass dieser Rezeptor TLQP-21 Ströme vermittelt. Stimulation der Mikroglia mit TLQP-21 erhöhte auch die intrazelluläre Calciumkonzentration , welche auch durch den C3AR1 Antagonisten blockiert werden konnte. Daher denken wir, dass in Mikroglia-Zellen die biologischen Wirkungen von TLQP-21 durch C3AR1 vermittelt werden. Es ist möglich, dass sowohl die Calcium-Signalgebung und Kaliumströme verbunden und an Funktionen der Mikroglia beteiligt sind.

Viele biologische Funktionen von VGF gilt es noch aufzudecken, ebenso wie verschiedenen Zelltypen auf VGF-abgeleitete Peptide reagieren. Noch viel weniger ist über die Beteiligung von VGF an der Krebspathologie bekannt- Zusammenfassend sind unsere Befunde nicht nur wichtig für die Krebsforschung, sonder auch für andere Bereiche der VGF Forschung, da sie die funktionellen Veränderungen der Hirnmakrophagen nach VGF-Peptid-Stimulation zeigen, welche bei anderen Krankheitsbildern wie Alzheimer oder Schizophrenie eine große Rolle spielen könnten.

9. Bibliography

a Dzaye, O. D., Hu, F., Derkow, K., Haage, V., Euskirchen, P., Harms, C., … Kettenmann, H. (2016). Glioma stem cells but not bulk glioma cells upregulate IL-6 secretion in microglia/brain macrophages via toll-like receptor 4 signaling. *Journal of Neuropathology & Experimental Neurology*, *75*(5), 429–440.

Aguilar, E., Pineda, R., Gaytan, F., Sanchez-Garrido, M. A., Romero, M., Romero-Ruiz, A., … Pinilla, L. (2013). Characterization of the reproductive effects of the Vgf-derived peptide TLQP-21 in female rats: in vivo and in vitro studies. *Neuroendocrinology*, *98*(1), 38–50. http://doi.org/10.1159/000350323

Annaratone, L., Medico, E., Rangel, N., Castellano, I., Marchiò, C., Sapino, A., & Bussolati, G. (2013). Search for neuro-endocrine markers (chromogranin A, synaptophysin and VGF) in breast cancers. An integrated approach using immunohistochemistry and gene expression profiling. *Endocrine Pathology*, *25*(3), 219–228. http://doi.org/10.1007/s12022-013-9277-4

Badie, B., & Schartner, J. M. (2000). Flow cytometric characterization of tumor-associated macrophages in experimental gliomas. *Neurosurgery*, *46*(4), 952–957.

Bartolomucci, A., Corte, G. La, Possenti, R., Locatelli, V., Rigamonti, a E., Torsello, A., … Bulgarelli, I. (2006). TLQP-21, a VGF-derived peptide, increases energy expenditure and prevents the early phase of diet-induced obesity A. *Pnas*, *103*, 14584–9. http://doi.org/10.1073/pnas.0606102103

Bartolomucci, A., Moles, A., Levi, A., & Possenti, R. (2008). Pathophysiological role of TLQP-21: gastrointestinal and metabolic functions. *Eating and Weight Disorders : EWD*, *13*(3), e49–54.

Bartolomucci, A., Pasinetti, G. M., & Salton, S. R. J. (2010). Granins as disease-biomarkers: Translational potential for psychiatric and neurological disorders. *Neuroscience*. http://doi.org/10.1016/j.neuroscience.2010.06.057

Bartolomucci, A., Possenti, R., Mahata, S. K., Fischer-Colbrie, R., Loh, Y. P., & Salton, S. R. J. (2011). The extended granin family: Structure, function, and biomedical implications. *Endocrine Reviews*. http://doi.org/10.1210/er.2010-0027

Becher, O. J., Hambardzumyan, D., Fomchenko, E. I., Momota, H., Mainwaring, L., Bleau, A.-M., … Holland, E. C. (2008). Gli activity correlates with tumor grade in platelet-derived growth factor-induced gliomas. *Cancer Research*, *68*(7), 2241–2249. http://doi.org/10.1158/0008-5472.CAN-07-6350

Benson, D. L., & Salton, S. R. J. (1996). Expression and polarization of VGF in developing hippocampal neurons. *Developmental Brain Research*, *96*(1-2), 219–228. http://doi.org/10.1016/0165-3806(96)00108-3

Bhat, K. P. L., Balasubramaniyan, V., Vaillant, B., Ezhilarasan, R., Hummelink, K., Hollingsworth, F., … Aldape, K. (2013). Mesenchymal differentiation mediated by NF-κB promotes radiation resistance in glioblastoma. *Cancer Cell*, *24*(3), 331–346. http://doi.org/10.1016/j.ccr.2013.08.001

Brait, M., Maldonado, L., Noordhuis, M., Begum, S., Loyo, M., Poeta, M. L., … Hoque, M. O. (2013). Association of promoter methylation of VGF and PGP9.5 with ovarian cancer progression. *PLoS ONE*, *8*(9), e70878. http://doi.org/10.1371/journal.pone.0070878

Brennan, C. W., Verhaak, R. G. W., McKenna, A., Campos, B., Noushmehr, H., Salama, S. R., … McLendon, R. (2013). The somatic genomic landscape of glioblastoma. *Cell*, *155*(2), 462–477. http://doi.org/10.1016/j.cell.2013.09.034

Canu, N., Levi, A., Trani, E., Rinaldi, A. M., & Possenti, R. (1992). Molecular cloning and sequence analysis of human VGF cDNA. *Society* for *Neuroscience (Abstract)* 18, 787.

Canu, N., Possenti, R., Rinaldi, A. M., Trani, E., & Levi, A. (1997). Molecular cloning and characterization of the human VGF promoter region. *J. Neurochem.*, *68*(4), 1309–1390.

Cero, C., Vostrikov, V. V., Verardi, R., Severini, C., Gopinath, T., Braun, P. D., … Bartolomucci, A. (2014). The TLQP-21 peptide activates the G-protein-coupled receptor C3aR1 via a folding-upon-binding mechanism. *Structure*, *22*(12), 1744–1753. http://doi.org/10.1016/j.str.2014.10.001

Charles, N. a., Holland, E. C., Gilbertson, R., Glass, R., & Kettenmann, H. (2011). The brain tumor microenvironment. *Glia*, *59*(8), 1169–1180. http://doi.org/10.1002/glia.21136

Chen, Y. C., Pristerá, A., Ayub, M., Swanwick, R. S., Karu, K., Hamada, Y., … Okuse, K. (2013). Identification of a receptor for neuropeptide VGF and its role in neuropathic pain. *Journal of Biological Chemistry*, *288*(48), 34638–34646. http://doi.org/10.1074/jbc.M113.510917

Coniglio, S. J., Eugenin, E., Dobrenis, K., Stanley, E. R., West, B. L., Symons, M. H., & Segall, J. E. (2012). Microglial stimulation of glioblastoma invasion involves epidermal growth factor receptor (EGFR) and colony stimulating factor 1 receptor (CSF-1R) signaling. *Molecular Medicine (Cambridge, Mass.)*, *18*, 519–527. http://doi.org/10.2119/molmed.2011.00217

D'Amato, F., Cocco, C., Noli, B., Cabras, T., Messana, I., & Ferri, G.-L. (2012). VGF peptides upon osmotic stimuli: changes in neuroendocrine regulatory peptides 1 and 2 in the hypothalamic-pituitary-axis and plasma. *Journal of Chemical Neuroanatomy*, *44*(2), 57–65. http://doi.org/10.1016/j.jchemneu.2012.05.001

D'Amato, F., Noli, B., Angioni, L., Cossu, E., Incani, M., Messana, I., … Cocco, C. (2015). VGF peptide profiles in type 2 diabetic patients' plasma and in obese mice. *PloS One*, *10*(11), e0142333. http://doi.org/10.1371/journal.pone.0142333

D'Amato, F., Noli, B., Brancia, C., Cocco, C., Flore, G., Collu, M., … Ferri, G. L. (2008). Differential distribution of VGF-derived peptides in the adrenal medulla and evidence for their selective modulation. *Journal of Endocrinology*, *197*(2), 359–369. http://doi.org/10.1677/JOE-07-0346

Ding, X., Boney-Montoya, J., Owen, B. M., Bookout, A. L., Coate, K. C., Mangelsdorf, D. J., & Kliewer, S. A. (2012). βKlotho is required for fibroblast growth factor 21 effects on growth and metabolism. *Cell Metabolism*, *16*(3), 387–393. http://doi.org/10.1016/j.cmet.2012.08.002

Fairbanks, C. A., Peterson, C. D., Speltz, R. H., Riedl, M. S., Kitto, K. F., Dykstra, J. A., … Vulchanova, L. (2014). The VGF-derived peptide TLQP-21 contributes to inflammatory and nerve injury-induced hypersensitivity. *Pain*, *155*(7), 1229–37. http://doi.org/10.1016/j.pain.2014.03.012

Fargali, S., Garcia, A. L., Sadahiro, M., Jiang, C., Janssen, W. G., Lin, W.-J., … Salton, S. R. (2014). The granin VGF promotes genesis of secretory vesicles, and regulates circulating catecholamine levels and blood pressure. *FASEB Journal : Official Publication of the Federation of American Societies for Experimental Biology*, *28*(5), 2120–2133. http://doi.org/10.1096/fj.13-239509

Feng, X., Szulzewsky, F., Yerevanian, A., Chen, Z., Heinzmann, D., Rasmussen, R. D., … Hambardzumyan, D. (2015). Loss of CX3CR1 increases accumulation of inflammatory monocytes and promotes gliomagenesis. *Oncotarget*, *6*(17), 15077–94.

Ferri, G. L., Levi, A., & Possenti, R. (1992). A novel neuroendocrine gene product: selective VGF8a gene expression and immuno-localisation of the VGF protein in endocrine and neuronal populations. *Molecular Brain Research*, *13*(1-2), 139–143. http://doi.org/10.1016/0169-328X(92)90053-E

Ferri, G. L., & Possenti, R. (1996). vgf: A neurotrophin-inducible gene expressed in neuroendocrine tissues. *Trends in Endocrinology and Metabolism*, *7*(7), 233–239. http://doi.org/10.1016/S1043-2760(96)00123-3

Fomchenko, E. I., & Holland, E. C. (2006). Mouse models of brain tumors and their applications in preclinical trials. *Clinical Cancer Research*, *12*(18), 5288–5297. http://doi.org/10.1158/1078-0432.CCR-06-0438

Fujihara, H., Sasaki, K., Mishiro-Sato, E., Ohbuchi, T., Dayanithi, G., Yamasaki, M., … Minamino, N. (2012). Molecular characterization and biological function of neuroendocrine regulatory peptide-3 in the rat. *Endocrinology*, *153*(3), 1377–1386. http://doi.org/10.1210/en.2011-1539

Galvao, R. P., Kasina, A., McNeill, R. S., Harbin, J. E., Foreman, O., Verhaak, R. G. W., … Zong, H. (2014). Transformation of quiescent adult oligodendrocyte precursor cells into malignant glioma through a multistep reactivation process. *Proceedings of the National Academy of Sciences of the United States of America*, *111*(40), E4214–23. http://doi.org/10.1073/pnas.1414389111

Garcia, A. L., Han, S. K., Janssen, W. G., Khaing, Z. Z., Ito, T., Glucksman, M. J., … Salton, S. R. J. (2005). A prohormone convertase cleavage site within a predicted α-helix mediates sorting of the neuronal and endocrine polypeptide VGF into the regulated secretory pathway. *Journal of Biological Chemistry*, *280*(50), 41595–41608. http://doi.org/10.1074/jbc.M509122200

Ginhoux, F., Greter, M., Leboeuf, M., Nandi, S., See, P., Gokhan, S., … Merad, M. (2010). Fate mapping analysis reveals that adult microglia derive from primitive

macrophages. *Science (New York, N.Y.)*, *330*(6005), 841–5. http://doi.org/10.1126/science.1194637

Glass, R., Synowitz, M., Kronenberg, G., Walzlein, J.-H., Markovic, D. S., Wang, L.-P., … Kettenmann, H. (2005). Glioblastoma-induced attraction of endogenous neural precursor cells is associated with improved survival. *The Journal of Neuroscience : The Official Journal of the Society for Neuroscience*, *25*(10), 2637–2646. http://doi.org/10.1523/JNEUROSCI.5118-04.2005

Goffart, N., Kroonen, J., & Rogister, B. (2013). Glioblastoma-initiating cells: Relationship with neural stem cells and the micro-environment. *Cancers*, *5*(3), 1049–1071. http://doi.org/10.3390/cancers5031049

Hahm, S., Fekete, C., Mizuno, T. M., Windsor, J., Yan, H., Boozer, C. N., … Salton, S. R. J. (2002). VGF is required for obesity induced by diet, gold thioglucose treatment, and agouti and is differentially regulated in pro-opiomelanocortin- and neuropeptide Y-containing arcuate neurons in response to fasting. *The Journal of Neuroscience : The Official Journal of the Society for Neuroscience*, *22*(16), 6929–6938. http://doi.org/20026687

Hahm, S., Mizuno, T. M., Wu, T. J., Wisor, J. P., Priest, C. a., Kozak, C. a., … Salton, S. R. J. (1999). Targeted deletion of the Vgf gene indicates that the encoded secretory peptide precursor plays a novel role in the regulation of energy balance. *Neuron*, *23*, 537–548. http://doi.org/10.1016/S0896-6273(00)80806-5

Hambardzumyan, D., Amankulor, N. M., Helmy, K. Y., Becher, O. J., & Holland, E. C. (2009). Modeling adult gliomas using RCAS/t-va technology. *Translational Oncology*, *2*(2), 89–95. http://doi.org/10.1593/tlo.09100

Hambardzumyan, D., Cheng, Y. K., Haeno, H., Holland, E. C., & Michor, F. (2011). The probable cell of origin of NF1- and PDGF-Driven glioblastomas. *PLoS ONE*, *6*(9). http://doi.org/10.1371/journal.pone.0024454

Hambardzumyan, D., Gutmann, D. H., & Kettenmann, H. (2015). The role of microglia and macrophages in glioma maintenance and progression. *Nature Neuroscience*, *19*(1), 20–27. http://doi.org/10.1038/nn.4185

Han, S., Zhang, C., Li, Q., Dong, J., Liu, Y., Huang, Y., … Wu, A. (2014). Tumour-infiltrating CD4(+) and CD8(+) lymphocytes as predictors of clinical outcome in glioma. *British Journal of Cancer*, *110*(10), 2560–2568. http://doi.org/10.1038/bjc.2014.162

Hanisch, U.-K. K., & Kettenmann, H. (2007). Microglia: active sensor and versatile effector cells in the normal and pathologic brain. *Nature Neuroscience*, *10*(11), 1387–1394. http://doi.org/10.1038/nn1997

Hannedouche, S., Beck, V., Leighton-Davies, J., Beibel, M., Roma, G., Oakeley, E. J., … Bassilana, F. (2013). Identification of the C3a receptor (C3AR1) as the target of the VGF-derived peptide TLQP-21 in rodent cells. *Journal of Biological Chemistry*, *288*(38), 27434–27443. http://doi.org/10.1074/jbc.M113.497214

Harry, G. J. (2013). Microglia during development and aging. *Pharmacology and Therapeutics*. http://doi.org/10.1016/j.pharmthera.2013.04.013 Associate Editor: C. Pope

Hawley, R. J., Scheibe, R. J., & Wagner, J. A. (1992). NGF induces the expression of the VGF gene through a cAMP response element. *The Journal of Neuroscience : The Official Journal of the Society for Neuroscience*, *12*(7), 2573–2581.

Hayashi, M., Bernert, H., Kagohara, L. T., Maldonado, L., Brait, M., Schoenberg, M., … Hoque, M. O. (2014). Epigenetic inactivation of VGF associated with Urothelial Cell Carcinoma and its potential as a non-invasive biomarker using urine. *Oncotarget*, *5*(10), 3350–3361.

Honda, S., Sasaki, Y., Ohsawa, K., Imai, Y., Nakamura, Y., Inoue, K., & Kohsaka, S. (2001). Extracellular ATP or ADP induce chemotaxis of cultured microglia

through Gi/o-coupled P2Y receptors. *The Journal of Neuroscience : The Official Journal of the Society for Neuroscience*, *21*(6), 1975–1982.

Hu, F., Ku, M.-C., Markovic, D., a Dzaye, O. D., Lehnardt, S., Synowitz, M., … Kettenmann, H. (2014). Glioma-associated microglial MMP9 expression is upregulated by TLR2 signaling and sensitive to minocycline. *International Journal of Cancer*, *135*(11), 2569–2578. http://doi.org/10.1002/ijc.28908

Huang, J. T.-J., Leweke, F. M., Oxley, D., Wang, L., Harris, N., Koethe, D., … Bahn, S. (2006). Disease biomarkers in cerebrospinal fluid of patients with first-onset psychosis. *PLoS Medicine*, *3*(11), e428. http://doi.org/10.1371/journal.pmed.0030428

Huang, Y., Hoffman, C., Rajappa, P., Kim, J. H., Hu, W., Huse, J., … Greenfield, J. P. (2014). Oligodendrocyte progenitor cells promote neovascularization in glioma by disrupting the blood-brain barrier. *Cancer Research*, *74*(4), 1011–1121. http://doi.org/10.1158/0008-5472.CAN-13-1072

Hussain, S. F., Yang, D., Suki, D., Aldape, K., Grimm, E., & Heimberger, A. B. (2006). The role of human glioma-infiltrating microglia/macrophages in mediating antitumor immune responses. *Neuro-Oncology*, *8*(3), 261–279. http://doi.org/10.1215/15228517-2006-008

Hussain, S. F., Yang, D., Suki, D., Grimm, E., & Heimberger, A. B. (2006). Innate immune functions of microglia isolated from human glioma patients. *Journal of Translational Medicine*, *4*, 15. http://doi.org/10.1186/1479-5876-4-15

Ingersoll, S. A., Martin, C. B., Barnum, S. R., & Martin, B. K. (2010). CNS-specific expression of C3a and C5a exacerbate demyelination severity in the cuprizone model. *Molecular Immunology*, *48*(1-3), 219–230. http://doi.org/10.1016/j.molimm.2010.08.007

Janeway, C. A., Travers, P., Walport, M., & Shlomchik, M. (2001). Immunobiology: The immune system in health and disease. *Immuno Biology 5*, 892. http://doi.org/10.1111/j.1467-2494.1995.tb00120.x

Jethwa, P. H., & Ebling, F. J. P. (2008). Role of VGF-derived peptides in the control of food intake, body weight and reproduction. *Neuroendocrinology*, *88*(2), 80–87. http://doi.org/10.1159/000127319

Jiang, C., & Salton, S. R. (2013). The Role of Neurotrophins in Major Depressive Disorder. *Translational Neuroscience*, *4*(1), 46–58. http://doi.org/10.2478/s13380-013-0103-8

Jo, H. Y., Kim, Y., Park, H. W., Moon, H. E., Bae, S., Kim, J., … Paek, S. H. (2015). The unreliability of MTT assay in the cytotoxic test of primary cultured glioblastoma cells. *Experimental Neurobiology*, 24(3), 235–245. http://doi.org/10.5607/en.2015.24.3.235

Katz, A. M., Amankulor, N. M., Pitter, K., Helmy, K., Squatrito, M., & Holland, E. C. (2012). Astrocyte-specific expression patterns associated with the PDGF-induced glioma microenvironment. *PLoS ONE*, *7*(2), e32453. http://doi.org/10.1371/journal.pone.0032453

Kennedy, B. C., Showers, C. R., Anderson, D. E., Anderson, L., Canoll, P., Bruce, J. N., & Anderson, R. C. E. (2013). Tumor-associated macrophages in gGlioma: Friend or foe? *Journal of Oncology*, *2013*, 486912. http://doi.org/10.1155/2013/486912

Kim, J.-W., Rhee, M., Park, J.-H., Yamaguchi, H., Sasaki, K., Minamino, N., … Yoon, K.-H. (2015). Chronic effects of neuroendocrine regulatory peptide (NERP-1 and -2) on insulin secretion and gene expression in pancreatic beta-cells. *Biochemical and Biophysical Research Communications*, *457*(2), 148–153. http://doi.org/10.1016/j.bbrc.2014.12.067

Klos, A. (2013). International Union of Basic and Clinical Pharmacology, *64*(1), 1–15. Retrieved from http://www.iuphar.org/

Klos, A., Tenner, A. J., Johswich, K. O., Ager, R. R., Reis, E. S., & Köhl, J. (2009). The role of the anaphylatoxins in health and disease. *Molecular Immunology*, *46*(14), 2753–2766. http://doi.org/10.1016/j.molimm.2009.04.027

Kopatz, J., Beutner, C., Welle, K., Bodea, L. G., Reinhardt, J., Claude, J., … Neumann, H. (2013). Siglec-h on activated microglia for recognition and engulfment of glioma cells. *Glia*, *61*(7), 1122–1133. http://doi.org/10.1002/glia.22501

Koroknai, V., Ecsedi, S., Vízkeleti, L., Kiss, T., Szász, I., Lukács, A., … Balázs, M. (2016). Genomic profiling of invasive melanoma cell lines by array comparative genomic hybridization. *Melanoma Research*, *26*(2).

Ku, M.-C., Wolf, S. A., Respondek, D., Matyash, V., Pohlmann, A., Waiczies, S., … Kettenmann, H. (2013). GDNF mediates glioblastoma-induced microglia attraction but not astrogliosis. *Acta Neuropathologica*, *125*(4), 609–620. http://doi.org/10.1007/s00401-013-1079-8

Le, D. M., Besson, A., Fogg, D. K., Choi, K.-S., Waisman, D. M., Goodyer, C. G., … Yong, V. W. (2003). Exploitation of astrocytes by glioma cells to facilitate invasiveness: a mechanism involving matrix metalloproteinase-2 and the urokinase-type plasminogen activator-plasmin cascade. *The Journal of Neuroscience : The Official Journal of the Society for Neuroscience*, *23*(10), 4034–4043.

Levi, A., Eldridge, J. D., & Paterson, B. M. (1985). Molecular cloning of a gene sequence regulated by nerve growth factor. *Science, 229*(4711), 393–395.

Levi, A., Ferri, G.-L., Watson, E., Possenti, R., & Salton, S. R. J. (2004). Processing, distribution, and function of VGF, a neuronal and endocrine peptide precursor.

Cellular and Molecular Neurobiology, *24*(4), 517–33. http://doi.org/10.1023/b:cemn.0000023627.79947.22

Lewis, J. E., Brameld, J. M., & Jethwa, P. H. (2015). Neuroendocrine role for VGF. *Frontiers in Endocrinology*, *6*(February), 1–8. http://doi.org/10.3389/fendo.2015.00003

Li, K., Anderson, K. J., Peng, Q., Noble, A., Lu, B., Kelly, A. P., … Sacks, S. H. (2009). Cyclic AMP plays a critical role in C3a-receptormediated regulation of dendritic cells in antigen uptake and T-cell stimulation Cyclic AMP plays a critical role in C3a-receptor – mediated regulation of dendritic cells in antigen uptake and T-cell stimulat. *Regulation*, *112*(13), 5084–5094. http://doi.org/10.1182/blood-2008-05-156646

Lian, H., Litvinchuk, A., Chiang, A. C.-A., Aithmitti, N., Jankowsky, J. L., & Zheng, H. (2016). Astrocyte-microglia cross talk through complement activation modulates amyloid pathology in mouse models of Alzheimer's Disease. *Journal of Neuroscience*, *36*(2), 577–589. http://doi.org/10.1523/JNEUROSCI.2117-15.2016

Liang, C.-C., Park, A. Y., & Guan, J.-L. (2007). In vitro scratch assay: a convenient and inexpensive method for analysis of cell migration in vitro. *Nature Protocols*, *2*(2), 329–333. http://dx.doi.org/10.1038/nprot.2007.30

Lin, W.-J., Jiang, C., Sadahiro, M., Bozdagi, O., Vulchanova, L., Alberini, C. M., & Salton, S. R. (2015). VGF and its C-terminal peptide TLQP-62 regulate memory formation in hippocampus via a BDNF-TrkB-dependent mechanism. *Journal of Neuroscience*, *35*(28), 10343–10356. http://doi.org/10.1523/JNEUROSCI.0584-15.2015

Lin, W.-J., & Salton, S. R. (2013). The regulated secretory pathway and human disease: insights from gene variants and single nucleotide polymorphisms. *Frontiers in Endocrinology*, *4*(August), 96. http://doi.org/10.3389/fendo.2013.00096

Liu, C., Sage, J. C., Miller, M. R., Verhaak, R. G. W., Hippenmeyer, S., Vogel, H., … Zong, H. (2011). Mosaic analysis with double markers reveals tumor cell of origin in glioma. *Cell*, *146*(2), 209–221. http://doi.org/10.1016/j.cell.2011.06.014

Liu, J. W., Andrews, P. C., Mershon, J. L., Yan, C., Allen, D. L., & Ben-Jonathan, N. (1994). Peptide V: A VGF-derived neuropeptide purified from bovine posterior pituitary. *Endocrinology*, *135*(6), 2742–2748. http://doi.org/10.1210/en.135.6.2742

Liu, X., & Ling, Z.-Q. (2015). Role of isocitrate dehydrogenase 1/2 (IDH 1/2) gene mutations in human tumors. *Histology and Histopathology*, *30*(10), 1155–1160. http://doi.org/10.14670/HH-11-643

Lively, S., & Schlichter, L. C. (2013). The microglial activation state regulates migration and roles of matrix-dissolving enzymes for invasion. *Journal of Neuroinflammation*, *10*(1), 75. http://doi.org/10.1186/1742-2094-10-75

Lombardo, A., Rabacchi, S. A., Cremisi, F., Pizzorusso, T., Cenni, M. C., Possenti, R., … Maffei, L. (1995). A developmentally regulated nerve growth factor-induced gene, VGF, is expressed in geniculocortical afferents during synaptogenesis. *Neuroscience*, *65*(4), 997–1008. http://doi.org/0306-4522(94)00538-G

Louis, D. N., Perry, A., Reifenberger, G., von Deimling, A., Figarella-Branger, D., Cavenee, W. K., … Ellison, D. W. (2016). The 2016 World Health Organization Classification of Tumors of the Central Nervous System: a summary. *Acta Neuropathologica*, *131*(6), 803–820. http://doi.org/10.1007/s00401-016-1545-1

Mamane, Y., Chan, C. C., Lavallee, G., Morin, N., Xu, L. J., Huang, J., … Mancini, J. A. (2009). The C3a anaphylatoxin receptor is a key mediator of insulin resistance and functions by modulating adipose tissue macrophage infiltration and activation. *Diabetes*, *58*(9), 2006–2017. http://doi.org/10.2337/db09-0323

Markovic, D. S., Vinnakota, K., Chirasani, S., Synowitz, M., Raguet, H., Stock, K., … Kettenmann, H. (2009). Gliomas induce and exploit microglial MT1-MMP expression for tumor expansion. *Proceedings of the National Academy of Sciences of the United States of America*, *106*(30), 12530–12535. http://doi.org/10.1073/pnas.0804273106

Masui, K., Mischel, P. S., & Reifenberger, G. (2016). *Molecular classification of gliomas*. *Gliomas* (1st ed., Vol. 134). Elsevier B.V. http://doi.org/10.1016/B978-0-12-802997-8.00006-2

Matsumoto, T., Kawashima, Y., Nagashio, R., Kageyama, T., Kodera, Y., Jiang, S.-X., … Sato, Y. (2009). A new possible lung cancer marker: VGF detection from the conditioned medium of pulmonary large cell neuroendocrine carcinoma-derived cells using secretome analysis. *The International Journal of Biological Markers*, *24*(4), 282–285.

Matsuo, T., Yamaguchi, H., Kageyama, H., Sasaki, K., Shioda, S., Minamino, N., & Nakazato, M. (2010). Localization of neuroendocrine regulatory peptide-1 and-2 in human tissues. *Regulatory Peptides*, *163*(1-3), 43–48. http://doi.org/10.1016/j.regpep.2010.04.007

Melis, M. R., Sanna, F., Succu, S., Ferri, G. L., & Argiolas, A. (2012). Neuroendocrine regulatory peptide-1 and neuroendocrine regulatory peptide-2 influence differentially feeding and penile erection in male rats: sites of action in the brain. *Regulatory Peptides*, *177*(1-3), 46–52. http://doi.org/10.1016/j.regpep.2012.04.007

Mishiro-Sato, E., Sasaki, K., Matsuo, T., Kageyama, H., Yamaguchi, H., Date, Y., … Minamino, N. (2010). Distribution of neuroendocrine regulatory peptide-1 and -2, and proteolytic processing of their precursor VGF protein in the rat. *Journal of Neurochemistry*, *114*(4), 1097–1106. http://doi.org/10.1111/j.1471-4159.2010.06827.x

Moin, A. S. M., Yamaguchi, H., Rhee, M., Kim, J.-W., Toshinai, K., Waise, T. M. Z., … Nakazato, M. (2012). Neuroendocrine regulatory peptide-2 stimulates glucose-induced insulin secretion in vivo and in vitro. *Biochemical and Biophysical Research Communications*, *428*(4), 512–517. http://doi.org/10.1016/j.bbrc.2012.10.073

Möller, T., Nolte, C., Burger, R., Verkhratsky, a, & Kettenmann, H. (1997). Mechanisms of C5a and C3a complement fragment-induced [Ca2+]i signaling in mouse microglia. *The Journal of Neuroscience : The Official Journal of the Society for Neuroscience*, *17*(2), 615–624.

Moss, A., Ingram, R., Koch, S., Theodorou, A., Low, L., Baccei, M., … Fitzgerald, M. (2008). Origins, actions and dynamic expression patterns of the neuropeptide VGF in rat peripheral and central sensory neurones following peripheral nerve injury. *Molecular Pain*, *4*, 62. http://doi.org/10.1186/1744-8069-4-62

Nakajima, K., Honda, S., Tohyama, Y., Imai, Y., Kohsaka, S., & Kurihara, T. (2001). Neurotrophin secretion from cultured microglia. *Journal of Neuroscience Research*, *65*(4), 322–331. http://doi.org/10.1002/jnr.1157

Nickles, D., Abschuetz, A., Zimmer, H., Kees, T., Geibig, R., Spiess, E., & Régnier-Vigouroux, A. (2008). End-stage dying glioma cells are engulfed by mouse microglia with a strain-dependent efficacy. *Journal of Neuroimmunology*, *197*(1), 10–20. http://doi.org/10.1016/j.jneuroim.2008.03.022

Noli, B., Brancia, C., D'Amato, F., Ferri, G.-L., & Cocco, C. (2014). VGF changes during the estrous cycle: a novel endocrine role for TLQP peptides? *PloS One*, *9*(10), e108456. http://doi.org/10.1371/journal.pone.0108456

Noli, B., Brancia, C., Pilleri, R., D'Amato, F., Messana, I., Manconi, B., … Cocco, C. (2015). Photoperiod Regulates vgf-Derived Peptide Processing in Siberian Hamsters. *PloS One*, *10*(11), e0141193. http://doi.org/10.1371/journal.pone.0141193

Norgauer, J., Dobos, G., Kownatzki, E., Dahinden, C., Burger, R., Kupper, R., & Gierschik, P. (1993). Complement fragment C3a stimulates Ca2+ influx in neutrophils via a pertussis-toxin-sensitive G protein. *European Journal of Biochemistry*, *217*(1), 289–294. http://doi.org/10.1111/j.1432-1033.1993.tb18245.x

Oberheim, N. A., Goldman, S. A., & Nedergaard, M. (2012). Heterogeneity of astrocytic form and function. *Methods in Molecular Biology*, *814*, 23–45. http://doi.org/10.1007/978-1-61779-452-0_3

Olah, M., Raj, D., Brouwer, N., De Haas, A. H., Eggen, B. J. L., Den Dunnen, W. F. A., … Boddeke, H. W. G. M. (2012). An optimized protocol for the acute isolation of human microglia from autopsy brain samples. *Glia*, *60*(1), 96–111. http://doi.org/10.1002/glia.21251

Orihuela, R., Mcpherson, C. A., & Harry, G. J. (2015). Microglial M1/M2 polarization and metabolic states. *British Journal of Pharmacology*, 649–665. http://doi.org/10.1111/bph.13139

Ostrom, Q. T., Gittleman, H., Liao, P., Rouse, C., Chen, Y., Dowling, J., … Barnholtz-Sloan, J. (2014). CBTRUS Statistical Report: Primary Brain and Central Nervous System Tumors Diagnosed in the United States in 2007–2011. *Neuro-Oncology*, *16*(Suppl 4), iv1–iv63. http://doi.org/10.1093/neuonc/nou223

van den Pol, A. N., Decavel, C., Levi, A., & Paterson, B. (1989). Hypothalamic expression of a novel gene product, VGF: immunocytochemical analysis. *J Neurosci*, *9*(12), 4122–4137.

Patel, A. P., Tirosh, I., Trombetta, J. J., Shalek, A. K., Gillespie, S. M., Wakimoto, H., … Bernstein, B. E. (2014). Single-cell RNA-seq highlights intratumoral heterogeneity in primary glioblastoma. *Science*, *344*(6190), 1396–1401

Peerschke, E. I. B., Yin, W., & Ghebrehiwet, B. (2008). Platelet mediated complement activation. *Advances in Experimental Medicine and Biology*, *632*, 81–91.

Penfield, W. (1925). Microglia and the Process of Phagocytosis in Gliomas. *The American Journal of Pathology*, *1*(1), 77–90.15.

Peng, Q., Li, K., Sacks, S. H., & Zhou, W. (2009). The role of anaphylatoxins C3a and C5a in regulating innate and adaptive immune responses. *Inflammation & Allergy Drug Targets*, *8*(3), 236–246. http://doi.org/10.2174/187152809788681038

Perry, A., & Wesseling, P. (2016). Histologic classification of gliomas. *Gliomas* (1st ed., Vol. 134). Elsevier B.V. http://doi.org/10.1016/B978-0-12-802997-8.00005-0

Petrella, C., Broccardo, M., Possenti, R., Severini, C., & Improta, G. (2012). TLQP-21, a VGF-derived peptide, stimulates exocrine pancreatic secretion in the rat. *Peptides*, *36*(1), 133–136. http://doi.org/10.1016/j.peptides.2012.03.035

Petrocchi Passeri, P., Biondini, L., Mongiardi, M. P., Mordini, N., Quaresima, S., Frank, C., … Possenti, R. (2013). Neuropeptide TLQP-21, a VGF internal fragment, modulates hormonal gene expression and secretion in GH3 cell line. *Neuroendocrinology*, *97*(3), 212–224. http://doi.org/10.1159/000339855

Pinilla, L., Pineda, R., Gaytan, F., Romero, M., Garcia-Galiano, D., Sanchez-Garrido, M. A., … Aguilar, E. (2011). Characterization of the reproductive effects of the anorexigenic VGF-derived peptide TLQP-21: in vivo and in vitro studies in male rats. *American Journal of Physiology. Endocrinology and Metabolism*, *300*(5), E837–47. http://doi.org/10.1152/ajpendo.00598.2010

Platten, M., Kretz, A., Naumann, U., Aulwurm, S., Egashira, K., Isenmann, S., & Weller, M. (2003). Monocyte chemoattractant protein-1 increases microglial

infiltration and aggressiveness of gliomas. *Annals of Neurology*, *54*(3), 388–392. http://doi.org/10.1002/ana.10679

Possenti, R., Muccioli, G., Petrocchi, P., Cero, C., Cabassi, A., Vulchanova, L., … Bartolomucci, A. (2012). Characterization of a novel peripheral pro-lipolytic mechanism in mice: role of VGF-derived peptide TLQP-21. *The Biochemical Journal*, *441*(1), 511–522. http://doi.org/10.1042/BJ20111165

Possenti, R., Eldridge, J. D., Paterson, B. M., Grasso, A., & Levi, A. (1989). A protein induced by NGF in PC12 cells is stored in secretory vesicles and released through the regulated pathway. *The EMBO Journal*, *8*(8), 2217–2223.

Prinz, M., Kann, O., Draheim, H. J., Schumann, R. R., Kettenmann, H., Weber, J. R., & Hanisch, U. K. (1999). Microglial activation by components of gram-positive and -negative bacteria: distinct and common routes to the induction of ion channels and cytokines. *Journal of Neuropathology and Experimental Neurology*, *58*(10), 1078–1089.

R Core Team (2015). R: A language and environment for statistical computing. R Foundation for Statistical Computing, Vienna, Austria. URL **https://www.R-project.org/**.

Rafehi, H., Orlowski, C., Georgiadis, G. T., Ververis, K., El-Osta, A., & Karagiannis, T. C. (2011). Clonogenic Assay: Adherent Cells. *Journal of Visualized Experiments*, (49), 15–17. http://doi.org/10.3791/2573

Riedl, M. S., Braun, P. D., Kitto, K. F., Roiko, S. A., Anderson, L. B., Honda, C. N., … Vulchanova, L. (2009). Proteomic analysis uncovers novel actions of the neurosecretory protein VGF in nociceptive processing. *The Journal of Neuroscience : The Official Journal of the Society for Neuroscience*, *29*(42), 13377–88. http://doi.org/10.1523/JNEUROSCI.1127-09.2009

Rindi, G., Licini, L., Necchi, V., Bottarelli, L., Campanini, N., Azzoni, C., … Ferri, G.-L. (2007). Peptide Products of the Neurotrophin-Inducible Gene *vgf* Are Produced in Human Neuroendocrine Cells from Early Development and Increase in Hyperplasia and Neoplasia. *The Journal of Clinical Endocrinology & Metabolism*, *92*(7), 2811–2815. http://doi.org/10.1210/jc.2007-0035

Ríos, M., Foretz, M., Viollet, B., Prieto, A., Fraga, M., Costoya, J. A., & Señarís, R. (2013). AMPK activation by oncogenesis is required to maintain cancer cell proliferation in astrocytic tumors. *Cancer Research*, *73*(8), 2628–2638. http://doi.org/10.1158/0008-5472.CAN-12-0861

Rizzi, R., Bartolomucci, A., Moles, A., D'Amato, F., Sacerdote, P., Levi, A., … Pavone, F. (2008). The VGF-derived peptide TLQP-21: a new modulatory peptide for inflammatory pain. *Neuroscience Letters*, *441*(1), 129–133. http://doi.org/10.1016/j.neulet.2008.06.018

Rossi, A., Granata, F., Augusti-Tocco, G., Canu, N., Levi, A., & Possenti, R. (1992). Expression in murine and human neuroblastoma cell lines of VGF, a tissue specific protein. *Int J Dev Neurosci*, *10*(6), 527–534.

Rozek, W., Kwasnik, M., Debski, J., & Zmudzinski, J. F. (2013). Mass spectrometry identification of granins and other proteins secreted by neuroblastoma cells. *Tumor Biology*, *34*(3), 1773–1781. http://doi.org/10.1007/s13277-013-0716-0

Sakamoto, M., Miyazaki, Y., Kitajo, K., & Yamaguchi, A. (2015). VGF, which is induced transcriptionally in stroke brain, enhances neurite extension and confers protection against ischemia in vitro. *Translational Stroke Research*, *6*(4), 301–308. http://doi.org/10.1007/s12975-015-0401-2

Salton, S. R., Ferri, G. L., Hahm, S., Snyder, S. E., Wilson, a J., Possenti, R., & Levi, a. (2000). VGF: a novel role for this neuronal and neuroendocrine polypeptide in the regulation of energy balance. *Frontiers in Neuroendocrinology*, *21*(3), 199–219. http://doi.org/10.1006/frne.2000.0199

Salton, S. R., Fischberg, D. J., & Dong, K. W. (1991). Structure of the gene encoding VGF, a nervous system-specific mRNA that is rapidly and selectively induced by nerve growth factor in PC12 cells. *Molecular and Cellular Biology*, *11*(5), 2335–2349. http://doi.org/10.1128/MCB.11.5.2335.Updated

Salton, S. R. J., Volonté C., & D'Arcangelo, G. (1995). Stimulation of vgf gene expression by NGF is mediated through multiple signal transduction pathways involving protein phosphorylation. *FEBS Letters*, *360*(2), 106–110. http://doi.org/10.1016/0014-5793(95)00086-O

Sassi, F. A., Brunetto, A. L., Schwartsmann, G., Roesler, R., & Abujamra, A. L. (2012). Glioma revisited: from neurogenesis and cancer stem cells to the epigenetic regulation of the niche. *Journal of Oncology*, *2012*, 537861. http://doi.org/10.1155/2012/537861

Sato, H., Fukutani, Y., Yamamoto, Y., Tatara, E., Takemoto, M., Shimamura, K., & Yamamoto, N. (2012). Thalamus-derived molecules promote survival and dendritic growth of developing cortical neurons. *The Journal of Neuroscience : The Official Journal of the Society for Neuroscience*, *32*(44), 15388–402. http://doi.org/10.1523/JNEUROSCI.0293-12.2012

Severini, C., La Corte, G., Improta, G., Broccardo, M., Agostini, S., Petrella, C., … Possenti, R. (2009). In vitro and in vivo pharmacological role of TLQP-21, a VGF-derived peptide, in the regulation of rat gastric motor functions. *British Journal of Pharmacology*, *157*(6), 984–993. http://doi.org/10.1111/j.1476-5381.2009.00192.x

Severini, C., Ciotti, M. T., Biondini, L., Quaresima, S., Rinaldi, A. M., Levi, A., … Possenti, R. (2008). TLQP-21 , a neuroendocrine VGF-derived peptide , prevents cerebellar granule cells death induced by serum and potassium deprivation, 534–544. http://doi.org/10.1111/j.1471-4159.2007.05068.x

Sharma, A., & Shiras, A. (2015). Cancer stem cell-vascular endothelial cell interactions in glioblastoma. *Biochemical and Biophysical Research Communications*, *473*(3), 688–692. http://doi.org/10.1016/j.bbrc.2015.12.022

Shimazawa, M., Tanaka, H., Ito, Y., Morimoto, N., Tsuruma, K., Kadokura, M., … Hara, H. (2010). An Inducer of VGF protects cells against ER stress-induced cell death and prolongs survival in the mutant SOD1 animal Models of Familial ALS. *PLoS ONE*, *5*(12). http://doi.org/10.1371/journal.pone.0015307

Sibilia, V., Pagani, F., Bulgarelli, I., Mrak, E., Broccardo, M., Improta, G., … Guidobono, F. (2010). TLQP-21, a VGF-derived peptide, prevents ethanol-induced gastric lesions: insights into its mode of action. *Neuroendocrinology*, *92*(3), 189–197. http://doi.org/10.1159/000319791

Sibilia, V., Pagani, F., Bulgarelli, I., Tulipano, G., Possenti, R., & Guidobono, F. (2012). Characterization of the mechanisms involved in the gastric antisecretory effect of TLQP-21, a vgf-derived peptide, in rats. *Amino Acids*, *42*(4), 1261–1268. http://doi.org/10.1007/s00726-010-0818-6

Siebzehnrubl, F. A., Reynolds, B. A., Vescovi, A., Steindler, D. A., & Deleyrolle, L. P. (2011). The origins of glioma: E Pluribus Unum? *Glia*, *59*(8), 1135–1147. http://doi.org/10.1002/glia.21143

Snyder, S. E., Peng, B., Pintar, J. E., & Salton, S. R. J. (2003). Expression of VGF mRNA in developing neuroendocrine and endocrine tissues. *Journal of Endocrinology*, *179*(2), 227–235. http://doi.org/10.1677/joe.0.1790227

Snyder, S. E., & Salton, S. R. J. (1998). Expression of VGF mRNA in the adult rat central nervous system. *Journal of Comparative Neurology*, *394*(1), 91–105.

Stephens, S. B., Schisler, J. C., Hohmeier, H. E., An, J., Sun, A. Y., Pitt, G. S., & Newgard, C. B. (2012). A VGF-derived peptide attenuates development of type

2 diabetes via enhancement of islet beta-cell survival and function. *Cell Metabolism*, *16*(1), 33–43. http://doi.org/10.1016/j.cmet.2012.05.011

Stock, K., Kuma, J., Synowitz, M., Petrosino, S., Imperatore, R., Smith, E. S. J., … Glass1. (2012). Neural precursor cells induce cell death of high-grade astrocytomas via stimulation of TRPV1. *Nature Medicine*, *18*(8), 1232–1238. http://doi.org/10.1038/nm.2827.Neural

Stupp, R., Mason, W. P., van den Bent, M. J., Weller, M., Fisher, B., Taphoorn, M. J., … National Cancer Institute of Canada Clinical Trials, G. (2005). Radiotherapy plus concomitant and adjuvant temozolomide for glioblastoma. *N Engl J Med*, *352*(10), 987–996. http://doi.org/10.1056/NEJMoa043330

Succu, S., Cocco, C., Mascia, M. S., Melis, T., Melis, M. R., Possenti, R., … Argiolas, A. (2004). Pro-VGF-derived peptides induce penile erection in male rats: possible involvement of oxytocin. *The European Journal of Neuroscience*, *20*(11), 3035–3040. http://doi.org/10.1111/j.1460-9568.2004.03781.x

Succu, S., Mascia, M. S., Melis, T., Sanna, F., Melis, M. R., Possenti, R., & Argiolas, A. (2005). Pro-VGF-derived peptides induce penile erection in male rats: Involvement of paraventricular nitric oxide. *Neuropharmacology*, *49*(7), 1017–1025. http://doi.org/10.1016/j.neuropharm.2005.05.015

Szulzewsky, F., Pelz, A., Feng, X., Synowitz, M., Markovic, D., Langmann, T., … Kettenmann, H. (2015). Glioma-associated microglia/macrophages display an expression profile different from M1 and M2 polarization and highly express Gpnmb and Spp1. *PLoS ONE*, *10*(2), 1–27. http://doi.org/10.1371/journal.pone.0116644

Thakker-Varia, S., Krol, J. J., Nettleton, J., Bilimoria, P. M., Bangasser, D. a., Shors, T. J., … Alder, J. (2007). The Neuropeptide VGF Produces Antidepressant-Like Behavioral Effects and Enhances Proliferation in the Hippocampus. *Journal of Neuroscience*, *27*(45), 12156–12167. http://doi.org/10.1523/JNEUROSCI.1898-07.2007

Thakker-Varia, S., Behnke, J., Doobin, D., Dalal, V., Thakkar, K., Khadim, F., … Alder, J. (2014). VGF (TLQP-62)-induced neurogenesis targets early phase neural progenitor cells in the adult hippocampus and requires glutamate and BDNF signaling. *Stem Cell Research*, *12*(3), 762–777. http://doi.org/10.1016/j.scr.2014.03.005

Thomas, A. A., Brennan, C. W., DeAngelis, L. M., & Omuro, A. M. (2014). Emerging therapies for glioblastoma. *JAMA Neurology*, *71*(11), 1437–44. http://doi.org/10.1001/jamaneurol.2014.1701

Toledo, C. M., Ding, Y., Hoellerbauer, P., Davis, R. J., Basom, R., Girard, E. J., … Paddison, P. J. (2015). Genome-wide CRISPR-Cas9 Screens Reveal Loss of Redundancy between PKMYT1 and WEE1 in Glioblastoma Stem-like Cells. *Cell Reports*, *13*(11), 2425–2439. http://doi.org/10.1016/j.celrep.2015.11.021

Toshinai, K., & Nakazato, M. (2009). Neuroendocrine regulatory peptide-1 and -2: novel bioactive peptides processed from VGF. *Cellular and Molecular Life Sciences : CMLS*, *66*(11-12), 1939–1945. http://doi.org/10.1007/s00018-009-8796-0

Toshinai, K., Saito, T., Yamaguchi, H., Sasaki, K., Tsuchimochi, W., Minamino, N., … Nakazato, M. (2014). Neuroendocrine regulatory peptide-1 and -2 (NERPs) inhibit the excitability of magnocellular neurosecretory cells in the hypothalamus. *Brain Research*, *1563*, 52–60. http://doi.org/10.1016/j.brainres.2014.03.038

Toshinai, K., Yamaguchi, H., Kageyama, H., Matsuo, T., Koshinaka, K., Sasaki, K., … Nakazato, M. (2010). Neuroendocrine regulatory peptide-2 regulates feeding behavior via the orexin system in the hypothalamus. *American Journal of Physiology. Endocrinology and Metabolism*, *299*(3), E394–401. http://doi.org/10.1152/ajpendo.00768.2009

Trani, E., Giorgi, a., Canu, N., Amadoro, G., Rinaldi, a. M., Halban, P. a., … Levi, a. (2002). Isolation and characterization of VGF peptides in rat brain. Role of PC1/3 and PC2 in the maturation of VGF precursor. *Journal of Neurochemistry*, *81*(3), 565–574. http://doi.org/10.1046/j.1471-4159.2002.00842.x

Trani, E., Ciotti, T., Rinaldi, a M., Canu, N., Ferri, G. L., Levi, a, & Possenti, R. (1995). Tissue-specific processing of the neuroendocrine protein VGF. *Journal of Neurochemistry*, *65*(6), 2441–9. http://doi.org/10.1046/j.1471-4159.1995.65062441.x

van den Pol, a N., Bina, K., Decavel, C., & Ghosh, P. (1994). VGF expression in the brain. *The Journal of Comparative Neurology*, *347*(3), 455–69. http://doi.org/10.1002/cne.903470311

Vazquez-Martinez, R., & Gasman, S. (2014). *The regulated secretory pathway in neuroendocrine cells*. *Frontiers in Endocrinology* (Vol. 5). http://doi.org/10.3389/fendo.2014.00048

Verhaak, R. G. W., Hoadley, K. a., Purdom, E., Wang, V., Qi, Y., Wilkerson, M. D., … Hayes, D. N. (2010). Integrated genomic analysis identifies clinically relevant subtypes of glioblastoma characterized by abnormalities in PDGFRA, IDH1, EGFR, and NF1. *Cancer Cell*, *17*(1), 98–110. http://doi.org/10.1016/j.ccr.2009.12.020

Vinnakota, K., Hu, F., Ku, M.-C., Georgieva, P. B., Szulzewsky, F., Pohlmann, A., … Kettenmann, H. (2013). Toll-like receptor 2 mediates microglia/brain macrophage MT1-MMP expression and glioma expansion. *Neuro-Oncology*, *15*(11), 1457–1468. http://doi.org/10.1093/neuonc/not115

Watkins, S., Robel, S., Kimbrough, I. F., Robert, S. M., Ellis-Davies, G., & Sontheimer, H. (2014). Disruption of astrocyte-vascular coupling and the blood-brain barrier by invading glioma cells. *Nature Communications*, *5*(May), 4196. http://doi.org/10.1038/ncomms5196

Wick, W., Platten, M., & Weller, M. (2001). Glioma cell invasion: regulation of metalloproteinase activity by TGF-beta. *Journal of Neuro-Oncology*, *53*(2), 177–185.

Wirsching, H.-G., Galanis, E., & Weller, M. (2016). Chapter 23 - Glioblastoma. *Handbook of Clinical Neurology* (Ed.), *Gliomas* (Vol. Volume 134, pp. 381–397). Elsevier. http://doi.org/http://dx.doi.org/10.1016/B978-0-12-802997-8.00023-2

Yamaguchi, H., Sasaki, K., Satomi, Y., Shimbara, T., Kageyama, H., Mondal, M. S., … Minamino, N. (2007). Peptidomic identification and biological validation of neuroendocrine regulatory peptide-1 and -2. *The Journal of Biological Chemistry*, *282*(36), 26354–26360. http://doi.org/10.1074/jbc.M701665200

Zhang, W., Ni, C., Sheng, J., Hua, Y., Ma, J., Wang, L., … Xing, Y. (2013). TLQP-21 protects human umbilical vein endothelial cells against high-glucose-induced apoptosis by increasing G6PD expression. *PloS One*, *8*(11), e79760. http://doi.org/10.1371/journal.pone.0079760

Zhuo, L., Theis, M., Alvarez-maya, I., Brenner, M., & Willecke, K. (2001). hGFAP-cre transgenic mice for manipulation of glial and neuronal function in vivo, *94*, 85–94. http://doi.org/10.1002/gene.10008

VI. List of publications

I. Related publications

Sassi, F. A., Hambardzumyan, D., Jordan, P., Wolf, S., Kettenmann, H (*In preparation*). VGF expression regulation in the PDGFb-induced glioblastoma by microglia cells affects tumor growth and host survival.

Sassi, F. A., Visser, J., Wendt, S., Semtner, M., Wolf, S., Kettenmann, H (*In preparation*). VGF-derived peptide-induced outward potassium currents affect ATP response in mouse microglia via C3AR1.

II. Abstracts

Sassi, F. A., Mersch, M., Jordan, P., Hambardzumyan, D., Wolf, S., Kettenmann, H. (2016). The novel role of VGF in the glioma microenvironment. 10th FENS Forum of Neuroscience. Copenhagen, Denmark.

Sassi, F. A., Mersch, M., Tamagno, I., Virk, S., Wolf, S., Hambardzumyan, D., Kettenmann, H. (2016)The novel role of VGF in the glioma microenvironmen (2015): 16th MDC.FMP PhD Retreat. Bad Saarow, Germany.

VII. Curriculum Vitae

For reasons of data protection, the curriculum vitae is not published in the electronic version

For reasons of data protection, the curriculum vitae is not published in the electronic version

For reasons of data protection, the curriculum vitae is not published in the electronic version

For reasons of data protection, the curriculum vitae is not published in the electronic version